

Integration of High- T_c Superconducting Cables in the Dutch Power Grid of the Future

Proefschrift

ter verkrijging van de graad van doctor
aan de Technische Universiteit Delft,
op gezag van de Rector Magnificus prof. ir. K.C.A.M. Luyben;
voorzitter van het College voor Promoties,
in het openbaar te verdedigen op
maandag 4 februari 2016 om 12:30 uur

door

Roy ZUIJDERDUIN

Elektrotechnisch ingenieur
Technische Universiteit Delft, Nederland
geboren te Pijnacker

This dissertation has been approved by the
Promotor: Prof.dr. J.J. Smit
Copromotor: Dr. O.A. Chevtchenko

Composition of the doctoral committee:

Rector Magnificus	chairman
Prof.dr. J.J. Smit	Delft University of Technology
Dr. O.A. Chevtchenko	HTS-powercables.nl

Independent members:

Prof.ir. M.A.M.M. van der Meijden	Delft University of Technology
Prof.dr. P. Palensky	Delft University of Technology
Prof.dr.ir. H.H.J. ten Kate	University of Twente
Prof.dr. M. Noe	Karlsruhe Institute of Technology
Prof.dr. N. Hayakawa	Nagoya University

This research project is sponsored by SenterNovem (nowadays RVO “Rijksdienst voor Ondernemend Nederland (RVO)”) as part of the research program “Energie Onderzoek Subsidie – Lange Termijn” (EOSLT07050)).

The project acronym of our research program is SuperNet.

Copyright © 2016 by R. Zuijderduin

All rights reserved

ISBN 978-94-028-0042-5

*To my dear
Janneke, Thijn, Linde & parents*

Summary

Integration of High- T_c Superconducting Cables in the Dutch Power Grid of the Future

Worldwide there is an increasing need for a more sustainable form of electrical power delivery with a growing share of renewable energy generation. In the distribution and transmission network, large-scale and small-scale wind and solar power plants will be introduced, in proportion to the annual economic growth. The transmission and distribution network will be expanded, focusing on the electricity transport, however, there will also be a need for exchanges with neighboring countries.

Alternative solutions are needed in order to support the changes of the future grid. High temperature superconductors are an alternative to conventional conductors, due to their high current density and very low AC loss, and therefore deserve more attention. The purpose of this study is to explore ways to integrate high-temperature superconducting cables in a future network and to compare their favorable technical properties with, e.g., the conventional XLPE cable.

The development of 2nd generation high temperature superconducting tapes results in a high tape quality, making it very attractive for use in superconducting power transmission cables. At the same time, the network requirements placed on the grid, based on society needs are changing, such as low magnetic field emissions, reducing space requirements, lower losses, minimizing visual intrusion, etc. Our study shows that superconducting cables compared to conventional cables score better on these societal requirements.

From our comparison of three practical low and high temperature superconductors we can conclude that Yttrium Barium Copper Oxide is the most suitable superconductor for use in transmission cables. Our techno-economic analysis shows that superconducting cables become already competitive with conventional cable in the AC transmission, such as XLPE cables. Possible future problems concerning the transport capacity in the power grid where high temperature superconducting cables can offer a solution have been identified. For one promising location, we have formulated the requirements for the design of a high-temperature superconducting cable. Next, we propose two types of cable systems (with cold and warm dielectric). For both types we describe the core, the electrical insulation, the screen, the cryostat, the cooling system, etc. Also for the distribution

grid a techno-economic investigation is conducted. To assess the feasibility of the application in distribution grids, we have experimentally demonstrated a reduction of AC conductor losses from 1 W/m to 0.1 W/m. We also carried out an experimental investigation to improve the developed cryostat design for a 6 km long cable connection. Despite these substantial technical improvements our economic study showed that the high-temperature superconducting distribution cable is not yet competitive with the present conventional distribution cable systems except for niche locations where additional advantages e.g. magnetic emission, reduced space usage, power density weighs more heavily.

Besides the HVAC grid the Netherlands has HVDC interconnections with neighboring countries and there are initiatives for the use of DC high voltage connections to wind farms further out to sea. In our study, we make reference to a suitable location, where the above mentioned attractive features of the superconducting cable are applicable as well. We advised a modified design of a HTS HVDC cable which enables a possible upgrade of the transmission capacity of the HVDC link at such location.

The main results from the investigation are that:

- Based on our techno-economic analysis HTS cables offer the most competitive solution in transmission grids. Introduction of such cables will reduce HTS tape price, which in turn will stimulate further applications.
- Conceptual designs of competitive HTS AC and DC transmission cables are formulated along with that for HTS AC distribution cable. Novel designs allow for much longer length between cooling stations.
- Our experimental research has shown that HTS cable core losses may be reduced by a factor 10 (down to 0.11 W/m/phas at 3 kA_{rms}, 77 K, 50 Hz).
- Dedicated low friction cable cryostat was developed and successfully tested for 47 meters length. Patented multi-layer thermal insulation improves the cable cryostat heat leak from 1 W/m to 0.1 W/m.

Samenvatting

Integratie van Hoge- T_c Supergeleidende Kabels in het Nederlandse Elektriciteitsnet van de Toekomst

Wereldwijd is er een toenemende behoefte aan een meer duurzame vorm van elektriciteitsvoorziening met een groeiend aandeel hernieuwbare energie opwekking. In het distributie- en het transmissienet zullen, al naar gelang de jaarlijkse economische groei, grootschalige en kleinschalige wind en zonne-energie centrales hun intrede doen. Het transmissie- en distributienet zal zich uitbreiden, gericht op de benodigde elektriciteitstransporten, waarbij er ook een behoefte zal zijn aan uitwisseling met omliggende landen.

Alternatieve oplossingen zijn nodig om de veranderingen van het toekomstig net te ondersteunen. Hoge temperatuur supergeleiders vormen dankzij onder andere de hoge stroomdichtheid en het zeer geringe AC verlies een alternatief voor conventionele geleiders en verdienen daardoor meer aandacht. Het doel van deze studie is om te onderzoeken welke opties er zijn om hoge temperatuur supergeleidende kabels in het toekomstig net te integreren en de gunstige technische eigenschappen van deze kabels te vergelijken met bijvoorbeeld de conventionele kunststof geïsoleerde kabel.

De ontwikkelstap naar 2^e generatie hoge temperatuur supergeleidende tapes geeft een dusdanig hoge kwaliteitsverbetering dat supergeleiders aantrekkelijk zijn voor het gebruik in transmissie energiekabels. Tegelijkertijd veranderen ook de eisen die vanuit de maatschappij aan het elektriciteitsnet gesteld worden, zoals lagere magneetveld emissies, reduceren van ruimtebeslag, lagere verliezen, minimaliseren van horizonvervuiling, etc. Uit onze studie blijkt dat supergeleidende kabels ten opzichte van de conventionele kabels beter scoren op deze maatschappelijke eisen.

Naar aanleiding van ons onderzoek naar drie praktische hoge- en lage temperatuur supergeleiders kan geconcludeerd worden dat Yttrium Barium Koper Oxide de meest geschikte supergeleider geleider is voor toepassing in transmissie kabels. De beperkte beschikbaarheid van metalen kan een nadelig effect hebben op de componentprijs. Hierdoor zullen in de toekomst alternatieven voor conventionele metalen geleiders interessant worden.

Uit onze techno-economische analyses blijkt dat supergeleidende kabels op dit moment al in het AC transmissienet concurrerend zouden kunnen zijn met conventionele kabels, zoals XLPE kabels. Mogelijk toekomstige knelpunten ten

aanzien van het transportvermogen in het transportnet waar hoge temperatuur supergeleidende kabels een uitkomst kunnen bieden zijn geïdentificeerd. Voor één kansrijke locatie hebben we de eisen voor een ontwerp van een hoge temperatuur supergeleidende kabel geformuleerd. Daaruit volgend zijn twee typen kabel systemen (koude- en warme diëlektrische kabel) voorgesteld, bestaande uit onder andere de kern, de elektrische isolatie, het scherm, de cryostaat, het koelsysteem, etc. Ook voor het distributienet is een dergelijk onderzoek verricht. Vanwege de haalbaarheid hebben we onder andere een AC geleider verlies reductie van 1 W/m naar 0.1 W/m aangetoond. Tevens hebben we een cryostaat ontwerp uitgewerkt voor een 6 km lange kabelverbinding. Uit deze studie is gebleken dat het voor hoge temperatuur supergeleidende distributie kabels nog niet haalbaar is om te concurreren met de huidige conventionele distributie kabelsystemen. Op niche locaties, waar de extra voordelen van hoge temperatuur supergeleidende kabels zwaarder meewegen, blijkt echter, dat een dergelijke kabel wel rendabel kan zijn.

Naast het HVAC transportnet heeft Nederland hoge gelijkspanningsverbindingen met buurlanden en zijn er initiatieven voor het gebruik van hoge gelijkspanningsverbindingen met windparken verder op zee. In onze studie brengen we aan de hand van een geschikte locatie de aantrekkelijke eigenschappen zoals de hoge stroomdichtheid en de verliezen die in de cryostaat zijn geconcentreerd van een dergelijke supergeleidende DC kabel naar voren. Voor zo'n netwerkverbinding hebben we een ontwerp voor een DC HTS kabelontwerp voorgesteld.

De voornaamste resultaten uit ons onderzoek zijn dat:

- Onze economische studie heeft aangetoond dat HTS kabels het meest concurrerend zijn in het transmissienet. Introductie van dergelijke kabels zal de tape prijs verlagen en daardoor toepassingen verder stimuleren.
- Conceptuele kabelontwerpen van concurrerende HTS AC en DC kabels zijn geformuleerd samen met die van een AC distributiekabel. Nieuwe ontwerpen maken langere afstand tussen koelsystemen mogelijk.
- Ons experimenteel onderzoek heeft laten zien dat kern verliezen van de kabelkern met een factor 10 gereduceerd kunnen worden (gereduceerd naar 0.11 W/m/fase at 3 kA_{rms}, 77 K, 50 Hz).
- Speciale lage wrijving kabel cryostaat was ontwikkeld en succesvol getest voor 47 meter lengte. Gepatenteerde multi-laag thermische isolatie verbetert de kabelcryostaat warmtelek van 1 W/m naar 0.1 W/m.

Table of Contents

Summary	V
Samenvatting	VII
1 Introduction	1
1.1 Practical superconductors	2
1.2 HTS power cables	6
1.3 Existing and future Dutch power transmission network	7
1.4 Scope & objectives	10
1.5 Thesis layout	10
2 HTS cable integration in the future power transmission network	13
2.1 Introduction	14
2.2 Expected bottlenecks in the future Dutch grid	14
2.3 Integration of a HTS power cable into the grid	18
2.3.1 Required transmission parameters	18
2.3.2 Modeled network example	21
2.3.3 Transmission characteristics	24
2.3.4 In-grid case study	29
2.3.5 Discussion on case study	38
2.3.6 Roadmap discussion	38
2.4 Conclusions	42
3 HTS 380 kV AC transmission cable design	45
3.1 Introduction	46
3.1.1 Conventional transmission	46
3.1.2 State of the art HTS transmission cables	46
3.2 Concept and interior arrangement of HTS cable	48
3.2.1 Cold dielectric HTS cable	48
3.2.2 Warm dielectric HTS cable	51
3.2.3 Laying arrangement	54
3.2.4 HTS core and shield	56
3.2.5 Electrical insulation	58
3.2.6 Cryostat	59
3.2.7 Terminations	60
3.2.8 Hydraulics of CD and WD HTS cables	64
3.2.9 Cooling	65
3.2.10 Cable system losses	67
3.2.11 Cable mass	70

3.2.12	Thermal cycling	71
3.3	General comparison of cables and OHL.....	72
3.4	AC Cable Activities.....	74
3.5	Conclusions	76
4	HTS AC cable integration in the distribution network	79
4.1	Introduction	80
4.1.1	Changing existing Dutch distribution network.....	81
4.2	HTS distribution cables	82
4.2.1	Dutch project	83
4.3	Feasibility study for integrating a HTS cable into the distribution network.....	88
4.3.1	Ampacity project costs	89
4.3.2	Estimation of the costs for Triax distribution cable in Dutch cable project.....	89
4.4	Discussion	92
4.5	Conclusions	93
5	HTS AC distribution cable design (50 kV).....	95
5.1	State of the art.....	96
5.2	Concept and interior arrangement	96
5.2.1	Design constraint for the HTS distribution cable	97
5.2.2	HTS core.....	97
5.2.3	AC losses in HTS conductors.....	98
5.2.4	Arrangement and manufacturing.....	99
5.2.5	Experimental setup	100
5.2.6	Measurement results.....	102
5.2.7	Electrical insulation.....	106
5.2.8	Cryostat and hydraulics	106
5.2.9	Measurement results	108
5.3	Terminations.....	110
5.4	Temperature profiles	111
5.5	Cooling	112
5.6	Intrinsic fault current limiter.....	113
5.7	Electrical imbalance modeling	115
5.8	Conclusions	119
6	HTS HVDC cables and Outlook	121
6.1	Introduction	122
6.2	HTS DC cable.....	122
6.3	HTS HVDC interconnection example.....	123
6.4	State of art commercial HTS HVDC cable.....	126
6.5	Concept and interior arrangement of HTS DC cable.....	126
6.5.1	HTS DC cable.....	126
6.5.2	Hydraulics of HTS DC cable.....	132

6.6	Outlook for DC HTS cables.....	133
6.7	Conclusions.....	135
7	Conclusions and recommendations	137
7.1	Main results of the study.....	138
7.2	Conclusions per chapter.....	138
7.2.1	Introduction.....	138
7.2.2	HTS AC cables in the power transmission network.....	138
7.2.3	HTS 400 kV AC transmission cable design.....	140
7.2.4	Integration of HTS AC cable in the distribution network.....	141
7.2.5	HTS AC distribution cable design.....	143
7.2.6	HTS HVDC cables and outlook.....	144
7.3	Opportunities for further research.....	145
	Appendix A.....	147
	Appendix B.....	153
	Appendix C.....	157
	Bibliography.....	163
	List of abbreviations.....	175
	List of symbols.....	179
	Acknowledgements.....	183
	Curriculum Vitae.....	185

1

Introduction

Due to the trend in energy policy to substantially increase the fraction of renewable power generation by the year 2030 one of the functions of the power grid is provide access to renewable energy resources to connect such sources over longer distances. High temperature superconductors could act as an enabler for accessing these large amounts of renewable energy in a sustainable way. This chapter gives an introduction of the HTS technology and provides the scope of the thesis.

- 1.1 Practical superconductors
- 1.2 HTS power cables
- 1.3 Existing and future Dutch power transmission network
- 1.4 Scope and objectives
- 1.5 Thesis layout

1.1 Practical superconductors

In 1911 Heike Kamerlingh Onnes discovered superconductivity by noticing that the electrical resistance of mercury became extremely small when cooling down with liquid helium. Since then many new superconducting materials & alloys were discovered. In 1987 a new type of high temperature superconductor (HTS) was discovered operating at liquid nitrogen temperature (77 K), see Figure 1.1.

The temperature below which the material becomes superconductive is called the critical temperature. Below the critical temperature, superconductors in practice can carry direct current with extremely small voltage drop. Above the critical current the voltage drop exceeds a threshold value.

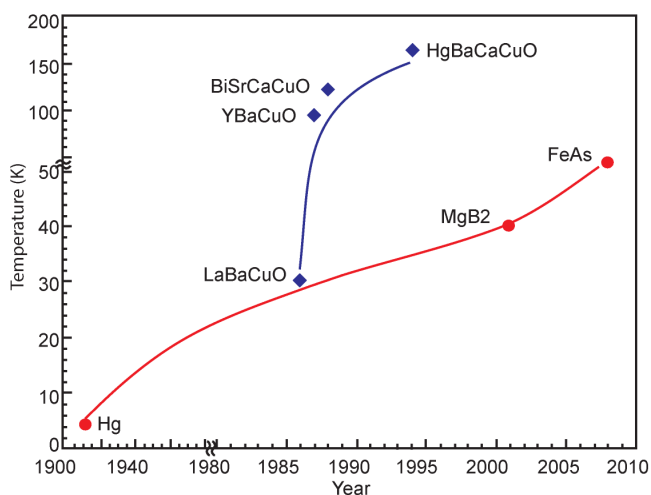


Figure 1.1 Critical temperature of superconductors, relevant to power applications, versus time ([1], the HTS and the LTS families are marked with the blue rhombi and the blue lines and with the red circles and the red lines respectively).

Today, practical HTS's are represented mainly by two generations of cuprate (copper compound) superconductors: the first generation (1G) uses bismuth strontium calcium copper oxide material (BiSrCaCuO or BSCCO), and the second generation (2G) contains a thin film of rare earth (RE) material in the form of e. g., yttrium and barium copper oxide (YBCO). The YBCO conductor is the most advanced coated conductor available. The interior arrangement of 1G and 2G wires is sketched in Figure 1.2. The first generation HTS conductor consists of a silver matrix filled with textured superconducting filaments and it is manufactured using so-called powder in tube process. The conductor is usually manufactured in the shape of a tape. The manufacturing process is similar to niobium composite superconductors that are produced for decades [1], which resulted into an efficient manufacturing process.

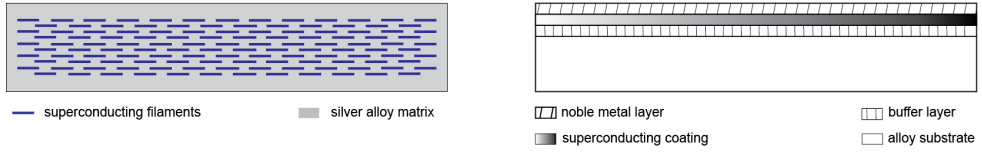


Figure 1.2 Schematic arrangements of 1G (left) and 2G tapes (right), where 2G in practical applications have an additional stabilization layer, e.g. copper or brass.

Table 1.1 Typical characteristics of practical superconductors with 1 mm² cross-section [1 – 3].

Parameter	MgB ₂	BSCCO (2223)	YBCO
Wire tape width, mm	Round, e.g. Ø1.13 mm	2.5 to 4.5, e.g. 4 mm	3 to 100 mm, e.g. 20 mm
Wire thickness, mm	Round, e.g. Ø1.13 mm	0.15 to 0.3, e.g. 0.25	0.05 to 0.2, e.g. 0.05
Sc/total filling factor	0.2	0.3	<0.02
Anisotropy, $\eta = H_{c2\parallel}(T)/H_{c2\perp}(T)$	1.5-5	50-200	5-7
Critical temperature T_c , K	~40	108	92
Operating temperature T_o , K	15	65	65
Critical current I_c (T_o , self-field), A	500*	225*	1850*
Irreversibility field $B^*(T)$, T	8 (4 K)	~0.2 (77 K)	5-7 (77 K)
Matrix resistivity ρ (T_c), $\mu\Omega\text{cm}$	0.4	~150-800	~40-60
Costs wire (T_o , self-field), €/kA·m	1	60	100
Critical current I_c (self-field), A at 15 K	500*	1125*	9250*
Cost wire (15 K), €/kA·m	1	20	25

* Lift factors for YBCO and BSCCO wire are assumed respectively of 2.5 and 2 times from 77 to 65 K and of 5 times from 65 to 15 K

The second generation YBCO superconductor is deposited as a thin film on an alloy substrate. The tape has several layers with an appropriate buffer and a highly textured surface as indicated in Figure 1.2. Additional layers on top of the buffer provide a secondary path for the current during the transition to the normal state. The HTS layer carrying the superconducting current I , is just 1 micrometer thick (while the total tape thickness is 50-100 μm). Produced tape is typically 100 mm wide and it can be sliced to almost any width, common for AC applications is 3-6 mm. For example a 4 mm wide and just 0.05 mm thick wire cooled to 77 K carries a DC current up to 150 A with very low ohmic loss (the voltage drop is below 10^{-4} V/m), corresponding current density is at present above 500 A/mm² (up on 0.1 T). As the filling factor of modern YBCO tapes is currently extremely low (Table 1.1), much higher critical currents can be expected in the future (e.g. due to

improved deposition techniques resulting in thicker HTS layers at the same current density and due to better pinning).

At present, high temperature superconductors in the form of coated conductor tapes are commercially available from several manufacturers: e.g., American Superconductor Corporation, Superpower, Fujikura, STI. Essential for applications is that the HTS tape price, expressed as cost performance ratio (CPR), can approach that of copper [4]. The cost performance ratio has unity, $\text{€}/(\text{kA}\cdot\text{m})$, indicating that the tape price is inversely proportional to the current carrying capacity of the tape. At present, the 4 mm wide YBCO tape has a DC critical current of 150 A and sells for about 250 $\text{€}/(\text{kA}\cdot\text{m})$ (77 K, self-field, in short length). As indicated in Table 1.1, operation at 65 K instead of 77 K results in a lift factor of 2.5 (in self-field) for the tape critical current of YBCO tape [5]. Therefore, the CPR for the YBCO wire is 100 $\text{€}/(\text{kA}\cdot\text{m})$ at this temperature and the CPR for BSCCO wire, at 77 K, is at present 125 $\text{€}/(\text{kA}\cdot\text{m})$ [6]. Similar to that the BSCCO wire CPR reduces to 60 $\text{€}/(\text{kA}\cdot\text{m})$ at 65 K, see Table 1.1.

Another interesting alloy for power applications is magnesium diboride (MgB_2). It belongs to the family of low temperature superconductors. It is occasionally referred to as a high-temperature superconductor due to its relatively high critical temperature, see Figure 1.1. This conductor has a relatively high critical temperature (40 K) and a remarkably low CPR (close to 1 $\text{€}/(\text{kA}\cdot\text{m})$ at present [7]), which makes it attractive for applications where the operating temperature around 15 K is acceptable (e.g., [8]).

Estimates show that at current prices BSCCO and YBCO tapes operated at 15 K will have a CPR's of respectively 20 and 25 $\text{€}/(\text{kA}\cdot\text{m})$, see Table 1.1. MgB_2 has a CPR much lower than that of YBCO and BSCCO, however the costs to keep this material at its operation temperature are higher as explained below.

Besides the wire costs, the cooling costs (including those of the cryocooler, cryostat and vacuum pumping), represent a considerable share of the cable system costs as shown in Table 1.2. In order to find the most appropriate wire to be used in HTS cables, a cost comparison is made for a HTS AC cable core consisting of MgB_2 , BSCCO and YBCO.

In the comparison the total wire and cooling costs are assessed for a cable wire core assuming operation at their operating temperature, T_o . The cores are assumed to have a DC critical current of 10 kA, with a nominal transport current of 2 kA.

AC cable core losses are determined by magnetisation, eddy current and transport current losses, which are depending on the current and magnetic- field amplitude. The wires in the core are exposed to perpendicular magnetic field amplitude of 0.01 T in order to estimate the magnetisation losses.

As a result the calculated core losses (assuming no decline of the critical current in the wire) are as follows: 0.59 W/m (wire $I_c = 140$ A, self-field, 77 K) estimated

from [9], 0.17 W/m ($I_c = 116$ A, self-field, 77 K) estimated from [3] and 0.03 W/m ($I_c = 120$ A, self-field, 77 K) estimated from our YBCO core AC loss measurement, (described in more detail in Chapter 5) for respectively MgB₂, BSCCO and YBCO wire. Based on the core losses, the cooling costs are derived. The assumed heat leaks for MgB₂, BSCCO and YBCO wire in the cryostat at 15 K and 77 K are respectively, 0.2 kW/km and 1 kW/km.

The MgB₂ cryostat costs are, however, much higher than that of the BSCCO and YBCO cryostat costs at the operating temperature estimated from technical analysis presented in [10, 18]. Refrigeration costs are estimated based on the cryostat and core heat load to be removed at the operation temperature following [12, 13]. As a result, the refrigeration costs are substantially higher for MgB₂ as compared to BSCCO and YBCO since it operates at lower temperature, hence cooling penalties (i.e. the ratio of the input power to the cooling power), are respectively, 250 to 500 W and 10 to 15 W [14].

Table 1.2 shows total costs for the MgB₂, BSCCO and YBCO cable core of 3, 1 and 2 M€/km, respectively. The total costs contain the costs for the wire, cryostat and cooling for each cable. It indicates substantial lower costs for a BSCCO and YBCO cables as compared to the MgB₂ cable. The wire costs for MgB₂ are substantially lower than BSCCO and YBCO, see Table 1.1, however it has the highest cryostat and refrigeration costs.

Table 1.2 Wire, cryostat and refrigeration costs of the cable core with the transport current of $2 kA_{rms}$, (the critical current of $10 kA_{dc}$) made of selected practical superconductors operated at T_o .

Component costs, M€/km	MgB ₂	BSCCO (2223)	YBCO (123)
Superconductor*	0.01	0.60	1
Cryostat	2.00	0.35	0.35
Cooling [▼]	0.62	0.22	0.20
Total	3	1	2

* Superconductor costs are based on Table 1.1

▼ Cooling costs are given in M€/km rather than €/W in order to be able to make a direct cost comparison between the cable core costs

Based on techno-economic analysis and considering that it is expected that with time YBCO tape costs will be lower than for BSCCO wire and for copper, we consider YBCO tape to be the most suitable superconductor to be used throughout this thesis.

1.2 HTS power cables

It is a general consensus that HTS power cable technology is on the way from demonstration stage to commercialization. Worldwide there are multiple HTS power cable projects started, running or completed [15].

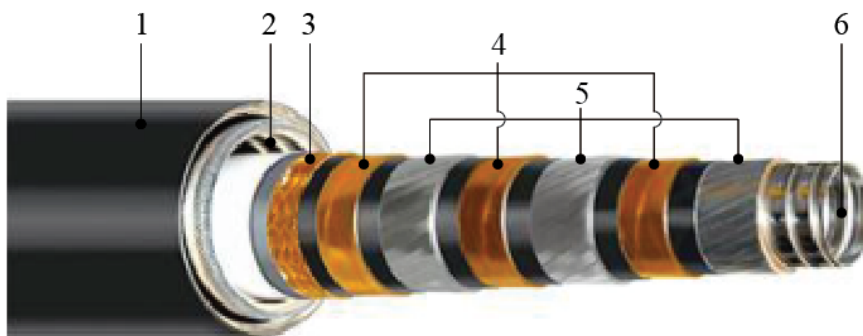


Figure 1.3 HTS cable example [15, 23]. (Courtesy Ultera® - A Southwire / nkt cables Joint Venture)

Several of these projects are focused on AC and a few on DC. AC projects are covering distribution and transmission voltages ranging from 10 kV to 275 kV, lengths from 30 m to 1 km [15, 22].

One example is the 13.8 kV, 4 kA HTS triaxial cable, linking two substations in Manhattan US.

Figure 1.3 shows an example of how a HTS distribution cable looks like. The cable core consists of three HTS phases that are made of HTS tape (5) and are electrically insulated from each other using special insulation material (4) developed to operate safely at low temperatures. The neutral (3) is on the outside core and is electrically isolated from the most outer phase. The cable core is thermally insulated by the cryostat (1), which prevents ambient heat to penetrate into the cold area of the cable. A coolant flows in the former (6) and in the area between the outer cable core diameter and cryostat inner diameter (2), allowing the cable core to operate at low temperatures.

Using HTS tapes enables a high current density in the HTS cable together with low loss. For example, HTS cables can transport about 5 and 10 times more power in comparison with copper cable of the same diameter operating at AC and DC voltage, respectively. More details on HTS cables arrangement and performance are provided in Chapters 3, 5 and 6.

1.3 Existing and future Dutch power transmission network

The Dutch power transmission grid is built with 380 kV system elements (Figure 1.4).

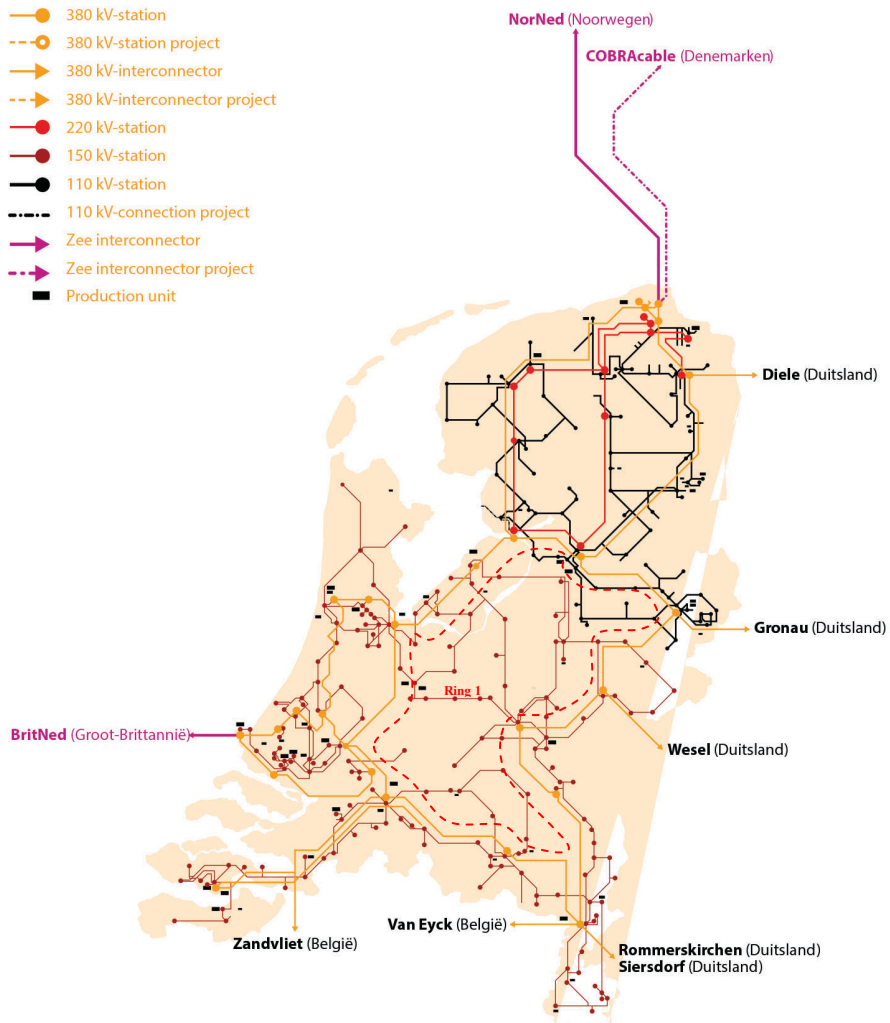


Figure 1.4 Dutch electricity network in year 2015, where EHV is indicated by the orange lines, generation plants by black squares. The orange arrows show connections to adjacent countries [16].

Depending on the connection lengths, several voltage steps towards end users can be taken (220, 150, 110 and 50 kV) to enable transmission of the about 26 GW installed power capacity. By means of the extra high voltage ring and its connections (EHV, 380 kV), large distances are covered, such as to large scale generation, neighbour countries and to the HV-grid, see Figure 1.4. Overseas connections are made with Norway (NorNed 1), England (BritNed) and cross-border capacity on land. General future developments on transmission level are: more power import and export through interconnections, additional large scale generation units mostly installed at coastal regions and increase of renewable energy sources (RES). The European Union (EU) plans 300 GW of available wind energy by 2030 and excess of energy will be traded through the interconnections.

If for instance the United Kingdom (UK) has an excess of wind power then the Netherlands could provide the link to disperse the power into the rest of Europe. Presumably, strengthening the BritNed connection is needed. The aim of the future EHV network is to keep a strong 380 kV network by having several 380 kV rings near the load centres and nearby generator units. For network stability two additional rings in the EHV network are being made. Then the rings could provide sustainable energy to be transferred directly to the load centres.

The existing 380 kV main ring is strengthened by two new rings. The new rings are the North - ring and South - ring, see Figure 1.5. Moreover, the main ring will transform in two smaller rings in year 2030, also shown in Figure 1.5. The connections that need power capacity upgrade for future use are illustrated by additional lines in Figure 1.5 in comparison with Figure 1.4.

The Dutch government has the objective to install 4.5 GW onshore and 6 GW offshore wind power in year 2020 [16]. The yearly load growth in the Netherlands is around 2% and in Europe 2% predicted by Union for the Coordination of the Transmission of Electricity (UCTE) [16]. The load increase in the Netherlands is mainly concentrated in western and central parts.

Figure 1.5 indicates the expected (by TenneT [16]) grid change for year 2030. The net power input value of the 380 kV grid is based on connected wind power, conventional production (coal, gas, nuclear, biomass), DC imports, DC exports and power exchanges with subordinated high voltage grids (220 kV, 150 kV, 110 kV). The overseas interconnections are using HVDC technology and submarine cables. Multiple convertor stations are able to provide a high power capacity link (up to 8 GW at present [17]). The capacity of the interconnection is limited by the cable rating, which has a capacity up to 1 GW. The Dutch target is to have a 14 % share of renewables by 2020 [18]. To reach this target, one expects that 35 % will be provided by the production of renewable electrical energy [19]. The share of sustainable generation provided by the renewables electricity sources; sun, wind and biomass in the Netherlands in year 2010 was 9.1% of the total consumed electricity [20].

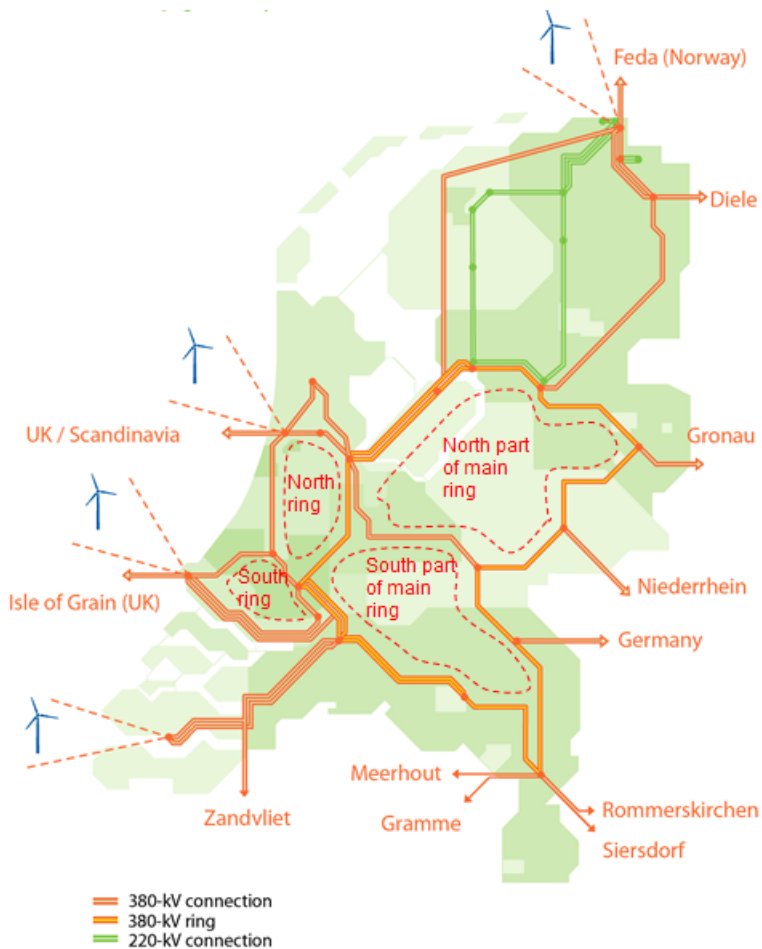


Figure 1.5 Dutch electricity network in the year 2030 [16].

This shows that about 25 % additional renewable energy production is needed in ten years towards 2020.

Electrical energy transmission and distribution to its consumers is accompanied by grid losses. The electrical power production and demand in the Netherlands in the years 2010 to 2013 was 110 TWh, and about 115 TWh was effectively consumed. About 4 % (4.5 TWh) of the total electricity consumption including export consisted of grid losses. HTS could contribute to a more efficient energy transportation and distribution, hence it deserves more attention.

Moreover, due to the aging of the power grid a replacement wave of a fraction of the grid components connectors is expected [15]. This creates an opportunity to apply HTS cables, however effort is needed in order to have a mature (E)HV cable ready to be integrated into the grid.

1.4 Scope & objectives

In the coming years many of the high voltage components in the existing energy network need to be replaced. It will soon be necessary to replace aged network components anyway, so it makes sense to look where new technologies can be applied. In that regard, the following objectives were set for this research:

- To investigate a possible integration of HTS AC cables in the Dutch electrical transmission and distribution grid in comparison with conventional technology;
- Based on future grid scenarios to identify prominent cases where HTS AC cables can be beneficial in solving foreseen capacity and societal problems in the Dutch electrical grid;
- To formulate the network requirements upon HTS HVAC and HVDC cable designs, for the most prominent grid locations;
- To elaborate a roadmap for the integration of HTS AC and DC cables in the Dutch grid of the future.

1.5 Thesis layout

In Chapter 2, the expected future bottlenecks in the Dutch electrical network (following from the scenarios of the Dutch transmission system operator TenneT) are examined for possible application of HTS cables. With time, HTS cables can be used to avoid many bottlenecks of the transmission network. The transition has to start somewhere and therefore it is important to identify a suitable location for this. In order to illustrate the potential of HTS transmission cables, we have selected a location in the network that will need higher capacity in three of the four future energy scenarios (of TenneT [16]). Network modelling, analysis and techno-economical comparison of available options for expansion (e. g, additional OHL, or XLPE cables, or HTS cables) will show if HTS cable is a good alternative. Based on the system requirements and desired performance of the connection, using the network modelling, demanded specifications of the HTS transmission cable are derived and transmission characteristics of the connection are calculated.

In Chapter 3 based on investigation of the state of the art for transmission cables the concept of a HTS transmission cable has been developed in accordance with the demanded specifications. The required cable interior arrangement is

explained and main components of the cable (HTS core, cold HV insulation, cryostat, terminations and cooling) are dealt with. Specifications and transmission characteristics of the cable are compared to those of conventional alternatives (OHL, XLPE cable).

In Chapter 4, possibilities to apply HTS cables in the distribution network of a selected Dutch operator are assessed by investigating expected future bottlenecks. The distribution network is facing also an increase in transport capacity to comply with the future needs. Analysis for implementing HTS cables to avoid expected bottlenecks at distribution level will be performed. Accordingly, a suitable location in the network is identified. The identified location is in the Network of Alliander (Dutch distribution network operator near Amsterdam). A system study including network modeling and techno-economic analysis will show in which way HTS distribution cables can compete with XLPE cables when HTS tape price is sufficiently low. Based on the desired system performance, required cable specifications are derived and network characteristics of the cable are evaluated.

In Chapter 5, the state of the art for distribution cables is presented together with the concept satisfying the required specifications. The interior arrangement of the HTS cable is explained, including the cable core, electrical insulation, cryostat, terminations and the cooling.

In Chapter 6 an outlook for HTS AC transmission and distribution cable systems is given. In addition, HTS HVDC power cables are covered. Using system approach and the network analysis, locations to integrate such cables are identified. A HTS cable concept is made based on an identified grid location and compared with another HTS DC cable concept. Other issues relevant to integration and the acceptance of new technology, such as social acceptance of HTS cables are addressed.

Chapter 7 provides the conclusions of the presented research and lays out opportunities for further investigation.

2

HTS cable integration in the future power transmission network

The main obstacle at present is the relatively high price of HTS conductor. However as the price goes down, initial market penetration of several HTS components (e.g.: cables, fault current limiters) is expected in the near future. In this chapter we discuss selected ways to integrate AC HTS EHV cables for various grid development scenarios in the Netherlands.

2.1 Introduction

2.2 Expected bottlenecks in the future Dutch grid

2.3 Integration of a HTS power cable into the grid

2.4 Conclusions

2.1 Introduction

Due to increasing fraction of renewable power generation, the electricity grid of the Netherlands is changing. The existing Dutch grid is not capable to handle the expected power transport in the year 2030. In this way, the Dutch grid needs strengthening in order to handle the power demands in year 2030. More decentralized electrical power generated by renewable sources will pass through the grid. Also, large scale electrical power is expected to be transported over longer distances due to generation at coastal regions and remote areas. This creates some potential grid issues, such as: power congestion and grid stability.

Most of the EHV grid components are in operation over 40 years. The existing components have an expected lifetime of about 50 years hence a replacement wave over 1-2 decades is expected. Moreover, societal concerns are growing such as the opposition to electrical lines, particularly in populated areas. Since the Dutch grid has a replacement policy, the introduction of HTS power components is an option as well. However, acceptance of a new innovation solution in the network is associated with a longer time period in comparison with the implementation time of proven assets. Several HTS pilot projects are completed and ongoing aiming to assure a reliable and efficient network operation [15]. HTS cables in the (E)HV grid are mainly likely to be promising for future network connections due to their current carrying capability, mechanical strength, low AC losses, network parameters etc.

The Dutch network operator TenneT (TSO) estimates the future energy demand and indicates expected grid bottlenecks by load flow calculations [16]. Places forming potential bottlenecks are identified according to four most likely future grid scenarios.

2.2 Expected bottlenecks in the future Dutch grid

The Dutch TSO TenneT estimated the necessary future grid change by means of four most likely scenarios for year 2030. The scenarios reflect the environmental and market dimensions and include four key locations of power generation: Borssele, Maasvlakte, IJmuiden (Beverwijk) and Eemshaven. In 2006 the EHV inputs from the production sites were respectively 0.9 GW, 1.1 GW, 0 GW, 2.4 GW. The expected key production capacities for 2030 are listed in Table 2.1. In TenneT's network study, load flows are estimated based on the grid voltages and nominal currents. The four scenarios are further detailed in [16, 24].

In this section we assume that HTS technology is mature and that the price of a HTS-based component is comparable to that of a conventional component. In each scenario we identify possible future locations where HTS technology could enforce the grid [25].

Table 2.1 Expected production capacity, GW at key locations in year 2030 [16].

Key location	Scenario			
	1	2	3	4
Borssele, GW	6.7	0.9	1.5	4.7
Maasvlakte, GW	5.4	4.0	8.6	5.1
IJmuiden-Beverwijk, GW	2.5	6.5	0.0	1.5
Eemshaven, GW	0.0	0.9	1.4	5.0
Total, GW	14.6	12.3	11.5	16.3

From all possible locations we select the most promising grid location to initiate HTS cable grid enforcement. This location is then used to analyse possible ways for the integration of HTS cables in the future Dutch power grid.

Scenario 1: Green revolution

The scenario postulates a large share of sustainable energy generation, using wind (generated at the North Sea and connection to Denmark), geothermal (connection to Norway) solar and biomass energy. Furthermore higher energy efficiency results in saving energy. Accordingly, sufficient CO₂ reduction is obtained. Besides the focus is on renewable energy and in this scenario a free market is concerned. The use of wind and solar energy makes the amount of generated energy unpredictable. Therefore, two extreme cases (windy, cloudy day and windless sunny day) are prominent in this scenario.

Load flow calculations from [16] show, that for a windy winter day connections 1.1a (Westerlee – Wateringen), 1.2a (Beverwijk – Oostzaan – Diemen), 1.3a to Belgium (Borssele - Zandvliet, <50 km), and 1.4a (Diemen – Lelystad – Ens) form potential transmission bottlenecks, see Figure 1.1 left. In case of a windless summer day the following connections form potential bottlenecks in the grid: 1.1b and 1.2b (Borssele – Geertruidenberg), 1.3b (Borssele - Zandvliet) and 1.4b (Geertruidenberg – Krimpen). Also the interconnection with Germany, 1.5b (Maasbracht - Rommerskirchen, <80 km) forms a bottleneck, see Figure 2.1, left.

Since TenneT vision demands for a strong EHV-ring with direct connections to large production capacities, in case of scenario 1, substantial parts of the transmission ring will require strengthening (see 1.4a, 1.4b, 1.6, 1.7 and 1.8 in Figure 2.1, left). Therefore, in this scenario connections 1.1a-1.4a, 1.1b-1.4b, 1.5b, 1.6, 1.7 and 1.8 are potential candidates for integration of HTS power cables. An example of our grid study (including comparison of overhead line, XLPE and HTS cables) for connection 1.3b is further detailed in [25].

Scenario 2: Sustainable transition

In this scenario the government regulates the market forcing society to make the transition to energy conservation and sustainability. Using bio-oil as a fuel for new

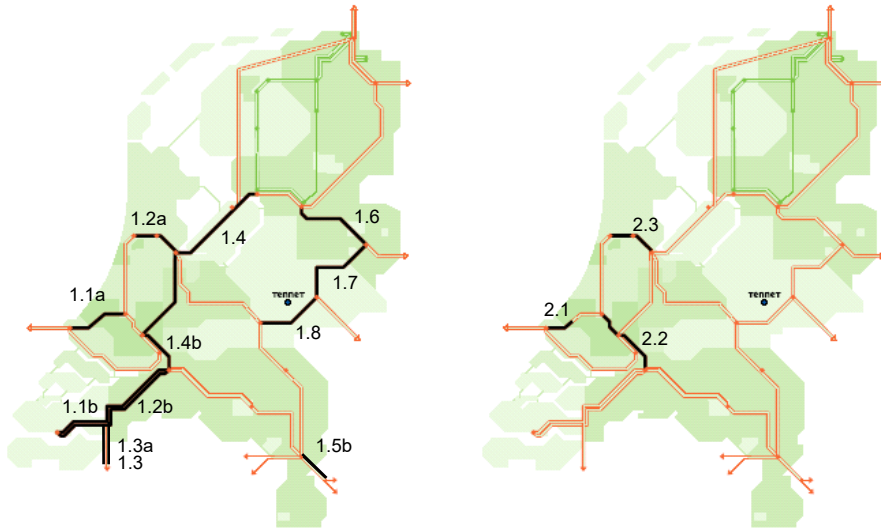


Figure 2.1 Potential bottlenecks in the grid of 2030: scenario 1 (left), cases of a windy winter day (a) and of a windless summer day (b); scenario 2 (right), case of a cold windy winter day [25].

power generation plants (such as combined heat and power plants) less CO₂ is emitted as compared to the more polluting coal plants. Homes produce solar energy and additional green energy is used from Scandinavian countries. Likewise to the green revolution scenario, two cases are assumed: when there is sufficient wind (excessive energy is exported to UK) and no wind but sunny (use of solar and import from neighbour countries).

The above mentioned new connection (Beverwijk - North Holland, 1.2a) is already reinforced with conventional cables [26]. Connections 2.1-2.3 (2.1: Maasvlakte – Westerlee, 2.2 Krimpen – Geertruidenberg, 2.3: Beverwijk – Oostzaan – Diemen) will exceed their capacity limit in case of high power generated at locations Maasvlakte (4 GW) and IJmuiden - Beverwijk (6.5 GW). Therefore, in this scenario, connections 2.1-2.3 are potential candidates for integration of HTS power cables [25].

Scenario 3: New strongholds

In this scenario a political tension is assumed leading to a trading block of oil and gas, see Figure 2. The position of power plants close to the North Sea makes the supply of fossil fuels possible, which leads to energy export. The energy increase is assumed to be only due to the additional export with no additional energy consumption. Sustainable energy and energy efficiency is used only when there is a need, so less wind is integrated.

Due to the increased power production at Maasvlakte, the overloaded connections: 3.1 (Maasvlakte – Crayestein - Krimpen), 3.2 (Maasvlakte - Bleiswijk), 3.3 (Geertruidenberg - Krimpen), 3.4 (Krimpen - Diemen) and 3.5 (Beverwijk – Diemen) require a power capacity upgrade, Figure 2 (left). Because of the large capacity at Maasvlakte, connections 3.3 and 3.4 are part of the main EHV ring. Therefore, in this scenario, connections 3.1-3.5 are potential candidates for integration of HTS power cables [25].

Scenario 4: Money rules

The scenario emphasizes globalization and liberalization, where social and environmental concerns are at low priority. Rising countries use a high share of gas and oil leading to a shortage in the EU. Consequently the EU must rely on other sources, like coal and nuclear. The Netherlands relies on gas to a large extent and hence more import of electrical energy is assumed requiring more interconnections.

Therefore, in this scenario, connections 4.1-4.3 are identified candidates for integration of HTS power cables [25].

At present, it is difficult to say which energy scenario will come to life. To our opinion, of all identified grid bottlenecks, connection Geertruidenberg – Krimpen stands out. Indeed, in three of the four future energy scenarios, connection Geertruidenberg – Krimpen needs strengthening.

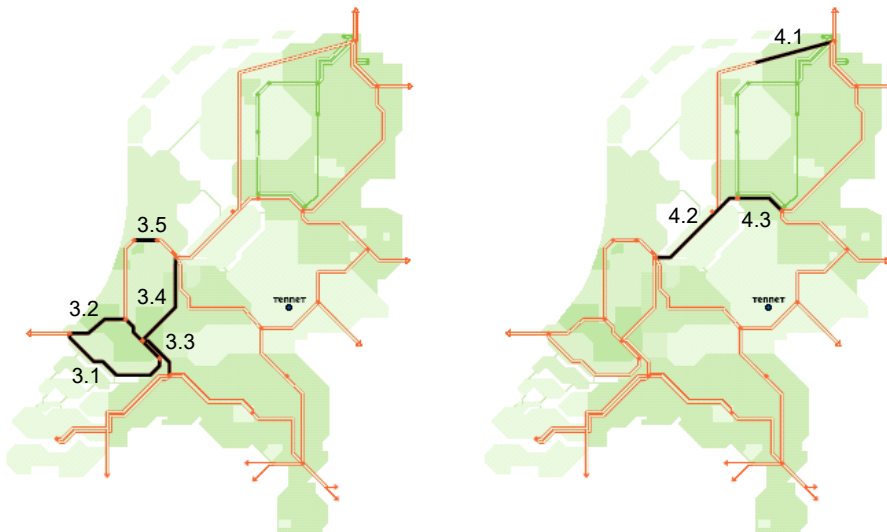


Figure 2.2 Potential bottlenecks in the grid of 2030: scenario 3 (left), cases of a windy winter day (a) and a windless summer day (b); scenario 4 (right), case of a windy or windless day [25].

Also, the expected load flow of this connection (7 GVA) and the load factor are sufficiently high. Furthermore, length of this connection (33.7 km) is such that it creates a problem for XLPE cable (limited to 25 km length at 380 kV) and allows demonstrating respective advantage of HTS cable (free of this limit) together with other advantages as further explained in section 2.3. Moreover, use of existing OHLs allows keeping reliability of the connection uncompromised after integration of HTS cable.

2.3 Integration of a HTS power cable into the grid

High temperature superconductors (HTS) can play an important role in solving these and other grid problems. Possible advantages to integrate HTS components at extra high voltages (EHV) are: more power with less permissions, intrinsic fault current limiting capability, lower AC loss, better control of power flow, reduced footprint, less magnetic field emissions, etc. [15].

In the (E)HV grid, HTS cables are not yet accepted as proven technology. Moreover in these networks the availability of the connection is of the utmost importance. For the introduction of HTS cables into the power grid we advise a two-step approach for the time being. At first, we propose to integrate the cables in parallel with existing OHL's that have an equal or higher power capacity as that of the existing OHL's. Hence the availability of the network is secured. Later on, when the OHL's have to be replaced, HTS cables may be used. As a result of this approach the connection will consist of completely of HTS cables finally. In order to initiate integration of HTS cables somewhere, we select the most suitable location from those identified in section 2.2.

After judging all future grid bottlenecks in the TenneT scenarios, we have identified location Geertruidenberg - Krimpen (1.4b in Figure 2.1, left) as the most promising location, since it requires strengthening in three of the four TenneT scenarios. Moreover it has a relatively short length (easier for reactive power compensation) and is part of the main ring and hence is therefore loaded more heavily [16].

For this location the HTS cable specifications are derived and compared to conventional alternatives. Using the circuit parameters and the redundancy criteria the integration of HTS cables at the connection Geertruidenberg - Krimpen is elaborated for the estimated power demand in the year 2030.

2.3.1 Required transmission parameters

The possibility to strengthen the connection is elaborated with HTS transmission cables laid in parallel to (or instead of) the existing OHL and using the same rights

of way. The existing connection Krimpen - Geertruidenberg has two OHLs with a nominal power capacity of 1.65 GVA each and operates under the $n-1$ criterion. At present there are plans to upgrade each OHL to a power capacity of 2.75 GVA, which is preferred over constructing additional connections next to the existing line.

First, we assume in this study that sufficiently long HTS cables at 380 kV will be developed within the required time frame. Next, since the availability of electrical energy supply is of outmost importance, the cases are considered of the connection with $n-1$ and $n-2$ redundancy. The redundancy criterion n describes the required availability of the power capacity: $n-1$ defines the required power availability for a single failure, e.g.: switching one circuit off the grid in occurrence of a connection fault, and $n-2$ criterion defines the required power availability that allows a single failure event during maintenance. Next to this, the TSO is able to lead power via other directions through the meshed grid, providing additional system redundancy.

Transmission parameters comprising the system inductance, capacitance and resistance for OHL, XLPE and HTS cable connections are listed in Table 2.2. For HTS cable the parameters are calculated using [27, 28] and dimensions in Table 3.2. The presented circuit parameters for OHL and XLPE cable are provided by TenneT [29].

The connection ratings for the year 2030 are a total load current of 10 kA, corresponding to a power load of about 7 GVA. The OHL, XLPE and HTS cables are all assumed to carry a 5 kA load current during normal operation and 7.5 kA in emergency situations. XLPE cables require 2 cables per phase to deliver the required power capacity, while HTS cables provide the power capacity with a single cable. In the hybrid options all the parallel cables need to be all switched off the grid if one cable circuit fails. Otherwise the maximum circuit current in the cable will be exceeded.

For a connection with two cables per phase the cable capacitance will approximately double and the inductance will decline to about half in theory, as compared to a single cable per phase circuit, see Table 2.2.

The characteristic impedance for the OHL is about 5 times higher than that of the XLPE and HTS cable, which results in a much lower surge impedance loading (SIL, also known as the natural loading [30]).

Due to the low impedance of cables as compared to OHL, in case of the parallel connection to OHL, most of the power will be transmitted via the cable. Operating near SIL requires the least reactive power. Hence, the HTS cable parameters (e.g., core diameter, winding twist pitch, insulation thickness) in this study are optimized in such a way that the nominal power loading is close to SIL. This yields a minimum of reactive power and subsequently of reactive power compensation.

Table 2.2 Three-phase transmission parameters at 380 kV of overhead line, of XLPE cables and of HTS cable suitable for the connection Krimpen - Geertruidenberg in year 2030.

Parameter	OHL [29]	XLPE [29]	XLPE double cable per phase [29]	Cold dielectric (CD) HTS [this work]
Resistance, mΩ/km	13.6	10.9**	6**	0.05
Inductance, mH/km	0.8	0.47	0.29	0.224
Capacitance, nF/km	14.5	202	426	116*
Current at $n-1$, kA	5*	2.5	5	7.5
Rated current, kA	5*	2.5	5	5
Characteristic impedance Z_0 , $\Omega, \sqrt{L/C}$	235	48	27	43
Rated power, MVA	3290	1645♦	3290	3290
Surge load impedance SIL , MW, U^2/Z_0	681	2994	5348	3379
Ratio of rated power and SIL	5	1.8	0.6	0.97
Charging current I_{ch} , A/km	1	16	30	8
Critical length for I_{ch}^\heartsuit , km	5002	180	170	622

* After wire upgrade

** Phase resistance at 90 °C

♦ Double rated current is possible for at least 30 days [26]

♥ Represents the maximum current for unloaded cable of which the maximum allowed current is reached at the sending end

* Calculated assuming Tyvek-PE electrical insulation

The maximum current (7.5 kA/cable) is defined by the load current (15 kA after 40 years of operation). Due to the cable capacitance a reactive power produced by the cable is proportional to the cable length. A critical length for a cable can be defined for the case when the rated power of the cable is equal to the produced reactive power [31]. At the critical length no transfer of active power is possible and compensation of reactive power is needed. The capacitive current is inherent with the amount of dielectric used, hence the longest length is obtained for OHL's. In turn, HTS cable is able to reach sufficiently longer lengths than XLPE cable with no compensation, since it has about 70 % lower capacitance, see Table 2.2.

Due to the public opposition, it is expected that in the near future parts of EHV ring will go underground, a recent Dutch project “Randstad” is a good example [32]. Higher voltage levels are an issue for conventional cables as more reactive power is generated, which requires more compensation. Possible options to compensate for reactive power production are; coils, capacitors and impedance matching. The impedance can be matched using e.g., flexible alternating current transmission systems (FACTS) [33]. In the next section we will analyse various network options with the emphasis on the integration of HTS cables.

2.3.2 Modeled network example

Using the derived transmission characteristics in Table 2.2 a network study of the connection was performed (for the case of business as usual at the power of 7 GVA expected in year 2030) and results of the study are listed in Table 2.3.

In Table 2.3 the following future options to strengthen the connection are compared:

- 1) Using OHL;
- 2, 3) Using HTS cables laid in parallel to existing OHL and using the same rights of way;
- 4) Using XLPE laid in parallel to existing OHL;
- 5) Using HTS cables laid instead of existing OHL and using less rights of way;
- 6) Using XLPE laid instead of existing OHL and using larger rights of way than that of HTS cables and smaller than that of OHL.

Under respectively $n-1$ and $n-2$ redundancy during maintenance criteria,

- Option 1) would require three and four OHL respectively;
- Option 2) would require two existing OHL (each upgraded to 5 kA) in parallel to two HTS cable circuits (each for 5 kA) and two existing OHL (each upgraded to 5 kA) in parallel to three HTS cables (each for 5 kA);
- Option 3) would require two existing OHL (each upgraded to 5 kA) in parallel to one HTS cable circuit in series with FACTS and two existing OHL (each upgraded to 5 kA) in parallel to two HTS cable circuits in series with a FACTS;
- Option 4) would require two OHL (each upgraded to 5 kA) in parallel to two XLPE circuits having a double cable per phase and two OHL (each upgraded to 5 kA) circuits in parallel to three XLPE circuits having a double cable per phase;
- Option 5) would require three HTS and four HTS circuits;
- Option 6) would require three XLPE circuits and four XLPE circuits, both with a double cable per phase.

The load flows are calculated using Vision Network Analysis program [35] for the abovementioned options and the results for year 2030 are presented in Table 2.3;

Table 2.3 Example of the grid study (7 GW business as usual) to strengthen the connection at Krimpen-Geertruidenberg with OHL (5 kA each), XLPE cables (2.5 kA each) and HTS cables (5 kA each) for year 2030.

Criteria	Length, km	Option	Nb. of Circuit x Type	Nb. of Core x In kA	P ₁	Q ₁	Q ₂	I ₂	ΔU	Loss*	Tot. Loss MW	Loss GWh per year	Tot. Loss GWh per year
					MW	MVA _r	MVA _r	kA	kV	MW			
n-1 33.7	1	3xOHL	9x5	6644	812	0	10.1	5.7	103	103	290	290	
	2	2xOHL	6x5	1436	-65	82	2.1		49	53	32	61	
		2xHTS	6x5	5366	-50	-82	8.1	0.05	4		29		
	3	2xOHL	6x5	3631	243	102	5.5		35	37	108	134	
		1xHTS*	3x5	3084	255	-282	4.7	-1.3	2		26		
	4	2xOHL	6x5	1799	81	-30	2.7		52		52	112	
2xXLPE		12x2.5	4962	219	30	7.5	1.7	7	59	61			
5	3xHTS	9x5	6811	-295	0	10.3	-0.3	11	11	44	44		
6	3xXLPE	18x2.5	6763	305	0	10.3	1.6	32	32	90	90		
n-2 33.7	1	4xOHL	12x5	6710	578	0	10.2	3.6	124	124	243	243	
	2	2xOHL	6x5	1030	-82	69	1.6		48	53	20	62	
		3xHTS	9x5	5784	-293	-69	8.9	-0.2	5		42		
	3	2xOHL	6x5	1474	1474	-779	2.5		50	55	39	50	
		2xHTS*	6x5	5038	5617	-2703	9.2	-7.9	5		11		
	4	2xOHL	6x5	1319	35	-28	2.0		49		32	85	
3xXLPE		18x2.5	5457	163	28	8.3	1.2	6	55	53			
5	4xHTS	12x5	6818	-535	0	10.3	-0.4	14	14	57	57		
6	4xXLPE	24x2.5	6776	218	0	10.3	1.1	39	39	75	75		

- Calculated for $\cos \varphi = 1$ of the load

- Load flow calculated using pi-network equivalent [34]

* FACTS in series enabling 95 % operation of rated power

♦ The AC loss is calculated assuming PPLP insulation

from left to right column are: transmitted power flow P_1 , reactive power Q_1 and Q_2 , for respectively the source and the load sites, receiving current I_2 , voltage drop ΔU , electric loss power per type of circuit in $MW/year$, and total loss per circuit in $GWh/year$. The last four columns (presenting the losses) are calculated assuming a load growth of 2 % per year and a 40-year long lifetime according to [32]. The assumed power load in year 2030 and at the end of the lifetime is 7 GVA (10 kA transport current) and 10 GW (15 kA), respectively. Under n-1 criterion the circuit could be loaded with double current for 60 hours. Therefore, e.g. three OHL's are needed for option 1 to allow a power capacity of 10 GW at the end of the lifetime.

Loss calculations presented in Table 2.3 for the studied cold dielectric HTS cable are made under the following assumptions:

The dielectric loss is 3 kW/km for three parallel cables, see section 3.2.5. Cryostat heat invasion loss is assumed at 1.5 kW/km/3 phases, see section 3.2.6. The loss is 0.4 kW/kA for 3 termination sets at both cable ends, see section 3.2.7, leading to a total loss of 3 kW for two three-phase terminations sets. The cable has a total

critical current of 19 kA and the AC conductor loss is deducted using the AC loss measurement results presented in Chapter 5.

For the transport currents of 5, 4.7, 4.6, 4.1, 3.5, 2.9 and 2.6 kA_{rms} the cable AC losses are respectively: 0.2, 0.16, 0.15, 0.10, 0.06, 0.04 and 0.03 kW/km/phase. Efficient cooling systems have a penalty factor of 10, this value is used to calculate the cable loss at room temperature, see for further information section 3.2.9.

Total circuit losses per year are calculated assuming fifty weeks of operation at full load (8424 hours) and subsequently two weeks of operation under $n-1$ and $n-2$ condition (336 hours). For simplicity, under $n-1$ or $n-2$ criteria the circuit losses for the hybrid options are calculated using the worst-case loss scenario, when one or two cable circuits fail under respectively $n-1$ and $n-2$. In this case more power runs through the OHL's, which leads to the highest transport losses.

For the future power scenario “business as usual” at respectively $n-1$ and $n-2$ redundancy, respectively three and four OHL's are needed, see Table 2.3, options 1. In the case when the HTS cables are used, under the $n-1$ redundancy two OHLs can be used in parallel to two HTS cables (option 2), or to one HTS circuit with FACTS (option 3) or instead three HTS cables can be used when the OHLs are not allowed (option 5). For instance for option 2 in case when one HTS cable fails, both HTS cables will be switched off as otherwise excessive current will flow in the remaining HTS cable circuit. For option 3 the FACTS takes care of a balanced power flow when e.g., one OHL fails. Replacement of two 5 kA HTS cables with one 10 kA HTS cable is not excluded, but will only be possible when corresponding circuit breakers are available. Respectively, under the $n-2$ criterion, two OHLs are needed in parallel to three HTS cables, two HTS circuits with FACTS or four HTS cables can be used when OHLs are not an option. Obviously, when three OHLs of 5 kA will operate (option 1), they will have about 2 times more spatial magnetic field pollution as compared to the currently existing two OHLs. On the other hand, when two OHLs operate in parallel with two HTS cables, the spatial magnetic field pollution will be even less than in the currently existing situation (as only 1/4 of the total power is transmitted by the two OHLs in this case), see option 2 in Table 2.3. Therefore an important conclusion of the study is that HTS cables laid in parallel to OHLs allow reducing of magnetic pollution from existing OHL [21].

Two HTS cables operated in parallel to the existing two OHLs (option 2) transmit most of the power (due to the low impedance) and at lower loss (reduced from 290 GWh to 61 GWh with corresponding annual savings of about 14.6 M€). The magnetic field emission in this case is reduced 3 times (as compared to option 1, Table 2.3). The voltage drop over this connection is negligible as compared to the case of three OHLs (5.7 kV, option 1). In case when a HTS cable uses Tyvek-PE as

electrical insulation, the total loss would be even lower, namely 48 GWh, see more in section 3.2.8, cable design 2.

Due to the public opposition and increasing value of land, it is likely that with time in the Netherlands transmission OHLs will be replaced by underground cables in many cases [36]. Use of OHLs close to residential areas is restricted. Moreover, cities are expanding, which forces the connections to go underground. In order to address this long term trend, option 5 with three HTS cables is introduced, having the total loss of 44 GWh, which is 40 % less than for option 2 (61 GWh). In case of cable design 2, the total loss would be 23 GWh.

When instead of HTS cables XLPE cables are used, similar results are obtained (Table 2.3, options 4 and 6), however on a longer term XLPE cables are more expensive than HTS cables, see Table 2.6; they require much more ROW, see section 3.2.1; their typical connection length is limited to about 25 km [37]; and heating from the cable core ages the electric insulation and influences the environment.

In case of $n-2$ redundancy, the use of four OHLs will lead to a total loss of 243 GWh, option 1. When instead three HTS cables are in parallel to two existing OHL (option 2), the total loss is reduced to 62 GWh (or to 42 GWh in case of HTS cable design 2). The magnetic field emission in this case is reduced almost three times (as compared to option 1). The voltage drop over this connection is negligible for option 2 as compared to option 1 (3.6 kV). The advantages of option 2 (as compared to option 1) are: no additional OHL towers needed, no additional permits, no additional occupation of land, reduced AC-loss, and less need for reactive power compensation. For a more distant future we include option 5 when existing OHL are fully replaced by four HTS cables (this allows TenneT to build OHL of the same length elsewhere and to use the land for other purposes).

2.3.3 Transmission characteristics

As cable electrical insulation is subjected to an alternating electric field, it acts as a capacitor. Accordingly, a charging AC current runs in the dielectric. The charging current causes resistive and capacitive current losses. The loss factor is deduced from the loss angle, which is the angle between the capacitive current vector and the charging current vector. The loss angle is small since the resistive loss is much smaller than the capacitive loss.

Thus, the capacitive charging current indicates energy stored in the cable capacitance and is limited by a thermal rated current in a conventional cable.

Similarly, in HTS AC cables the “thermal rated current” is a current limit set by the conductor AC losses. Moreover, the reactive power depends on the length whereby a maximum line length can be defined. By definition, at the maximum length no active power is transferred anymore.

The XLPE cable insulation heats up mainly by the electrical losses developed in the conventional core, insulation and sheath limiting the power capacity. The heat removal from the cable depends on e.g., soil properties, cable laying conditions, nearby heat sources. The loss produced in the HTS cable core is substantially lower than in a XLPE cable core and furthermore it is produced at much lower temperature, see Table 3.7. Hence, the XLPE cable design is specified as such that the maximum operational insulation temperature will not be exceeded typically 105 °C (for higher temperatures the crosslinking will be lost). The conventional core loss can be reduced by selecting a larger core cross-section or by adding parallel cables.

The transferrable power for an OHL or a cable (XLPE and HTS) for a radial network can be expressed as follows [38]:

$$P_L = \sqrt{S_g^2 - (\omega C \cdot l \cdot U^2 \cdot 10^{-6})^2} \quad \text{Eq. 2.1}$$

where P_L is the transferrable power, S_g is the apparent power, ω is the angular frequency, C is the capacitance per length, U is the system voltage and l is the length of the connection. For the transmission parameters listed in Table 2.2 the transferrable power as function of the circuit length calculated using Equation 2.1 and the rated power is shown in Figure 2.3: for the OHL by the black solid line, for the XLPE single cable by the red solid line, for the XLPE double cable per phase by the red dashed line and for the HTS cable by the blue line.

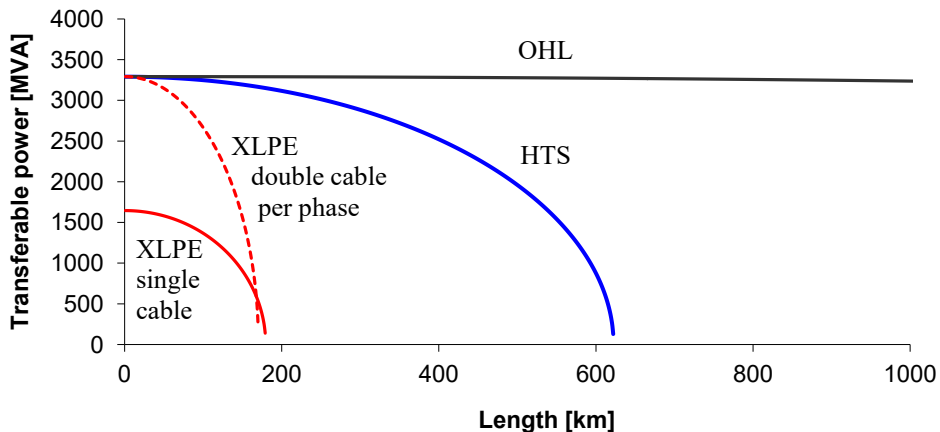


Figure 2.3 Transmittable power as function of the length at 380 kV during no-load and for a radial network for OHL (the black line), for HTS and XLPE one phase and two cables per phase (the red line and the red dashed line).

The theoretical circuit critical length l_1 (at which transmitted active power becomes zero), is 5000 km for OHL, 180 km for XLPE single cable per phase, 170 km for XLPE double cables per phase and 622 km for HTS cable.

When the cable is connected to the grid at one side, the cable capacitance will give rise to the voltage at the cable open end (Ferranti effect) [30]. Without any action, at the critical length l_2 , the open voltage rise is within 10% of the rated voltage [30, 39, 40]. For HTS and XLPE cables as listed in Table 2.2, l_2 is respectively 270 km and 33 km (calculated as in [30] with the voltage rise approximated by assuming a loss-less line and no compensation used). Thus, the cables are limited in their length by the open-end voltage rather than by the charging current if no actions are taken. While for XLPE cable the derived length limit of 33 km is close to 25 km length limit that is generally accepted and is a restriction for applications [37], for HTS cable the length limit of 270 km (in a country like the Netherlands) is well beyond the application demand. The calculated respective open-end voltage and current profiles for OHL, XLPE and HTS cables are shown in Figures 2.4 and 2.5 below.

Important practical conclusion is that for HTS cable the critical l_2 (270 km) is sufficiently large to make any connection in a country like the Netherlands, in contrast to that of XLPE cable.

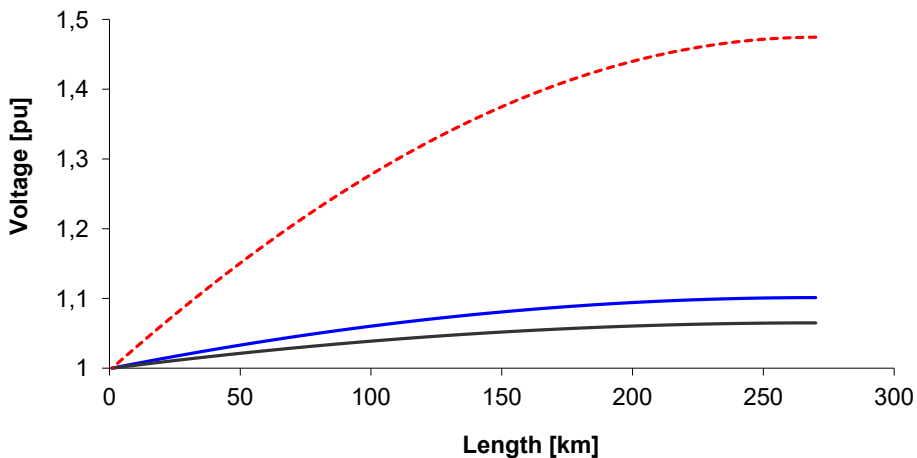


Figure 2.4 No-load voltage rise profile (during receiving end open circuited) for OHL (black line), XLPE (the red dashed line) and HTS (blue line).

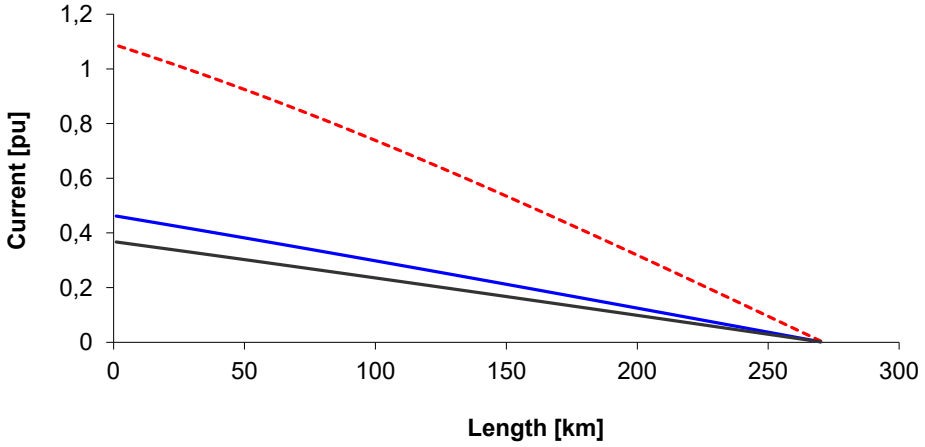


Figure 2.5 No-load voltage rise profile (top) and current profile (bottom) during receiving end open circuited for OHL (black line), XLPE (the red dashed line) and HTS (blue line).

The reactive power transfer through the connection can be written in terms of the connection line length l , angular frequency ω , inductance per length L , capacitance per length C , transferrable power P and the natural power P_n [38]:

$$Q = \omega \cdot l \cdot \sqrt{L \cdot C} \cdot (P^2 - P_n^2) / P_n \quad \text{Eq. 2.2}$$

Using Equation 2.2 and the parameters in Table 2.2, the reactive power production is calculated for a 33.7 km long OHL, XLPE and HTS connection.

The results are shown in Figure 2.6 for OHL, XLPE single cable phase, XLPE double cable per phase (dashed line) and HTS connection. It is clear that for the same transmitted power, the HTS cable produces the least amount of reactive power as compared to OHL and XLPE cables over the most of the range of transmitted power (except for 0 to 1.6 GVA, where OHL performs better).

Moreover, at no-load the reactive power for HTS is just 160 MVAR, and is the lowest for the compared cables. Matching of the SIL to the rated (or any other preferred value of) power for HTS cable can be achieved more easily as compared to conventional cables because in a conventional cable most of the core cross-section is occupied by the conductor, while for the HTS cable the conductor cross-section is a very small fraction of the core cross-section, see Chapter 3. This feature makes operating close to SIL more feasible for HTS cables. When the active power is smaller than SIL there is an excess of inductive power that is absorbed by both system ends.

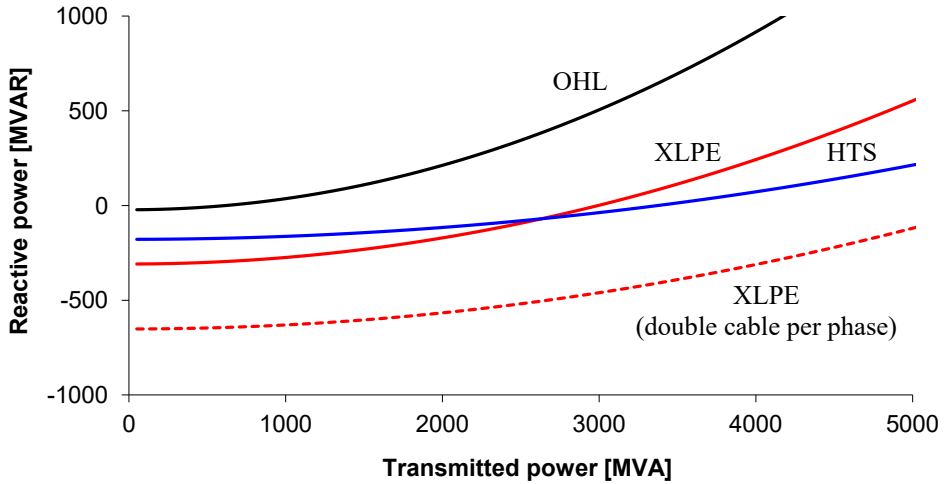


Figure 2.6 Reactive power as function of the transmittable power. The zero reactive power crossing indicates the SIL, for OHL (the black line), XLPE one phase and two cables per phase (red line and red dashed line) and HTS cables (blue line).

On the other hand when the active power is larger than SIL, the connection consumes reactive power supplied from both system ends. The reactive power flow is illustrated by a vector diagram in Figure 2.7. In Figure 2.7, the power triangles are shown for an inductive (I lags U , $Q_{\text{inductive}}$) and capacitive (I leads U , $Q_{\text{capacitive}}$) loading, which represents the power loading of an OHL and a cable, respectively. A cable generates reactive power and a line absorbs reactive power (Figure 2.6). Obviously, the apparent power S cannot be adjusted and therefore any increase in reactive power (Q capacitive or inductive) will decrease the transferrable active power P .

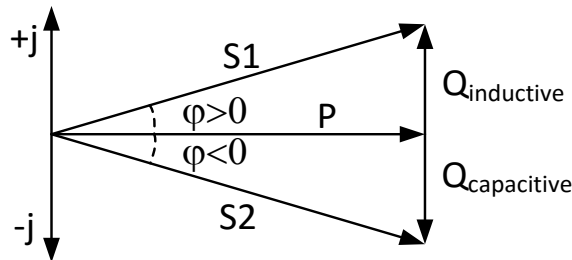


Figure 2.7 Power triangles for inductive and capacitive load.

The consumption of reactive power will create a distributed voltage over the connection between the buses at both ends. The maximum voltage of the cable connection at no-load is found in the middle [30]. The derived maximum voltage at no-load for a connection with two OHL in parallel to two HTS is 0.19 kV (below 1.05 of nominal value). Such a maximum voltage increase is no issue in the electrical cable insulation design.

As mentioned above, to improve the critical length of conventional cables, shunt compensation is frequently used [40]. It also minimizes the impact of voltage transients.

In general, the critical length of a connection depends on the capacitive reactive power and may be different for each network. It has to be evaluated individually, taking into account the capability of the grid to sustain such a reactive power load [31]. Before a new network component will be introduced to the grid, load flows need to be calculated to verify if the grid change affects the network operation [16], as recommended in section 7.3.

In the next section the voltage stability at the connection Krimpen - Geertruidenberg is examined using a network model.

2.3.4 In-grid case study

Network voltages during steady state operation for Krimpen (KIJ) and Geertruidenberg (GTB) are calculated to examine if the bus voltages are within acceptable limits excluding unstable network operation. In this way we analyse the network ability to transfer power through the network accounting for the voltage drop due to reactive power transfer and the reactive power losses (I^2X) mainly due to active power delivery, which is one of the three aspects of voltage stability. The other two aspects are load restoration dynamics (operation of dynamic network components such as motors, tap changers) and voltage control at generators in the network which are outside the scope of our study. The network options listed in Table 2.3 are used in this study.

As mentioned before, when cables are introduced to the grid, the reactive power production in the network increases, which affects the system voltage. A 5% voltage variation in the network is accepted by TSO's.

The Dutch electrical grid is roughly represented by the network as shown in Figure 2.8. Verification of the system bus voltages at Krimpen - Geertruidenberg provides an indication if the network voltages are within the limits (5 % voltage variation) or that additional compensation is required. The network model is implemented in the Network program Matpower® [41] which enables to study the network voltages by load flow calculation. In Figure 2.8, both generators, Thévenin equivalents 1, 2 ($Z_{th} = jX_{th} + R_{th}$) and buses 1, 4 represent the total Dutch electrical grid in a simplified way, buses 2 and 3 show voltages V_1 and V_2 at substations Krimpen and Geertruidenberg, respectively.

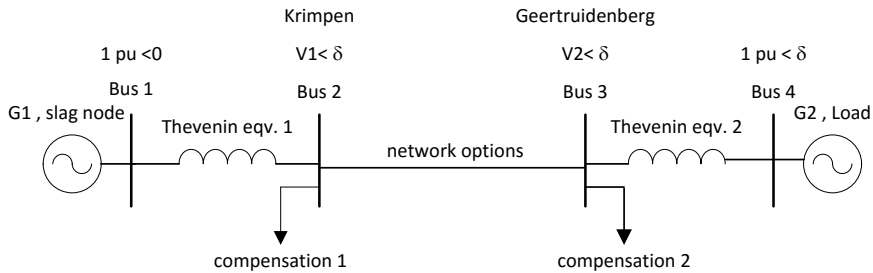


Figure 2.8 Simplified representation for the EHV network where possible network options are connected between bus 2 and 3 as listed in Table 2.3.

The connection between Krimpen and Geertruidenberg are indicated by “network options” from Table 2.3. The Thévenin equivalents are derived by short circuit calculations at both substations and are provided by TenneT [29].

The two generators G1, G2 (at bus 1 and bus 4 respectively) represent the Thévenin voltage which is 1 pu with a voltage angle (δ) (base voltage is 380 kV, which is equal to 1 pu). Generator 1 acts as a slag node, providing the power demand to bus 4, having a voltage angle of 0 degrees. The power demand for the connection is set by generator 2. If the voltages on bus 2 and 3 are larger than $\pm 5\%$, shunt (reactive) and series (capacitive) compensation can be applied as indicated with compensation 1 and 2. At this moment at station Krimpen are available: two capacitor banks with a total capacity of 267 MVA and three reactors with a total capacity of 245 MVAR connected to the tertiary transformer winding (50 kV), for substation Geertruidenberg: two reactors are connected, comprising 75 MVA each. The listed compensations are discounted in the Thévenin equivalents.

The following network options with a load at generator 2 for option 1: 0 GVA and 1.6 GVA and for option 2 to 5: 0 GVA and 6.6 GVA are studied:

- 1) Two OHL and 1645 MVA transport capacity for each circuit (benchmark case);
- 2) Three OHL circuits and 3290 MVA transport capacity for each circuit;
- 3) Two OHL in parallel to two HTS circuits and 3290 MVA transport capacity for each circuit;
- 4) Two OHL in parallel to two XLPE (double cable per phase) and 3290 MVA transport capacity for each circuit;
- 5) Three HTS circuits and 3290 MVA transport capacity for each circuit;
- 6) Three XLPE (double cable per phase) and 3290 MVA transport capacity for each circuit.

Network option 3 is not included since the required reactive power in this case is assumed to be adjusted by the FACTS.

Table 2.4 Results for simulated bus voltages for network options to strengthen connection Krimpen - Geertruidenberg.

Option	Nb. of Circuit x Type	In <i>kA</i>	Load at Generator <i>2</i> <i>MVA</i>	from bus 1 total injection		to bus 2 total injection		bus 1		bus 2		bus 3		bus 4	
				<i>P,</i> <i>MW</i>	<i>Q,</i> <i>MVA_r</i>	<i>P,</i> <i>MW</i>	<i>Q,</i> <i>MVA_r</i>	<i>U1,</i> <i>V</i>	<i>δ1,</i> <i>deg</i>	<i>U2,</i> <i>V</i>	<i>δ2,</i> <i>deg</i>	<i>U3,</i> <i>V</i>	<i>δ3,</i> <i>deg</i>	<i>U4,</i> <i>V</i>	<i>δ4,</i> <i>deg</i>
*															
0	2xOHL	2x2.5	0	0	-21	0	-24	1	0	1,001	-0,004	1,001	-0,004	1	-0,001
			1645	1656	-77	-1651	-115	1	0	0,994	-5,5	0,995	-8,3	1	-13
1	3xOHL	3x5	0	0	-33	0	-34	1	0	1,001	-0,007	1,001	-0,007	1	0,003
			2x3290	6922	-202	-6864	1214	1	0	0,935	-18	0,942	-27	1	-44
2	2xOHL// 2xHTS	2x5//2x5	0	0,22	-201	-0,22	-208	1	0	1,008	-0,041	1,008	-0,04	1	0,02
			2x3290	6846	-758	-6842	245	1	0	0,963	-17	0,967	-20	1	-36
4	2xOHL// 2xXLPE	2x5//2x5	0	2,56	-701	-2,56	-722	1	0	1,028	-0,144	1,028	-0,15	1	0,06
			2x3290	6854	-1214	-6830	-138	1	0	0,983	-17	0,986	-20	1	-36
5	3xHTS	3x5	0	0,39	-267	-0,39	-279	1	0	1,011	-0,05	1,011	-0,05	1	0,03
			2x3290	6840	-869	-6839	610	1	0	0,967	-17	0,971	-19	1	-36
6	3xXLPE	3x5	0	5,55	-1042	-5,55	-1075	1	0	1,041	-0,2	1,041	-0,22	1	0,08
			2x3290	6844	-1734	-6818	-222	1	0	0,998	-17	1	-19	1	-35

* Calculated with existing short circuit power

The short circuit powers in year 2010 and 2020 at Krimpen and Geertruidenberg are provided by TenneT: 18 GVA and 21 GVA) and 24 GVA and 22 GVA, respectively.

Short circuit currents for year 2030 are not available and are deduced using the short circuit powers of year 2010 and 2020, as follows.

The future fault current is assumed to decline, since there are expected to be more converters integrated in the 2030 grid (e.g. increasing HVDC interconnections and the aim for an off-shore grid connecting wind energy [42]). Accordingly, a 50 % lower short circuit power increase between 2020 and 2030 is assumed, compared to the short circuit power increase between 2010 and 2020. In Table 2.4 two extreme load cases are simulated for each network option to emphasize the strongest voltage variation, namely for no load and for maximum load.

Findings from this study confirm that additional compensation is needed for option 1 under maximum load¹.

Using the network model, the circuit critical length l_3 for network options 3 to 6 is estimated for no-load and maximum load and the results are listed in Table 2.5.

Using the model enables the possibility to estimate the maximum connection length allowing a voltage variation of 5% on bus 2 and 3.

Table 2.5 Calculated maximum connection length for the network options based on a maximum 5% bus voltage variation, where no load and maximum load is applied.

	Network option									
	3xOHL		2xOHL// 2xHTS		2xOHL// 2xXLPE		3xHTS		3xXLPE	
Load, MVA	0	2x3290*	0	2x3290	0	2x3290	0	2x3290	0	2x3290
Critical l_3 , km	1150	34	195	500	59	118	149	340	40	74

* Requires a minimum of 275 MVA additional compensation at bus 2 and bus 3

¹ As expected the bus voltages at bus 1 (KIJ) (0 MVA: 1.001 pu, 1645MVA: 0.994 pu) and bus 2 (GTB) (0 MVA: 1.001 pu, 1645MVA: 0.995 pu) for option 0 are within the voltage boundaries in both load cases. For option 1, the voltage is within the 5% boundary for 0 MVA at KIJ (1.001 pu) and GTB (1.001 pu), however in case of the maximum load (6580 MVA) the bus voltages exceeded the acceptable voltage limit; at KIJ, 0.935 pu and at GTB, 0.942. For option 2, the bus voltages are within the limits; KIJ) 0 MVA: 1.008 pu, 6580 MVA: 0.963 pu, GTB) 0 MVA: 1.008 pu, 6580MVA: 0.967 pu. Also for option 4) the bus voltage are with the acceptable limit; KIJ) 0 MVA: 1.028 pu, 6580MVA: 0.983 pu, and GTB) 0 MVA: 1.028 pu, 6580MVA: 0.986 pu. And the voltage is within the limit for option 5; KIJ) 0 MVA: 1.011 pu, 6580MVA: 0.967 pu, GTB) 0 MVA: 1.011 pu, 6580MVA: 0.971 pu. For option 6, consisting of 3 XLPE circuits shows no limitation on the bus voltages: KIJ) 0 MVA: 1.041 pu, 6580MVA: 0.998 pu, GTB) 0 MVA: 1.041 pu, 6580MVA: 1 pu.

Alternatively, additional connections can be established enabling closer operation at SIL. Hybrid connections improve the critical length, especially by using a hybrid HTS connection. The critical lengths for hybrid HTS and XLPE connections are 500 km and 118 km, respectively. If the connection comprises only cables, the XLPE connection is more limited in length than the HTS connection, see Table 2.5. The XLPE connection is limited to 40 km, whereas the HTS connection is limited to 340 km.

This study shows that HTS cables are suitable for longer lengths with regards to the corresponding bus voltages and in particular for the connection Krimpen-Geertruidenberg they allow to save on additional compensation otherwise required for connection made of OHL or XLPE cables, Table 2.5 (the effect of tap changers are not included in the model).

HTS cable is one of the five technologies that could improve the transmission grid [33]. When HTS cables will become a tool for changing the grid depends on (among other factors) if they are economically attractive as compared to the alternatives. When the technology could be economically sound, remaining issues to be resolved are e.g.: life expectancy, reliability, maintenance. These issues can be properly addressed, for instance by a pilot project to be operated in the grid.

The following study uses the connection Krimpen - Geertruidenberg as an example and provides answers to the question: at which HTS tape price levels HTS underground cables are economically competitive with XLPE cables and overhead lines?

The costs below are estimated assuming a lifetime of 40 years. In Table 2.6 the investment and lifetime costs are compared for the network options of Table 2.3.

For simplicity, only the redundancy criterion $n-1$ is presented here. From left to right Table 2.6 lists: the option number (see Table 2.3 for detail), the HTS tape cost performance ratio in €/kA·m, the number and type of the circuits comprising the connection, their nominal currents in kA, the costs of the circuit (CC, in M€/km) consisting of three phases, the investment costs (IVC, in M€) per circuit component, the lifetime generation capital costs (LGCC, in M€, representing the capital costs for the installation of new generation plant(s) that provide additional electrical energy to compensate the maximum AC losses developed in the grid), the total investment costs (TIVC, in M€), the maintenance costs (MNC, in M€), the lifetime costs of energy loss (LELC, in M€, representing the costs related to the additional generation of energy to compensate transport losses), the dismantling costs (DMC, in M€), and the total lifetime costs (TLTC in M€) [43].

The estimated investment costs for upgrading the existing OHLs (from 2.5 kA to 5 kA capacity each) are 101 M€, assuming the cost of the existing OHL follow [44] and 20 % additional costs for increase in the right of way, as indicated for options 1 to 4 in Table 2.6. Investment costs of HTS cable depend largely on the price of YBCO tapes.

Table 2.6 Comparison of connection costs for OHL, HTS and XLPE cables of Krimpen - Geertruidenberg.

Option	CPR, €/kA·m	Circuits: number & type	I_{nom} , kA	CC, M€/km	IVC, M€	LGCC, M€	TIVC, M€	MNC, M€	LELC, M€	DMC, M€	TLTC, M€
1		2xOHL [♥]	2 x 5	3	101	418	658	3	695	51	1462
		1xOHL	1 x 5	4	140						
2a	129	2xOHL [♥]	2 x 5	3	101	221	1173	3	147	51	1435
		2xHTS	2 x 5	25	855						
2b	25	2xOHL [♥]	2 x 5	3	101	221	596	3	147	51	850
		2xHTS	2 x 5	4	278						
3	25	2xOHL [♥]	2 x 5	3	101	152	432	3	321	51	837
		1xHTS*	1 x 5	5	179						
4		2xOHL [♥]	2 x 5	3	101	239	1178	3	270	51	1794
		2xXLPE	2 x 5	25	838						
5a	136.5	3xHTS	3 x 5	39	1328	57	1385	28	105	62	1580
5b	25	3xHTS	3 x 5	12	413	57	469	28	105	62	665
6		3xXLPE	3 x 5	37	1257	130	1386	28	216	409	2039

[♥] Two existing OHL upgraded from 2.5 kA to 5 kA transport current each

* With FACTS in series (36 M€ accounted in redundant case)

Table nomenclature:

CPR – cost performance ratio, €/kA·m

I_{nom} – nominal current, kA

CC – total circuit costs, M€/km

IVC – investment costs, M€/km

TIVC – total investment costs, M€

LGCC – lifetime generation capital costs, M€

LELC – lifetime energy loss costs, M€ (discounted at 6% over the lifetime)

DMC – dismantling costs, M€

MNC – maintenance costs, M€

TLTC – total life time costs, M€.

The indicative price performance ratio of a good quality YBCO tape today is 350 €/kA·m and total annual production is about 1000 km/year [4]. Larger tape orders can increase the annual production and reduce the tape price. For example, the costs of a standard YBCO tape can be reduced to below 10 €/kA·m assuming that one new factory is opened producing and selling 5000 km/year of such tapes [4]. Recently such prices were indeed demonstrated in a business case model [46] see Chapter 3 for more details. A single HTS circuit for the connection Krimpen - Geertruidenberg will require 16000 km of such HTS tapes (for details see section

3.2.4). Therefore, the assumed HTS tape price of 25 €/kA·m (Table 2.6) is realistic, e.g., when a decision is taken to integrate a reasonable amount of HTS transmission cables into the grid (i.e. 20 km/year) such HTS tape price can be expected within 5-10 years [4].

Other assumptions for the HTS cable component costs are: 10% for other (than HTS tape) conductor components, 10% for conductor contingency in fabrication and 5% for fabrication, added on top of the total HTS tape costs; vacuum system according to [48]; single cryostat according to [11]; electrical cable insulation and three-phase terminations (at both sides), which for one circuit are: 52, 350, 25 and 180 €/m, respectively. For the metallic shield 30 % of the total HTS conductor costs are added [47].

To provide sufficient redundancy for the HTS cable refrigeration, two times the required costs for refrigeration systems are added, resulting in a total investment cost of 0.4 M€/km [13]. The HTS circuit laying costs are assumed 0.63 M€/km, which is 80% lower than that of XLPE cable (3.8 M€/km [32]) since only three cables are laid instead of six, the HTS cable has substantially lower mass and lighter machinery can be used (see Table 3.8). Moreover, the laying formation is much more compact (section 3.1) resulting in less ROW and reduced laying time.

The total circuit costs for the copper 2500 mm² XLPE enamelled cables with a double cable per phase, including the accessories and tests, are 8.5 M€/km [33]. On top of that, the compensation costs for XLPE and HTS cables have to be included. The total compensation costs are calculated according to the cable capacitance as presented in Table 2.3. The compensation costs are 0.02 M€/MVAR [32].

The total life time cost are calculated assuming electricity selling price to industrial consumers of 60 €/MWh [11]. The lifetime generation capital costs (LGCC) are calculated using 102 €/kW which represents the capital cost for installing extra power generation equipment [43, 48], see Table 2.6.

Dismantling and maintenance costs are added to the life time costs and are 0.02 M€/km and 0.0012 M€/km respectively for OHL and respectively 0.1 M€/km/circuit and 0.01 M€/km/circuit for XLPE [32]. The HTS dismantling costs are estimated using the known costs of dismantling XLPE cables, which mainly consists of excavation works. The dismantling costs of HTS cables are assumed to be 0.02 M€/km/circuit, which are subsequently supported in Chapter 3. The maintenance costs for XLPE include yearly partial discharge measurements of joints and the cable sheath, which is assumed to be similar for HTS cables, namely 0.01 M€/km/circuit. For new OHL costs of ROW at 1.85 M€/km are included in the investment costs [44], for details see section 3.2.3.

It follows from Table 2.6 that the investment costs and total lifetime costs are in increasing order:

- The investment costs (IVC): 241, 280, 379, 413, 393, 956, 1257 and 1328 M€ for options: 1, 3, 2b, 5b, 4, 2a, 6 and 5a respectively;
- The total investment costs² (TIVC) are: 432, 469, 596, 658, 1173, 1178, 1385, and 1386 M€ for options: 3, 5b, 2b, 1, 2a, 4, 5a and 6 respectively;
- The total lifetime costs are: 665, 837, 850, 1435, 1462, 1580, 1794 and 2039 M€ for options: 5b, 3, 2b, 2a, 1, 5a, 4 and 6 respectively.

Accordingly, the lowest costs of the eight options are achieved in increased order:

- For TIVC: by options 3, 5b and 2b (all using HTS cables);
- For TLTC: by options 5b, 2b and 3 (all using HTS cables).

The following savings are obtained for three listed options above:

- Option 5b as compared to options 1, 2a, 2b, 3, 4, 5a saves on TIVC and TLTC respectively: 189 and 797, 704 and 770, 126 and 186, -38 and 172, 709 and 1129, 916 and 916 M€;
- Option 2b as compared to options 1, 2a saves on TIVC and TLTC respectively: 63 and 611, 577 and 584 M€;
- Option 3 as compared to options 1, 2a, 2b saves on TIVC and TLTC respectively: 227 and 625, 742 and 598, 164 and 14 M€;
- Options 1, 2a, 2b, 3 as compared to option 4 save on TIVC and TLTC respectively: 520 and 332, 5 and 359, 582 and 944, 746 and 957 M€;
- Options 1, 2a, 2b, 3, 4 as compared to option 5a save on TIVC and TLTC respectively: 727 and 118, 212 and 145, 789 and 730, 953 and 743, 207 and -214 M€;
- Options 1, 2a, 2b, 3, 4, 5a and 5b as compared to option 6 save on TIVC and TLTC respectively: 728 and 577, 213 and 604, 790 and 1188, 954 and 1202, 208 and 245, 1 and 459, 917 and 1374 M€.

It is therefore clear, that option 1 (OHL) with regards to TIVC is more expensive as compared to options 2b, 3 and 5b, all using HTS cables at the HTS tape price of 25 €/kA·m) and is cheaper than options 2a, 4, 5a and 6. With regards to TLTC option 1 is more expensive as compared to options 2a, 2b, 3, 5b and is cheaper than options 4, 5a and 6. Besides, option 1 has other disadvantages when compared to use of HTS cables as further explained in Figure 3.8.

Option 4 (XLPE cables) with regards to TIVC and TLTC is more expensive than options 1, 2a, 2b and 3; option 6 (XLPE cables) with regards to TIVC and TLTC is more expensive than options 1, 2a, 2b, 3; 4, 5a and 5b. Therefore, options 4 and 6 are the most expensive and besides they limit the connection length to 25 km (for

² The TIVC are the lifetime generation capital costs (LGCC) added to the investment costs (IVC).

1.63 and 3.25 GVA transport power for respectively single and double cable per phase) as explained above, see Figure 2.3. Besides, option 4 and 6 have other disadvantages when compared to use of HTS cables as further explained in Figure 3.8.

Moreover, at the HTS price-performance ratios of 193 and 129; 133 and 36 €/ (kA·m) option 2 has the same TLTC and the same TIVC as options 4 and 1 respectively. At the HTS price-performance of 356 and 283; 241 and 103 €/ (kA·m) option 3 has the same TLTC and the same TIVC as options 4 and 1 respectively. At the HTS price-performance of 192 and 137; 122 and 48 €/ (kA·m) option 5 has the same TLTC and the same TIVC as options 6 and 1 respectively. Therefore, when the HTS tape price-performance ratio is below 241 and 103 €/ (kA·m), option (3) using HTS cables competes economically with conventional options 4, 6 and 1 with regard to the total investment costs TIVC and to the total lifetime costs TLTC.

When the HTS tape price of 25 €/ (kA·m) is achieved, the HTS option is more economically sound than the conventional OHL and the XLPE option. This will lead to a substantial saving in total investment and total lifetime costs. An important conclusion from the former section is that option 3 results in the lowest costs, assuming a tape price of 25 €/ (kA·m). Accordingly, option 3 results in 227 and 625 M€ investment costs savings and 954 and 1202 M€ lifetime costs savings compared to option 1 and 6, respectively.

When option 3 instead of option 1 is used, the underground connection can be installed in the same right of way as the remaining OHL's. This results in a substantial reduction in magnetic field emissions. Not only because of the consistent width of the corridors, but also due to the fact that less current is transported through the existing OHLs.

The decline in magnetic field emission is an important feature for the TSO's, as residential areas are built closer to the OHLs. Furthermore, option 3 as compared to option 1, results in less spatial planning permits and lower operational losses. Notably, the hybrid connection enables the grid to be expanded with cables. Thus, resulting in an equally reliable network option. When a failure occurs in a cable, the redundant OHLs can retain the power transport capacity.

The required power transport capacity by year 2050 for K-G is 10 GW. As stated in Tables 2.3, 2.4, 2.6, in compliance with the power demand, one HTS cable circuit is sufficient to replace the remaining OHL's.

2.3.5 Discussion on case study

When in option 3 the OHLs are aged and replaced with new OHLs with the same transmission capacity and using the same ROW, an investment of 220 M€ is needed. If the aged OHLs in option 3 are replaced with two HTS cables instead (that is, option 3 turns into option 5b), an additional investment of 278 M€ is needed. Also, the additional investment of 58 M€ for option 2b is justified, since option 5b allows complete undergrounding of the connection and consequently enables undergrounding of the Dutch 380 kV transmission network.

With regard to the costs, it is more interesting to underground a connection at once, hence the connection changes directly into option 5b. From an economical point of view, the total investment costs for option 3 and 5 show to be cheaper than option 1, respectively 63 and 189 M€. Moreover, 611 and 797 M€ could be saved, respectively, on total lifetime costs in comparison to option 1. This shows that direct undergrounding of a connection that contains aged OHLs is profitable. Notably, additional savings are to be expected since excavating a trench for three sequentially cable circuits will be much faster than excavating cable trenches separately.

In comparison to a conventional connection consisting of only cables (option 6), option 5b is associated with i.e.: the lowest total investment costs, lifetime costs, AC losses, magnetic field pollution and right of way, as described in Chapter 3. Therefore, option 5b (as compared to option 6) is technically and economically superior to enable undergrounding of the Dutch 380 kV transmission network.

As mentioned before, upgrading existing OHLs with parallel HTS cables allows keeping the circuits availability. When the existing OHLs are aged and the HTS cables have shown their successful operation, the transition to a circuit with only HTS cables is an adequate option.

The total grid length is 2127 km (single circuit, 380 kV). When assuming that the transition would expand to the whole transmission grid, the total investment and total lifetime cost savings for the whole grid would be 5 and 13 B€, respectively.

When the HTS cable has proven its superior behavior in the grid using i.e. option 3, it could be decided that the aged OHLs are to be replaced by HTS cables. In our study, we assume that the project (option 2 or 3) will start a few years from now. When the transmission grid expands by year 2050, then beyond year 2050 the replacement of the remaining OHLs could be started. In this way, the grid transforms completely underground, as shown in option 5b.

2.3.6 Roadmap discussion

This study shows that HTS cables are able to effectively strengthen and to underground the future grid at the same or reduced costs and therefore deserve more attention. Accordingly, a roadmap for the Dutch transmission grid evolution is made using three scenarios, as will be explained below [48]:

Scenario 1 (long term vision of TenneT on the (E)HV grid, years 2010 – 2030): business as usual; the grid consists of mainly conventional OHL (95 % of transmission grid consist of OHL) and uses underground cables only where it is impossible to use OHL, the cables comprise a small fraction (<5 % of the transmission grid). The public issues of visual and magnetic pollutions remain; the estimated total transmission loss is 1.5 TWh/year and the consumption is 150 TWh/year. There may be a need to use 750 kV instead of 380 kV as foreseen by ENTSO-E.

Scenario 2 (vision of Supernet project, years 2025 - 2050): alternatively, the grid connections consist mainly of OHLs and expansion is made underground. We assume that the grid is strengthened with HTS cables in parallel, using the same right of way as the OHL (Figure 2.9). The public issues of visual and magnetic pollutions remain, but they are relieved by the facts that the grid expands underground with HTS cables and because HTS cables reduce magnetic pollution in existing OHL. The cost advantage of expanding the whole 380 kV grid using HTS cable instead of OHLs will lead to 5 and 13 B€ of savings, respectively for the investment and lifetime costs. The consumption can be as high as 200 TWh/year and the estimated grid losses are below 0.7 TWh/year. The transmission voltage level is kept at 380 kV (there is no need to go to 750 kV as it is foreseen by ENTSO-E [49]).

Scenario 3 (vision of Supernet project, beyond year 2050): HTS cables are assumed to be a dedicated technology as they, already, have been operating for 25 years in the grid. TSO's are familiar with their specification and operation in the network. Specifications such as maturity, availability, maintenance, repair time, high power switching material have been demonstrated in the field. Therefore, there are no expected problems for using HTS cables instead of OHLs. This results in a cheaper, more compact grid, without magnetic field and visual pollution. As discussed before, the 380 kV grid will be transformed in a grid consisting of HTS cables (Figure 2.10). We assume here for simplicity that the HTS cables follow the same routing as that of the OHLs. However, the advantage of a cable routing is that its routing can be selected on the need, e.g. in many cases the shortest direct length, or just one high capacity cable link enabling to keep the n redundancy criteria, etc. This advantage can be used in scenario 3 for optimising the transmission routes [50]. Defining new HTS cable routings is outside the scope of this study. The additional costs to completely underground the connections are estimated on 4 B€, including scrapping the remaining OHLs and installation of one additional HTS cable circuit. These costs are justified by the achieved savings in scenario 1 and 2. The consumption can be as high as 400 TWh/year, with an estimated grid loss below 0.4 TWh/year.

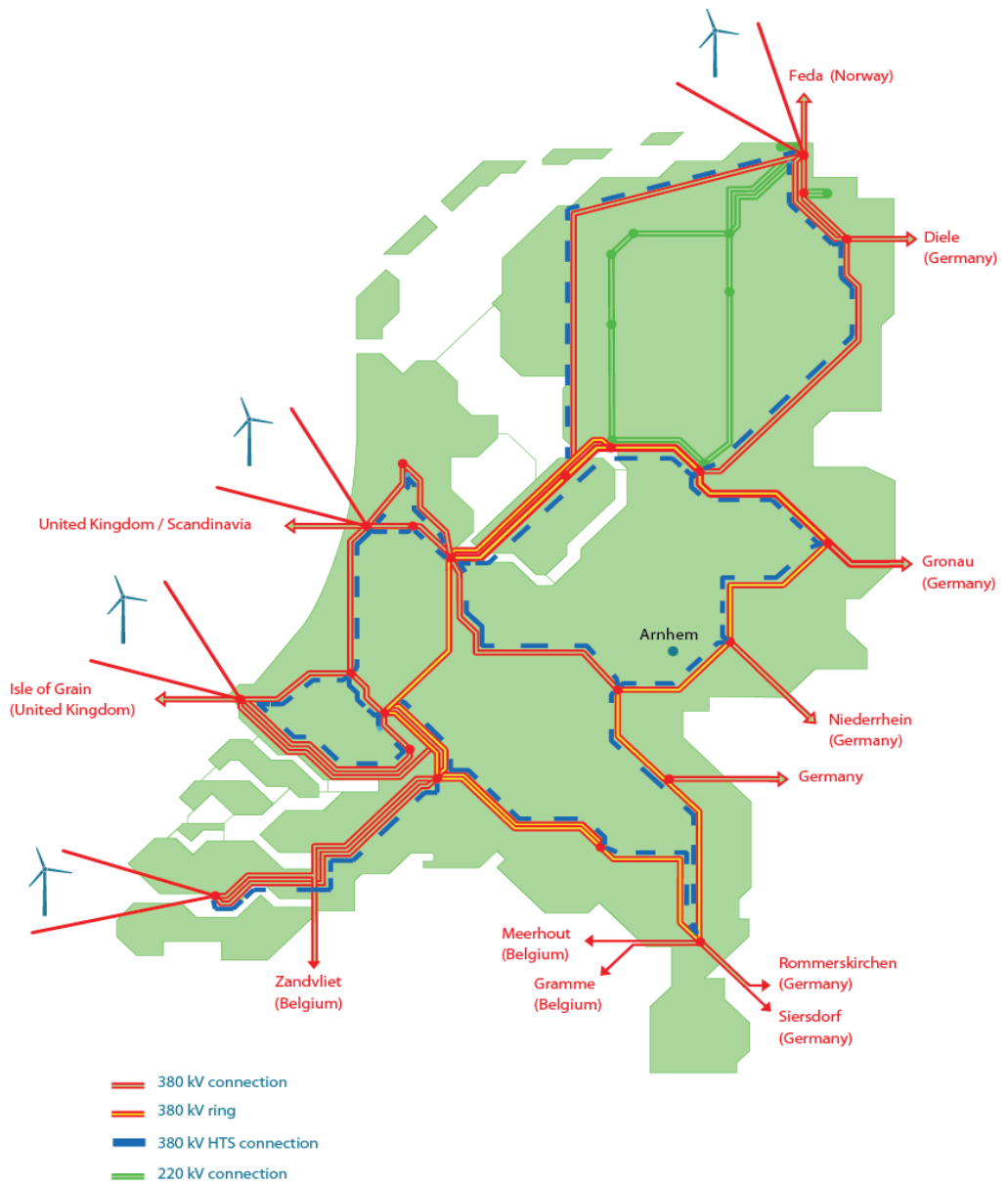


Figure 2.9, Foreseen evolution of the Dutch transmission network, with HTS cables installed in parallel to the existing grid (2020-2040) [16].

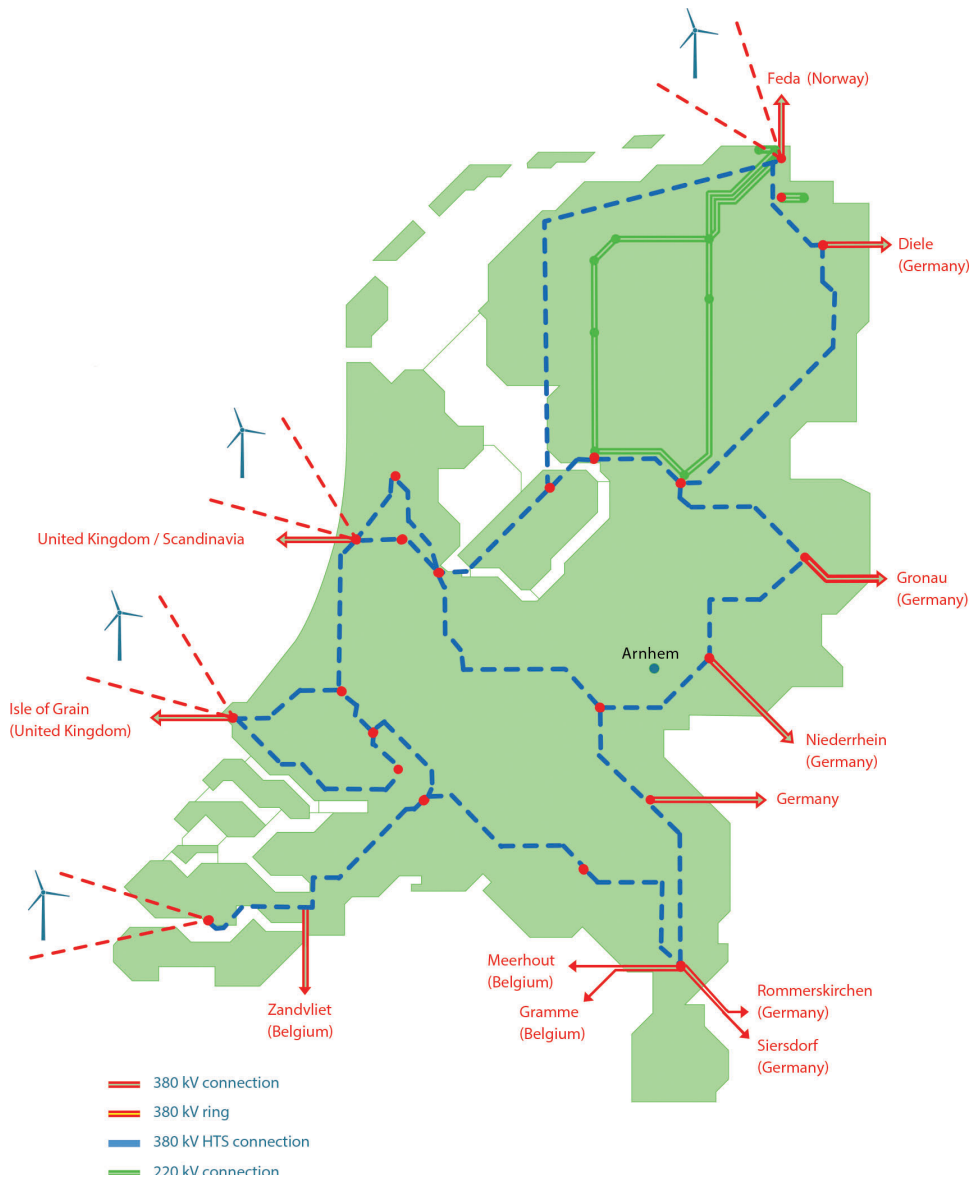


Figure 2.10 Foreseen evolution of the Dutch transmission network, with OHLs are completely replaced by underground HTS cables (double circuit [16]).

To give an example, when the whole 380 kV transmission grid (single circuit length was 2127 km in year 2012 [48]) is expanded by HTS cables instead of OHLs, this will lead to an average saving (extrapolated over 40 years lifetime and assuming option 3) for investment and lifetime costs of respectively 125 M€/year and 325 M€/year. To compare, earnings before interest and taxes (EBIT) of TenneT in year 2012 were 118 M€ [51]. Apart from investment, we must strive to overcome some concerns, as example: roll out the cooling infrastructure, social acceptance, repair times, tape price, etc.

2.4 Conclusions

In this Chapter, we identified the bottlenecks in the future Dutch 380 kV grid using energy scenarios of TenneT. Of these, connection Krimpen-Geertruidenberg is selected as the most promising for integration of HTS cable.

Using network study for this 7 GVA, 33.7 km long connection comprised of OHLs, or XLPE or HTS cables, or their combinations, we derived required transmission parameters for this connection. HTS cables allow easier matching of SIL to rated power.

Load flows are compared for available transmission options (option 1- OHLs, 2- OHLs and HTS cables in parallel; 3- OHLs, HTS cable and FACTS, 4- OHLs and XLPE cables in parallel, 5- HTS cables, 6- XLPE cables). Due to use of cables in parallel with OHLs, reliability of the connection is preserved; furthermore, most of the load current flows in cables (due to their lower impedance), therefore connection losses are reduced and magnetic emission from OHLs is diminished.

Comparison of the transmission characteristics shows that the cable length is limited not so much by the charging current, but rather by the voltage at the cable open end (Ferranti effect). While for the XLPE cable the limit is 33 km, for the proposed HTS cable it is 270 km, which is acceptable for most of applications in a country such as the Netherlands.

In-grid case study shows that expected maximum voltages for HTS cable present no obstacle for the electrical insulation management (are within 1.05 of the nominal voltage).

From economic point of view, it is attractive to replace the connection K-G option 4 with 3 (or 2) at a HTS tape price of 356 to 283 (195 to 135) €/((kA·m) and below. Moreover, it makes sense to replace option 1 with 3 (or 2) at a tape price from 241 to 143 (135 to 36) €/((kA·m) and below. These tape prices are expected to be reached within 3 to 12 years.

New advances such as better ReBCO tapes, better thermal insulation, more efficient cooling could speed up the integration of HTS cables in the transmission grid.

With our assumptions our findings show that by the year 2050 there will be no limitations to an underground 380 kV transmission grid. We conclude regarding the transmission grid;

- HTS cables laid in parallel to the existing OHLs reduce the magnetic emission of the connection substantially. HTS cables are a favorable option to strengthen the transmission grid together with a reduction in transmission loss;
- HTS cables enable the use of long connection lengths (about 150 km) together with lower voltage drops;
- FACTS will spare one HTS circuit as compared to the same circuit option without a FACTS (option 3 compared with option 2b);
- Due to the high transport capacity of HTS cables, the transmission voltage can be kept at the same level using HTS cables;
- HTS cable routing can be selected on the need, e.g. shortest distance therefore total length of future transmission grid can be substantially reduced, while keeping redundancy unchanged. This is used in the long term scenario for optimising the transmission routes. Moreover HTS cables allow undergrounding the Dutch transmission grid for more or less the same investment.

3

HTS 380 kV AC transmission cable design

A concept design is explained of a HTS transmission cable with the specifications derived in Chapter 2. Such cable consists of HTS core, electrical insulation, cryostat, cooling system, terminations, etc. Concepts of HTS cables using cryogenic or warm dielectrics are elaborated and compared to each other and with conventional alternatives.

- 3.1 Introduction
- 3.2 Concept and interior arrangement of HTS cable
- 3.3 General comparison of cables and OHL
- 3.4 Outlook AC cables
- 3.5 Conclusions

3.1 Introduction

3.1.1 Conventional transmission

At present electrical energy is transmitted through HV OHL and cables. OHL are in use for more than 100 years and are made of various structures. Pylons of an OHL are made of several shapes, depending on the operating voltage, magnetic field emissions and visual pollution.

In the Dutch grid one phase typically has three or four wire bundles with a crosssection of 460 mm² and 620 mm² [26]. Upgrades to four bundles of 660 mm² enable a transport current of 4 kA [26]. The distance between pylons is about 400 m [52]. The ROW is mainly determined by the width of magnetic field corridor for the OHL (e.g. 250 m for 380 kV, 2.5 kA). In order to reduce the visual effect and ROW, new pylons types are used nowadays. New pylons have a reduced magnetic field corridor of about 80 m, and are spaced 350 to 400 m from each other [52]. However, investment costs are about 5 times higher, which makes the costs of modern OHL comparable to those of underground cables [53].

AC OHLs are currently available for voltages of more than 1000 kV (UHV) and capable of transmitting about 4 GW. Increasing the operating voltage enhances its power capacity with about the same loss, however it requires a larger structure since larger clearance is needed. Such larger pylons are not preferred as they are difficult to integrate in the landscape.

As mentioned in Chapter 2, one can expect more undergrounding in the coming years, in particular in populated areas. For instance in the Netherlands, the 380 kV Randstad cable was recently successfully installed [54]. Also, the Dutch government decided to underground 110 and 150 kV OHL close to residential areas within 15 years starting from year 2017 [36].

Due to the need for undergrounding, HTS cables are beneficial in comparison to the existing solutions, which will be further addressed in this chapter. More about conventional transmission technology is treated in more detail in Appendix A, which is used for comparing the properties with the HTS cable technology throughout the chapter.

3.1.2 State of the art HTS transmission cables

The first HTS transmission cable (> 100 kV) is operating in a grid since 2008 [56]. The project goal is to demonstrate the commercial viability of HTS systems. The cable was installed in The Long Island Power Authority (LIPA) network that is located in New York, US. The cable has a length of 600 meter and is able to transport 574 MW at a voltage of 138 kV_{rms}, resulting in 2.4 kA_{rms} per phase. This cable runs successfully, powering 300.000 homes which shows that this is a mature technology to be applied in the network. The cable is made of BSCCO tape, because YBCO tape was not available at the time.

In the currently second phase of the project, the existing BSCCO core of one cable will be replaced with an YBCO core to get more experience. Notably, in the future a similar periodic upgrade of the HTS cable core with modern tapes could allow keeping transmission capacity needs in the future at the same extra high voltage level. The superconductor from the aged HTS core can be recycled (or used elsewhere if the wires are still in good condition).

Another interesting example is a 275 kV, 3 kA HTS cable of Furukawa (Figure 3.1). This cable is developed by Furukawa Electric which is also part of the HTS roadmap or the Korean network [56].

Regardless the operation voltage, HTS cables use two concepts for electrical insulation, namely cold dielectric (CD) and warm dielectric (WD) design. The electrical insulation for the WD HTS cable is placed around and outside the cryostat, in the ambient environment. As a result, extruded insulation as in conventional cables can be an option for a WD HTS cable with minor adjustment. This brings the advantage that dielectric losses are outside the cryostat leading to better economics. However, the cryostat of a WD cable operates at the rated voltage, which makes repairs more difficult.

For a CD HTS cable the electrical insulation is immersed in the coolant whereby the cooling penalty needs to account for dielectric loss as well.

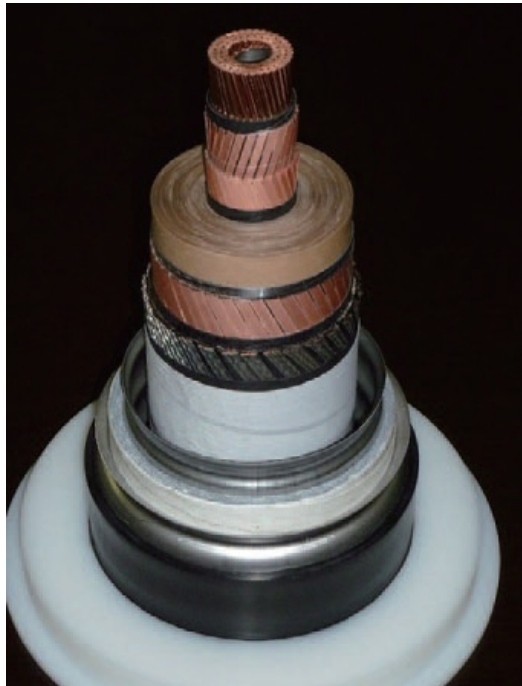


Figure 3.1 Interior arrangement of Furukawa 275 kV, 3 kA, YBCO HTS cold dielectric cable [56, 57]. (Photo courtesy of the author of the first article Mr. M. Yagi)

Table 3.1 Comparison of main advantages for CD and WD HTS cable.

CD	The cryostat is electrically grounded, enabling faster repair
	Aging of electrical insulation is less pronounced
	In trefoil configuration one cryogenic envelope could be used, which saves in costs and the cross-section
WD	Extruded XLPE insulation is applicable and is widely used in conventional cables, which increases reliability and saves installation time
	Lower dielectric losses are possible at ambient temperature

Extruded electrical insulation at cryogenic temperatures is complicated and is only researched [58].

The main advantages for a CD and WD cable are listed in Table 3.1 and will be further explained thereafter. A more detailed comparison is depicted in Table 3.10.

So far there is a HTS cable design made up to 275 kV.

Most important remaining challenges of HTS cables are: relatively high costs, short distance between cooling stations, uncertainty in reliability, reduction of electric and thermal losses, as shown in Table 3.10.

3.2 Concept and interior arrangement of HTS cable

In this section, the 380 kV HTS transmission cable concept and interior arrangement are explained according to the specifications derived in Chapter 2. The AC cable has three identical phases and where possible for simplicity one phase is discussed. In a cable, 380 kV is voltage present between any two phases, the phase to ground voltage is 230 kV for every phase (assuming symmetrical load). Direct buried HTS cable laying arrangement is assumed, since it has its own environment and adequate outer protection. Since the cable core has active cooling, HTS cables do not rely on soil properties for heat removal. The total system consists of the HTS cable, cryostat, terminations, two cooling stations at the cable ends and a control and protection system. When later on HTS cables are compared to XLPE cables, we assume same transmitted power and same outer dimensions.

3.2.1 Cold dielectric HTS cable

Design constrains

In order to be competitive, the CD HTS cable has to have an outer diameter comparable to that of a conventional XLPE cable for the same transferable power. The 2500 mm² enamelled core XLPE cable for 380 kV has a transport current of about 2500 A assuming a soil resistivity of 0.5 Km/W (corresponding to 1.5 m depth), flat direct burial laying arrangement with two cables per phase, 750 mm spacing between adjacent cables, and no circulation current due to cross bonding of the sheath [26].

Outer diameter of the XLPE cable is 141 mm [59].

For a 5 kA transport current (Table 2.3), two such cables per phase are needed. With this in mind and spacing between the two phases accounted, the maximum CD HTS cable outer diameter is limited to 350 mm.

From the design point of view, the heat load must be limited to achieve an acceptable pressure drop in the cable. Therefore, the cooling channel sizes are carefully selected. Also, the cryostat thickness should match the allowed heat leak. Notably, a certain space is needed to provide mechanical integrity of the cable, i.e. to make bending possible.

The resulting concept interior arrangement of the CD cable (dimensions, materials) as explained in Figure 3.2 and Table 3.2, has the outer cable dimension of 266 mm, well within the 350 mm restriction.

The cable concept in case of the CD design is explained in Figure 3.2. Only one phase (of three identical phases) is shown. Starting from the inside, the cable phase has the cooling channel 1 (1, 5), the former (2) around which copper stabiliser (3) and HTS tapes are placed (4), a support tube (6), inner semiconducting layers (7, 9), electrical insulation (8), outer semiconducting layers (9), the screen (10), return cooling channel (11), the cryostat (12,13,14), and the protective layer (15).

- Cooling channels (1) and (5) are used for the “go” flow of refrigerant, which is pressurised liquid nitrogen in this case;
- The former (2) provides mechanical support for current carrying layers and it can be made for instance a stainless steel spiral with a hydraulically smooth (internal) surface;
- The copper stabiliser (3) is electrically connected to the HTS layers and it takes the full current during short circuits;
- The HTS tapes (4) are wound over the copper stabilizer with a minimized gap size, between the adjusted tapes, see Chapter 5 for more details;
- The support tube (6) defines the outer dimension for channel (5) and supports the semiconducting layers (7,9) and the electrical insulation (8);
- The electric and HTS magnetic screens (10) are placed around the electrical insulation, able to completely screen the magnetic field produced by the HTS core [22];
- The ‘return’ cooling flow is in the channel (11) between the outer surface of the electrical insulation (8) and the inner cryostat wall (12);
- The cryostat (12-14) thermally isolates the cold part of the cable from room temperature, it encompasses the inner and the outer walls (12, 14) and the thermal multilayer insulation (MLI) layers and spacers in high vacuum space (13);
- An extruded protection layer (14) placed over the cryostat.

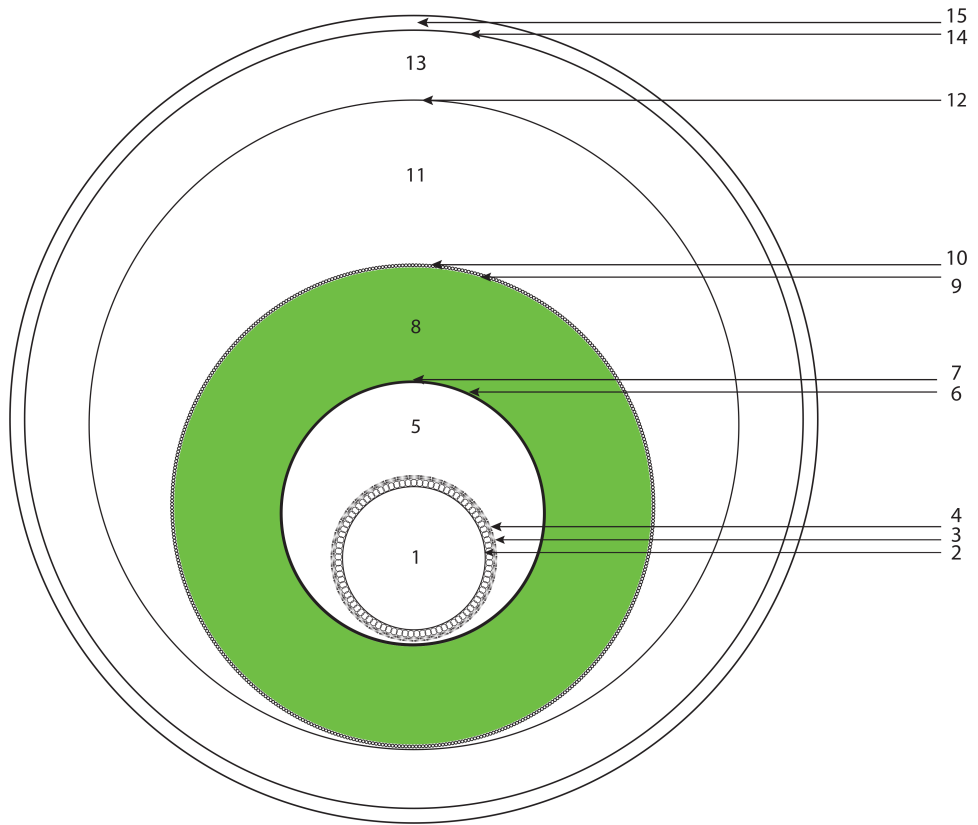


Figure 3.2 Cross-section of the HTS cable using cold dielectric design (380 kV phase to phase voltage).

Further details of the cable interior arrangement are shown in Table 3.2.

Table 3.2 Dimensions and materials (of one phase) for the CD HTS cable: 380 kV, 5 kA.

Part		Outer diameter [mm]	Thickness [mm]	Material
1	Cooling channel (1)	47.8		LN ₂ pressurised
2	Former	49.8	1	Stainless steel (SS)
3	Stabiliser	53.8	2	Copper
4	Phase conductor	54	0.1	YBCO tapes
5	Cooling channel (1)			LN ₂ pressurised
6	Support tube	90	1	Corrugated or flexible SS
7	Semiconductor tape	91	0.5	e.g. black carbon
8	Electrical insulation	171	40	PPLP impregnated, EPR, Tyvek-PE
9	Semiconductor tape	172	0.5	e.g. black carbon
10	Metallic shield	174	1	e.g. copper, aluminium or HTS
11	Cooling channel (11)	176	17	LN ₂ pressurised
12	Inner cryostat wall	210	1	Corrugated or flexible SS
13	MLI, spacers in vacuum	252	20	*(for corrugated, additional 8 mm)
14	Outer cryostat wall	256	1	Corrugated or flexible SS
15	Protection layer	266	5	e.g. polyethylene

3.2.2 Warm dielectric HTS cable

Design constrains

The objective for the WD concept cable is to make a design which is closely related to that of a XLPE cable with respect to the outer dimension and materials that are used. Therefore we assume an outer cryostat dimension that is limited by that of the 2500 mm² XLPE cable core. The HTS cable uses XLPE electrical insulation, the same as conventional cables.

The internal arrangement for the 5 kA WD cable with its dimensions and materials is listed in Table 3.3. The resulting total outer cable dimension is 144 mm and is close to that of a single XLPE cable with a 2500 mm² core.

The concept view of WD HTS cable interior arrangement is shown in Figure 3.3, with only one of the three identical phases shown.

Starting from the inside, the single phase cable has the cooling channel (1); the former (2) around which the copper stabiliser (3) and the HTS tapes (4) are placed, the cooling channel (5) enclosed by the inner cryostat wall (7) or the optional metallic screen (6) (HTS is optional), located at the inner side of the cryostat and simultaneously acting as a support tube, the cryostat (7-9), optional location of the metallic screen (10), inner semiconducting layers (11), electrical insulation (12), outer semiconducting layers (13), the optional metallic screen (14), and the protective layer (15).

- The cooling channel (1) is used for the “go” flow of the pressurised liquid nitrogen and it hosts the transport current carrying layers of the cable phase that are made semi-transparent for the coolant (we assume that cooling channel (1) is thermally insulated from cooling channel (5));
- The former (2) provides mechanical support for current carrying layers and it can be made for instance of stainless steel spiral with hydraulically smooth (internal) surface;
- The copper stabiliser (3) is electrically connected to the HTS layers and it takes the full current during short circuits;
- The HTS layers (4) are wound over the copper stabilizer using the whole cylinder area;
- The support tube (6), which can be the metallic screen layer and when no screen is applied the inner cryostat, which mechanically separates channel (5) from the outer cable layers. The outer cryostat wall is acting as a support tube for the semiconducting layers and electrical insulation;
- The electric shielding and optional magnetic screen on top of the insulation are optimized to partly or completely screen (HTS tape screen) the magnetic field outside the cable by using an aluminium or copper conductor;
- The ‘return’ cooling flow is in the channel (5) surrounding the cable end enclosed by the inner cryostat wall;
- The cryostat to thermally isolate the cable from the ambient environment and hosts, MLI layers and spacing material in high vacuum;
- The outer protection layer is extruded over the screens.

In Table 3.3 dimensions and materials of the cable components are listed.

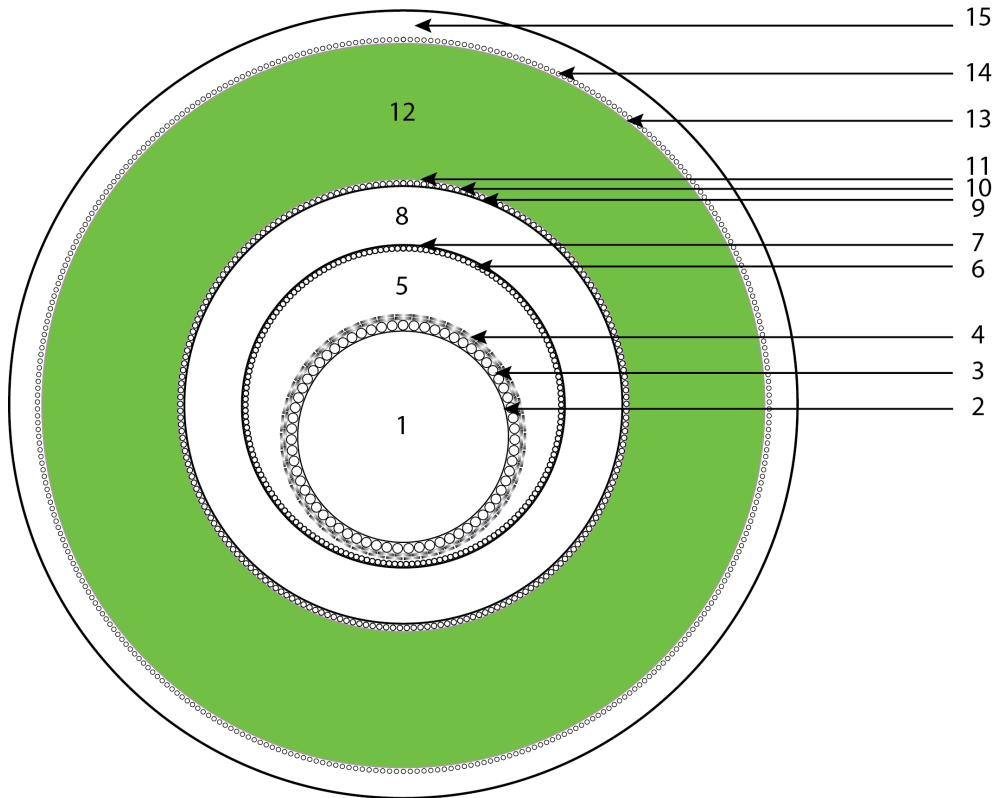


Figure 3.3 Cross-section of the WD HTS cable design concept (380 kV phase to phase voltage).

Table 3.3 Dimensions and materials (of one phase) for the WD HTS cable: 380 kV (phase to phase), 5 kA for 1-phase flat laying configuration.

Part		Outer diameter, mm	Thickness, mm	Material
1	Cooling channel (1)			LN ₂ pressurised
2	Former	39.5	1	Stainless steel (SS)
3	Stabiliser	43.5	2	Copper
4	Phase conductor	43.7	0.1	YBCO tapes
5	Cooling channel (5)			LN ₂ pressurised
6	<i>Optional magnetic screening</i>			e.g. copper or aluminium
7	Cryostat inner wall	61	0.5	Corrugated or flexible SS
8	MLI and spacers material	79	9	Vacuum
9	Outer cryostat wall	80	0.5	Corrugated or flexible SS
10	<i>Optional magnetic screening</i>			e.g. copper or aluminium
11	Semiconductor paper tape or extruded layer	81	0.5	e.g. black carbon
12	Dielectric	131	25	e.g. XLPE type
13	Semiconductor paper tape or extruded layer	132	0.5	e.g. black carbon
14	Ground shield and metallic shield	134	1	e.g. copper or aluminium
15	Protection layer	144	5	e.g. polyethylene

3.2.3 Laying arrangement

As mentioned, a flat HTS cable configuration consist of three single cables each enclosed in its own envelope, which enables close spacing, see Figure 3.4. For about 7 GVA of transmission power, the total corridor for HTS CD configuration (Figure 3.4a) is about 1.5 m, which is only 15% of that of a XLPE corridor for the same power (Figure A.3). For the WD cable the total corridor for the same power is less than 1 m wide (Figure 3.4b). We assume herein a minimum cable spacing of 10 mm. This results in more compact laying arrangement: e.g., in case of three WD HTS cables in flat configuration the circuit corridor is about 452 mm, while one XLPE cable circuit need about 3900 mm (same power capacity as one HTS circuit), see Figure A.3.

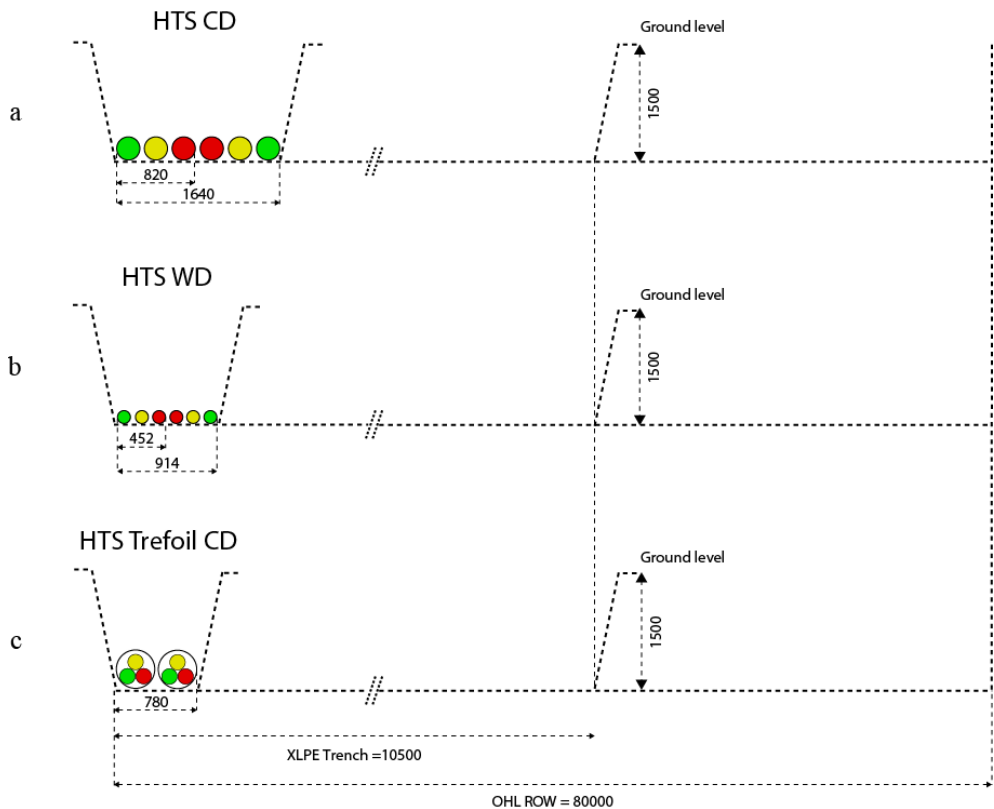


Figure 3.4 Trenches representing flat buried: a HTS CD, b HTS WD and c HTS trefoil configurations.

Excavation works is one of the main root failure causes of power cable circuits. Therefore it is recommended to install two circuits with sufficient spacing to reduce the risk of one than one failed cable circuit during an excavation activity.

When needed, HTS trefoil configuration could also be an option. This arrangement would offer the least corridor (780 mm) which also enables faster installation, since the three phases are housed in one cryogenic envelope (Figure 3.4c). In this cable design both cooling flows (“go” or “return”) can be arranged the (three-phase) cable, e.g. “go” or “return” in the inner formers area and “go” or “return” in the area between the cable surfaces and the inner cryostat wall. Obviously, this single cryostat cable arrangement has the advantage of one cryostat heat invasion accounted in the total loss instead of three. The overall cable design is more compact, but when one phase fails, it is likely that all three phases must be replaced, resulting in longer repair time. Assuming that the CD trefoil

configuration comes later in time, it is considered to be out of the scope of this study.

Obviously, the three WD single cable designs as shown in Figure 3.4b could also be arranged triangular leading to savings in installation and space.

3.2.4 HTS core and shield

As explained in Chapter 1, at present HTS tapes are relatively expensive, meaning that an economically sound HTS cable requires a carefully optimized core design. The resulting specifications for the HTS CD and WD core designs are compared in Table 3.4. At the specified transport current the AC losses at a given transport current [23 and Chapter 5] should be within the design limits and on the other hand it has to fit inside the cooling channel, see Tables 3.3, 3.4 and section 3.3.8. Besides the HTS arrangement in the HTS core, the diameter and the HTS tape critical currents have a large effect on the total core losses. The outer core diameter defines the number of tapes in the core layer. The cable core AC loss target (Table 3.4) sets the required critical current of the core, which is obtained by selecting proper critical currents of HTS tapes. The core is explained in Chapter 6 even as the dependence of the core AC losses on the transport and on the tape critical currents. This HTS core amply meets to the AC loss requirements.

Furthermore, we assume that the critical current of the cable is kept constant over the length even though the core temperature is changing (see example for CD cable in the subsection “CD core and shield”). For example, for the CD HTS cable (Figure 3.2, Tables 3.2, 3.4) when to assume that HTS core temperature is 77 K anywhere, 88 tapes each with the critical current of 216 A (in external field of 0.1 T) would be needed in order to arrive at the core critical current of 19 kA, Table 3.4. In practice however, the core temperature changes from 65 to about 77 K (section 3.2.8).

Table 3.4 Core specifications for CD and WD HTS cables.

Parts	CD design 1, Table 3.2	WD design, Table 3.3
Nominal transport current I_{tn} , kA ($I_{max} = 7.5$ kA)	5	5
Cable I_c , kA (at 77 K)	19	23
Tape I_c , A (at 77 K, 0.1T)	216	261
Number of tapes	88	88
Former diameter, mm	53	42
AC loss ($I_r = 5$ kA), W/m/core	0.56	0.16
AC loss ($I_r = 7.5$ kA), W/m/core	0.8	0.55
AC loss, W/ circuit (at 5 kA)	1.68	0.48
AC loss, W/ circuit ($n-1$)	2.4	1.65

Consequently, the required critical current of each individual tape (at 77 K, 0.1 T) changes from 122 to 295 A with the average (over the cable length) value of 183 A. Therefore, by such adjustment of the critical current of individual tapes a reduction of nearly 15% (183 A vs. 216 A) in the HTS tape costs is achieved. Similar result is obtained for WD HTS cable.

During a short circuit, a copper stabilizer provides a secondary path for the current (such that the cable will not be excessively heated) and is assumed to handle the mechanical forces.

CD core and shield

The cable core (two layers of 3 mm wide YBCO tapes) is built around a hollow flexible spiral duct (non-magnetic materials e.g., stainless steel, plastic), Figure 3.2 and Table 3.2. It has two helically wound layers with total of 88 of 3 mm-wide YBCO tapes each with the average (over the cable length) critical current of 259 A at 77 K (and self-field), see Chapter 5 for more details.

The tapes are wound with a winding angle of 12 degree with a minimized gap between the tapes. The critical current of the cable of 19 kA is kept constant over the whole cable length as explained above. Thus, at the rated transport current of 5 kA_{rms} the cable operates at 37 % of the critical current.

Outside the cable the magnetic field produced by the transport current in the core shall be completely compensated by the shield. This enables a very low inductance for the CD cable. The same tapes are used in the shield as in the core. As HTS tapes are expensive today, an alternative could be to use conventional material such as aluminium or copper (when cooled to 77 K, copper resistivity is 10 times lower than at room temperature and this results in a more efficient shielding than room temperature shielding). Also, a BSCCO tape could be an alternative since this tape is cheaper than YBCO tape at the moment.

It is recommended in case of using an alternative shield conductor, to assess the electromagnetic shielding performance. A joint design is out of the scope of this study, however an example of a joint design can be found in [55].

WD core and shield

The WD core is made of 3 mm-wide YBCO tapes that are wound on the former, similar to the CD core. The assumed maximum transport current in the core is 5 kA. The winding angle, the former diameter and the number of tapes are the same as for the CD core, namely 12 degrees, 42 mm and 88 tapes. To achieve a 0.16 W/m AC loss target at the transport current of 5 kA_{rms}, a cable critical current of 23 kA is required. As for the CD cable, in the WD cable we assume that the critical current of the cable is kept constant over the length even though the core temperature is changing. When to assume that the HTS core temperature is 77 K anywhere, 88 tapes - each with the critical current of 261 A (in external field of 0.07 T) - are needed in order to arrive at the core critical current of 23 kA, Table 3.4. In practice however, the core temperature changes from 65 to 73 K (see

section 3.2.8). Thus, the required critical current of an individual tape (at 77 K, 0.07 T) changes from 120 to 300 A with the average (over the cable length) value of 210 A. Therefore, by such individual adjustment (grading) of the critical current of tapes in the core a reduction of nearly 20% (210 A vs. 261 A) in the HTS tape costs is achieved.

Options to screen magnetic field are at the inner or outer sides of the electric insulation, Figure 3.3. As the HTS core produces almost no heat, more current is allowed in the same shield as compared to the XLPE cable. In section 3.2.10 the shield loss are explained in more detail. Since the extruded insulation is subjected to negligible amount of heat, a longer lifetime can be expected.

In case the shield is located at the outside of the insulation, cross bonding can be used, in the same way as for conventional cables [60].

3.2.5 Electrical insulation

Electrical insulation is an important component of the cable. It enables separation between cable components at different potentials. In the CD cable the dielectric is located in the coolant. Liquid nitrogen in this case penetrates through the insulation, removes the heat and acts as part of the electrical insulation. This is why a laminated paper (PPLP) is widely used as an electrical insulator. The lapped insulation is comparable to the insulation used in oil pressure cables for many years by ambient temperature.

PPLP immersed in liquid nitrogen (LN_2) as used in the LIPA and Furukawa cables, is relatively environment friendly and has lower dielectric losses as compared to the oil immersed variants. Also, it can handle high mechanical stresses and has good expansion properties at cryogenic temperatures. Thermal aging of electrical insulation at this temperature is less pronounced [58, 61, 62]. At transmission voltage levels, dielectric losses dominate, see Table 3.6. Recent studies have shown that Tyvek-PE insulation is a good alternative to PPLP since the loss can be reduced by almost five times (in comparison to PPLP insulation) at the same voltage [63]. As soon as the Tyvek-PE insulation will be certified for use in HTS transmission cables, the total losses for the basic design for CD HTS cable can substantially improved see section 3.2.8 (and Table 2.3). As a result, in the CD design we assume Tyvek-PE insulation.

Excessive heat load attributed to a lapped insulation can result in a gaseous state of the coolant (e.g., during or right after a fault current). This must be prevented as the dielectric strength declines. One way to prevent such occasions is to pressurize the coolant [64].

Alternatively, cryogenic extruded insulation e.g. XLPE or EPR could also be an option [58, 65], but requires substantial research effort.

The electrical insulation of the WD cable is located at ambient temperature. XLPE insulation is a logical choice in this case, since it is widely used in conventional

transmission cables for many years. As mentioned, in comparison to the XLPE copper cable, the WD insulation of HTS cable will experience less heating (section 3.2.8).

CD concept

Polypropylene laminated paper (PPLP) is assumed in the CD cable concept. The insulation thickness is about 40 mm, based on the Furukawa 275 kV HTS cable, which has a comparable outer core diameter [65]. The Furukawa cable has selected their dielectric thickness after undergoing a serious test program: AC withstand tests, impulse voltage tests, Partial Discharge Inception Electric field strength (PDIE) tests, 30 year voltage endurance test and dielectric loss measurements. In this way one believes that the insulation will have high reliability [56].

The insulation thickness enables close operation to SIL at nominal power. The calculated insulation stress (with respect to the interior dimension) is 7.6 kV/mm at the surface of the cable core and 3.3 kV/mm at the surface of the inner shield and is well below the design stress limit of PPLP. The cable insulation thickness is almost twice that of conventional cables. It is assumed that the mechanical strength of the cable insulation is not jeopardized since it consists of many thin layers (<0.1 mm).

WD concept

For the WD design, conventional extruded or lapped insulation can be used to electrically insulate the core. In this design we assume a conventional XLPE insulation that is applied around the outer cryostat wall. We assumed equal insulation thickness as for a conventional 380 kV XLPE cable, since the inner support former diameter whereon the insulation is extruded is equal to that of the conventional copper cable at the same voltage. As a result, the WD HTS cable outer dimension is equal to that of a copper XLPE cable, as shown in Table 3.3.

As mentioned, the insulation is not thermally stressed as in a conventional cable, therefore a higher shield current is allowed. It might be possible to select a thinner insulation.

Flexible parts require more attention due to the bellow heads wherein the electric field needs to be controlled, which could be done by appropriate filler material. These flexible parts require being flexible, therefore a flexible filling material, e.g. rubber, is possible. Alternatively, a helically wound metal strip covering the bellow heads with a layer of semiconductor or paper is an option to extrude the insulation [66]. The electric field strength calculated at the core and at the screen surface is 11 and 6.7 kV/mm, respectively.

3.2.6 Cryostat

The cryostat has the purpose to provide a thermal barrier for a heat flow from room temperature into the cold area. The cryostat comprises two concentric stainless steel tubes, wherein efficient thermal insulation is applied, which are separated by a

vacuum and spacer material. The heat penetrates the barrier by conduction, convection and radiation mechanisms. The efficiency of the cryostat has a direct effect on the distance between two cooling stations and the refrigerator size. Cryostat technical requirements are the following: reasonable mechanical strength, high thermal performance and vacuum property, low electrical conductivity and non-magnetic [67]. The cryostat thermal performance relies mainly on: thermal insulation materials, spacer design, manufacturing factors, vacuum level, outgassing, etc.

The cryostat of the designed HTS cables uses relatively long straight sections and short flexible parts that are used where needed [68]. The outer diameters of the flexible sections are larger because of the bellow heads, which have a typical height of 8 mm [69].

In the cryostat annular region contains a high vacuum of 1×10^{-3} Pa, which acts as a thermal convection barrier [70]. To further increase the thermal efficiency, multi-layer insulation (MLI) is applied in the annular region. The MLI is composed of reflecting aluminium layers separated by low thermal conducting spacer material, such as fine glass fibre fabric. Getter material is applied to outgas the evacuated space in order to maintain a high vacuum for a long period without the use of external pumps [71]. Currently, a cryostat heat invasion of 1 W/m/phase is reported, e.g. for LIPA project cryostat [72]. In the near future a cryostat heat leak can be expected of 0.3 W/m, with a vacuum lifetime period of 10 years without the need for external pumping [73].

Cryostat of a CD HTS cable

The cryostat is outside of the electrical insulation and operates at the ground potential. This allows relatively simple access to the cryostat in case of a repair. The cryostat loss target, 0.5 W/m, is listed in Table 3.7 and agrees well with the expectations [73]. Accordingly, the MLI requires a thermal heat conductivity of 0.125 mW/m/K.

Cryostat of a WD HTS cable

The cryostat operates at HV potential and is more difficult to access, as it is covered by the HV insulation. Furthermore, the WD design has a more demanding heat loss target, because of the more confined dimensions, Figure 3.3 and Table 3.3. The heat leak target of 0.1 W/m, Table 3.7 yields an apparent thermal conductivity of just 0.03 mW/m/K, which is a very demanding figure. According to [74], such thermal conductivity can be reached.

3.2.7 Terminations

Terminations enable the connection to the substation at both cable ends. A circuit consisting of three phases with a single cable per phase needs in total six

terminations, similar to the studied HTS cable for Krimpen-Geertruidenberg, see Chapter 2.

To summarize, HTS terminations take care of:

- The transition from high voltage to ground potential;
- Interface from cryogenic to ambient temperature;
- Cable shrinkage/expansion, e.g. during a thermal cycle.

In the termination the electric field is graded by specially shaped insulation that makes sure that no excessive fields occur.

Up to now, HTS cable prototype terminations are successively built for system voltages of 275 kV_{rms} [65].

Most termination designs use a copper current lead cooled with liquid nitrogen by a secondary cooling path [47]. The termination heat load is thus dependent on the transport current. For a three phase termination (total three terminations for one cable end), a loss of 1 and 0.2 kW is assumed at rated and at zero current respectively. Termination loss is determined in the following way [75]:

$$P_{current\ lead} = 2I\sqrt{\rho K\Delta T} \quad Eq. 3.1$$

where, I is the rms transport current, ρ the average resistivity of the current lead, ΔT the temperature difference between the warm and cold ends of the lead and K the thermal conductivity. For a copper lead, with warm and cold end temperatures of 300 K and 65 K respectively and 5 kA_{rms} transport current, K is 400 Km/W, ρ_{copper} is 0.017 $\mu\Omega\text{m}$, the heat loss for the conduction cooled lead is 0.4 kW. With some margin accounted the total loss of 0.5 kW for a single phase CD and WD termination is assumed.

Basically, the termination is divided into a vertical and horizontal part, see Figures 3.5 and 3.6. The vertical part ensures the temperature transition and the electrical connection to the grid. The horizontal part connects the cable with the termination and manages the thermal contraction of the cable system and connections to the cooling system.

In order to provide a proper insulation clearance, the radial and parallel field stress must be limited. More details about the insulation coordination in a cryogenic stress cone are presented in Annex B, based on a stress cone design for dielectric type testing. The termination designs for the CD and WD cable are further discussed by means of the conceptual drawings as shown in Figures 3.5 and 3.6, respectively and in the text below.

CD termination

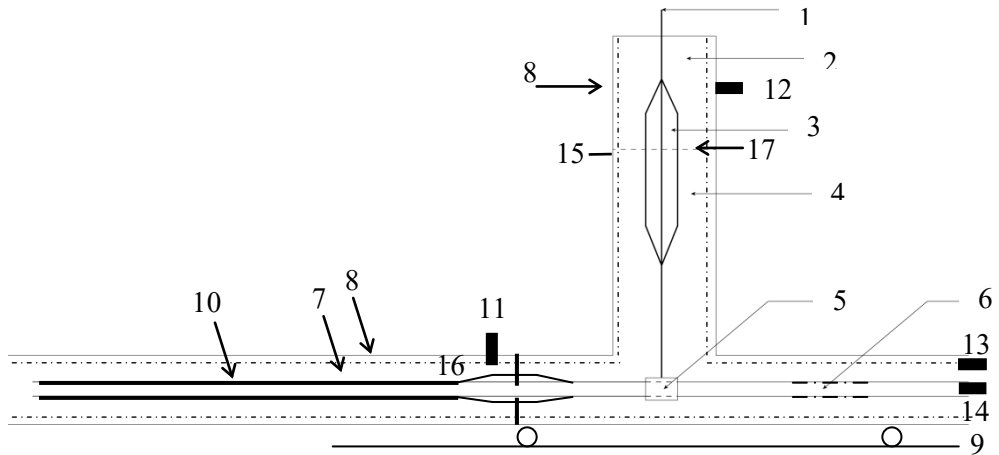


Figure 3.5 Cross-section of a simplified CD termination design, where: 1 is the HV connection, 2 gaseous space, 3 stress cone, 4 LN₂ space, 5 connection of core to conventional bushing, 6 inner cooling channel, 7 outer cooling channel, 8 thermal insulation, 9 sliding rail, 10 electric insulation, 11-14 cooling leads, 15 ground connection, 16 stress cone, 17 thermal barrier.

The cable core is located in the cryogenic envelope and is connected to a copper joint (5) to provide a connection to the termination lead (1). It has a duct to provide a path for the inner coolant channel. The core insulation (10) is terminated close to the location of the vertical bushing. Stress cone (16) provides a gradual reduction of the electrical strength and limits the creepage length. Accordingly, the maximum electrical field strength parallel to the stress cone surface does not exceed 2 kV/mm [77]. In the middle of the stress cone the cooling of the outer channel is closed. In this way the cooling for the bushing and the cable are separated and (11) provides the connection to the refrigerator. The inner cooling channel (6) is electrically insulated by a plastic pipe and connected to the refrigerator using cooling lead (14). The conventional current lead in the vertical bushing can be copper or brass tube and or a braided wire to increase the mechanical flexibility. The vertical part of the termination consist of two compartments namely, the gaseous space (2) and the LN₂ (4) space. In this way a gradual thermal transition is provided, separated by a thermal barrier (17), e.g. vacuum compartment or a flange. The electric field stress between the compartments is controlled by the vertical stress-cone (3). A ground connection is made at the vertical bushing (15), of which the electric field strength is properly graded. To provide additional dielectric strength, the current lead can be covered by a glass fibre reinforced plastic (GFRP). The cooling to the vertical part

of the bushing is provided by cooling connections (12) and (13). Thermal insulation (8) indicated by the dashed lines is used to reduce the heat leaks. When the cable expands or contracts in longitudinal direction, the termination slides along the rail (9).

WD termination

The WD HTS cable cryogenic envelope encloses: the cable core (12), cryostat (11) and electrical insulation (10). The cable is feed through the outer envelope of the cable insert (9) and through the outer by the copper joint (6). The copper joint provides the electrical connection to the vertical bushing (3), and is made with two cooling channels feed troughs that enable the connection with the inner and outer cooling channel. Hereby, cooling tubes are connected between joint and refrigerator connections (13) and (14). However, the tubes are properly electrically insulated at (4) and (5), respectively. Furthermore, a ground connection is provided at (12) and when the cable expands or contracts in longitudinal direction, the termination slides along rail (16).

Other termination examples for a WD termination design are given in [77] and [78].

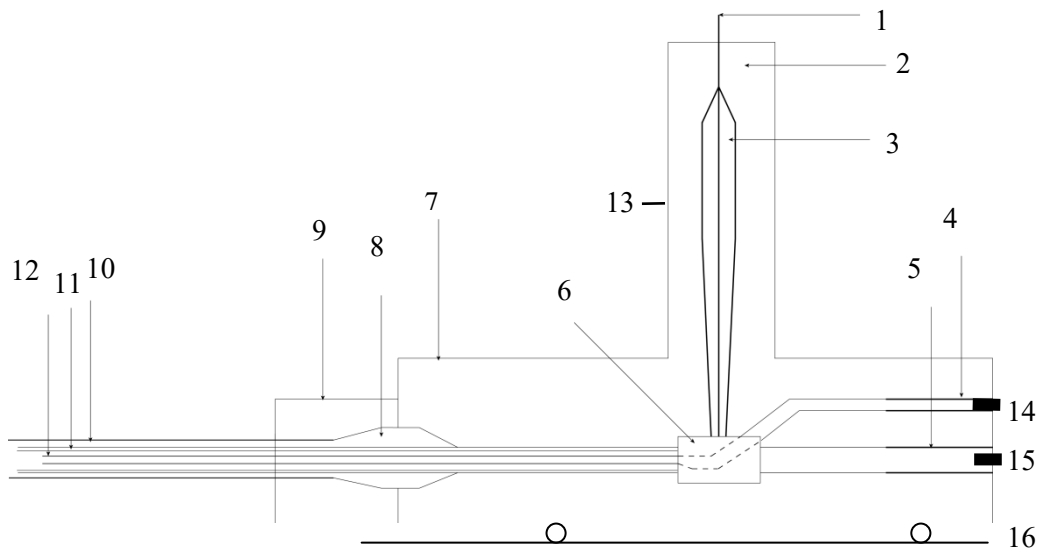


Figure 3.6 Cross-section of a simplified WD termination design, where: 1 is the HV connection, 2 space inside bushing, 3 stress cone, 4 electrically insulated cooling tube of inner cooling channel, 5 electrically insulated cooling tube of outer cooling channel, 6 connection of the core to the conventional bushing, 7 outer envelope of termination, 8 stress-cone cable lead through, 9 outer envelope of cable insert, 10 electrical cable insulation, 11 cryostat, 12 cable core, 13 earth connection, 14-15 connection to cooling leads, 16 sliding rail.

3.2.8 Hydraulics of CD and WD HTS cables

In Table 3.5 hydraulic parameters are listed for the CD and WD cables (Figures 3.2 and 3.3 respectively) assuming that the cooling is provided only from the connection ends. Cooling profiles along the cable are similar to that in [72]. As mentioned the outer diameter of the WD cable is more challenging than that of the CD cable due to the confined cross sectional area of the cooling channel. It is therefore more challenging to achieve acceptable pressure drops for the WD cable. If longer distances are required for a WD cable, the coolant area can be increased using both cable cooling channels as a “go” flow and a fourth separated tube as a return flow. To achieve a balanced cooling, the “return” tube should have a cross-section comparable to that of the “go” flow of all the cables in the circuit. Furthermore, the coolant is pressurized in such a way that no gas bubbles are formed in the cooling channel along the whole cable length. The pressure drop in the conduit is based on the equations given in section 5.2.8 with friction factors deduced from [70].

CD cable

Table 3.5 shows the hydraulics for the CD and WD cable. The inlet temperature has a temperature of 65 K to improve the cable performance and to optimize the refrigeration costs. The output temperatures on the cable end for the inner and outer cooling channel are 76.7 and 77 K as shown in Table 3.5. The inner cooling channel carries the “go” flow and the outer cooling channel the “return flow”. In the calculation, as mentioned above, the cooling channels are assumed to be separated by a thermal barrier, hence the heat loss dissipation in the dielectric is only attributed to the outer cooling channel and the core’s AC loss to the inner cooling channel [79].

Table 3.5 Hydraulic characteristic for CD and WD concepts of HTS cable.

Cooling parameters	CD ($I_{tr} = 7.5$ kA) $I_c = 19$ kA		WD ($I_{tr} = 5$ kA) $I_c = 23$ kA	
	inner	outer	inner	outer
Cooling channel	inner	outer	inner	outer
Heat invasion, W/m	0.8	0.82*	0.16	0.1
T_{in} , K	65	65	65	65
T_{out} , K	76.7	77	77	73
Mass flow rate, kg/s	1.16	1.16	0.14	0.14
Cross-sectional area of flow, cm^2	45	140	11	13
Friction coefficient of rigid sections	0.04	0.03	0.03	0.035
Friction coefficient of bellows sections	0.3	0.3	0.2	0.3
Total pressure drop, atm.	9	1.2	8	8

* Tyvek-PE insulation

The flow cross-sections for the “go” and the “return” channels are 45 and 140 cm² resulting in an equal mass flow rate in both channels (1.16 kg/s). The equal mass-flow rates provide the flow integrity. The friction factors agree with [68, 69]. In order to enable bending and to reduce the pressure drop, 10 % bellows parts are assumed (of the total length). The remaining length is manufactured with straight parts. Hence, a total pressure drop of 9 and 1.2 atm. is calculated for the inner and outer channels respectively, which are acceptable from practical point of view.

WD cable

As shown in Table 3.6, the heat loss targets for this cable are 0.16 W/m and 0.1 W/m for the “go” and the “return” flow channels respectively. The cross-sectional area of the cable phase channel is restricted to 11 cm² which corresponds to an outer dimension of 38 mm. The “return” channel has a cross-section of 13 cm² having an outer diameter of 60 mm. The temperatures of the refrigerant for the cable outlet for the inner and outer channels are assumed 77 and 73 K, respectively. The friction factors are accounted for the length comprised of 10 % bellows and 90 % straight sections same way as for the CD cable. Despite of the confined area of the cooling channels, the pressure drops are calculated to be both 8 atm. The assumed cable maximum transport current is 5 kA_{rms} in this case. The WD pressure is larger than the CD cable, although such a pressure drop is acceptable, a maximum pressure on the outer wall should be limited to about 10-15 atm.

To note that the outer dimension of the WD cable is very close to the outer dimension of a XLPE cable, Table 3.3. Obviously, one can optimise the pressure drops if larger outer dimensions are allowed.

3.2.9 Cooling

The heat load arising in the HTS cable system (Table 3.6) is removed by liquid nitrogen provided by the cooling system.

Most efficient cooling is provided when the cable is cooled using a refrigeration cycle and terminations that are cooled with a liquefaction cycle.

The refrigeration system of HTS cable must be: reliable, with long intervals between maintenance, small footprint, low costs and efficient.

Various refrigeration cycles are known, one example is shown in Figure 3.7 [55]. This modular system is capable to remove a heat load of 22 kW at 72 K and 12 kW at 65 K and is known for its very low vibrations, efficiency over a large temperature range, and long operating lifetime. Connection K-G has a total heat load of 0.8 and 0.82 W/m in the inner and outer cooling channel. This results in a total heat load of 120 kW at one side of the connection to be removed. Deduced from the above stated heat removal specifications, the heat removal at 77 K is 29 kW.

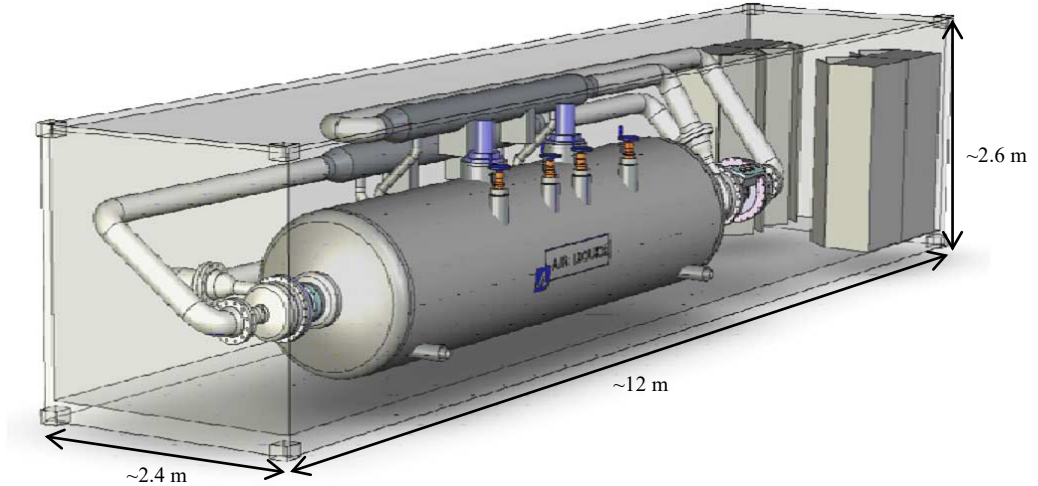


Figure 3.7 Reverse turbo-Brayton cycle refrigerator concept for LIPA project [55]. (Illustration courtesy of the authors of the article: Mr. C. Condrand, Mr. F.Schmidt, J. Maguire)

Accordingly, four turbo Bryton cycle refrigerators are required to remove the heat load at one side of connection K-G, which encompasses with 7 and 1 M€, for single side CD and WD cable circuit refrigeration, respectively. A CD cable with Tyvek-PE insulation needs two refrigerators at each side of the connection, which corresponds to 4 M€. Selecting Tyvek-PE instead of PPLP insulation could save 6 M€ per circuit on refrigeration.

In case of the WD cable, 16 kW of cooling power is required at 77 K. This requires one Turbo Bryton refrigerator at each connection end without redundancy accounted for.

In a refrigeration cycle, as mentioned before, the ratio of the input power P to the cooling power Q is the cooling penalty ε :

$$\varepsilon = P/Q = \frac{T_p/T_Q}{\eta} \quad \text{Eq. 3.2}$$

where, η is the relative efficiency of a real cycle compared to an ideal thermodynamic Carnot cycle (for the latter $\eta=1$ holds), T_Q is the temperature of the cold end, and T_p is the ambient temperature where the heat is rejected. For efficient practical cycles $\eta \sim 0.25$, $T_p = 300K$, $T_Q = 70K$ and $\varepsilon \sim 12$ [3].

The Brayton cycle refrigeration system (Figure 3.7) operates at 28 % of Carnot efficiency, which results in a cooling penalty of 13 W/W at 77 K, Equation 3.2. The efficiency increases for larger cooling capacities (such as needed for Krimpen-Geertruidenberg), therefore we have assumed a cooling penalty of 10 W/W, see also [66]. New advances can make HTS cables more attractive for instance by using gas-driven compressors at the cable cooling stations, which could contribute to a climate in nearby buildings (with heat pumps fed by cable cooling losses) [21].

3.2.10 Cable system losses

The CD and WD cables have the following losses: in the conductor core, in the dielectric, in the hydraulic loops, in the shield, in the cryostat, in the terminations, etc. These are listed in Table 3.6 and are used to calculate the total cable losses.

The losses are presented for a single CD, WD HTS and XLPE cable, respectively, at 7.5 kA_{rms}, 5 kA_{rms}, transport current and 2.5 kA_{rms} current. XLPE cable losses have to be multiplied by two for a 5 kA_{rms} transport current. This allows for a comparison of the HTS cable with conventional cables at full load. As detailed in the section 3.2.9, the removal of the losses from cryogenic temperature to room temperature has the cooling penalty of 10 and 20 W/W, respectively for the cable components and the terminations.

Table 3.6 380 kV system voltage sources of loss for CD (7.5 kA) and WD single cable (5 kA_{rms}) and XLPE cable double cable per phase (total of 5 kA_{rms}).

Source	CD	WD	XLPE
Conductor core, W/m	0.8 [*]	0.16 [*]	85
Dielectric loss ⁺ , W/m	0.23 ^{**}	1	1
Hydraulic losses (pump power), W/m	0.07 [*]	0.1 [*]	na.
Loss in shield, W/m	0.09 ^{**}	0 [▼]	na.
Cryostat heat load, W/m	0.5 [*]	0.1 [*]	na.
Termination losses [*] , W/m	0.07 [*]	0.09 [*]	na.
Total cable loss (to be removed at ambient temperature) [*] , W/m	12 ^{**}	5.5 [*]	86

^{*} Coolant loss (a cooling penalty 10 W/W is applied for cable and 20 W/W for termination)

⁺ Dissipation factor for CD and WD, XLPE is 5×10^{-4} and 2×10^{-4} , respectively

^{**} Deduced from the neutral loss estimated in [47]

[▼] 68% shielding can be provided assuming same temperature rise of a XLPE cable for the same power

[♦] Loss is based on Tyvek-PE insulation

^{*} In W/m at rated power based on the lead loss, in kW/kA and divided by the cable length, 33.7 km in order to be able to compare the result with the other cables

As shown in Table 3.6, the total losses for CD, WD and XLPE cables operating at 5 kA_{rms} are: 12, 5.5 and 86 W/m, respectively. This indicates that the total losses for the CD and WD cables are respectively about 85 % and 90 % lower as the XLPE cable for the same power.

The HTS core losses for the CD and WD cable concepts are estimated using the loss measurement, as explained in Chapter 5.

The single cable losses developed in the WD and XLPE dielectric are both about 1 W/m, assuming that the same insulation type and thickness is used. To compare the dielectric loss of the CD cable with that of the WD and XLPE cable the cooling penalty must be accounted. This is why the dielectric losses for the CD cable (using Tyvek-PE insulation) are about 2 times higher as compared to that of the WD HTS cable and of XLPE cable, see Table 3.6. The dielectric loss depends on the dissipation factor ($\tan \delta$), voltage (U_f), cable capacitance (C) and the angular frequency and is given by:

$$P_{dielectric} = \omega C U_f^2 \tan \delta \quad Eq. 3.3$$

Similar to the Furukawa cable [66] the dissipation factor of 5×10^{-4} is obtained for the CD (PPLP) HTS cable of this study. The WD cable is assumed to have the same dissipation factor as XLPE insulation, which is 2×10^{-4} [81]. Using Eq. 3.3 and the cable capacitances (Table 2.2), the calculated values of the dielectric losses for CD, WD HTS and XLPE cables respectively are, 0.23, 1 and 1 W/m.

As a result, cooling of the cable is less demanding as explained in section (3.2.7) and the cable hydraulics is simplified, see section 3.2.8.

The pumping losses are due to the circulation of the coolant through the cooling channels. The pumping losses depend on: pressure drops and the velocity of the coolant. The calculated pumping losses for CD and WD HTS cables are rather small, see Table 3.6.

The shielding requirement depends on where a cable circuit will be located, for instance in residential areas, screening would be more essential as compared to rural areas. Complete shielding of the magnetic field is more practical in the CD cable than in the WD cable and should lead to the lower shield loss using HTS tapes in the shield. A loss of 0.09 W/m is accounted for the shield, which is about 11 % of the core loss [47].

The HTS WD core loss is only a fraction as that of the XLPE cable. Also the dielectric loss is only a fraction of that of the total loss, since no cooling penalty is accounted. As mentioned before, a higher shielding current is allowed in the WD cable, which reduces the magnetic field emission and leads to a lower cable inductance. For an ambient temperature of 20°C and assuming a temperature drop of 5°C over the screen, the screen temperature will be 65°C. Assuming the same properties for the screen as that of the core would lead to about 70 % screening of

the magnetic field produced by the core. This leads to a more compact laying arrangement for the WD cable as compared to the XLPE cable.

A higher current in the shield leads to higher costs, thus there is an optimum between the cable spacing and shielding in a WD cable design. Moreover, the loss for a WD cable with 70 % shielding (52.5 W screen loss leading to total WD losses of 58 W/m), is still 24 % lower than that for a XLPE circuit.

It shows that screening for the WD cable is an option and could be further optimized by studying the screen materials.

As mentioned, the cable cooling can be provided in several ways, of which open loop cooling and closed loop refrigerators are preferred. In order to estimate the return on investment time (ROI) for a CD cable and WD cable cooling system in the connection Krimpen-Geertruidenberg, a comparison is made between the open loop cooling and the closed loop cooling (refrigerators). The results are presented in Table 3.7. Assumed is that half of the required system heat load is supplied by each cooling system located at each connection end.

As shown in Table 3.7, the yearly liquid nitrogen consumption for an open cooling system required for the CD and WD cable is, 31 and 5 ML respectively, assuming that the CD cable operates at 7.5 kA_{rms} and the WD cable at 5 kA_{rms} continuously. This would require respectively 12 and 2 liquid nitrogen truckloads a week (assuming a 50 m³ truck capacity). The selling price of LN₂ for such a quantity is 46 €/m³ [82], including the lease price of 10 k€/year for the liquid nitrogen storage tank and the operating costs.

Results of this study show that the investment into the refrigeration system can be returned after 2 years and 5 years, for respectively the CD and WD cable systems, see Table 3.7. Hence, investing in a refrigeration system intended to operate for forty years is reasonable.

Table 3.7 Refrigeration for CD and WD concept cables (three phases), connection Krimpen-Geertruidenberg.

	CD	WD
Heat load for the refrigeration on one side at ambient temperature (incl. terminations), kW	1507	233
ΔT inner channel, K	11.7	12
ΔT outer channel, K	12	8
Latent heat evaporation of LN ₂ , kJ/kg (L_v)	198	
Density of LN ₂ , kg/L	0,808	
Heat capacitance LN ₂ , kJ/kg/K (C_v)	1.038	
LN ₂ consumption, ML/year	31	5
Required nr. of LN ₂ truck loads a 50m ³ /week	12	2
Costs estimate for LN ₂ supply, M€/year	1	0.24
Estimated cost for refrigerator, M€*	1	1
Return on investment time, years*	1	5

* Calculation method as described in [13]

3.2.11 Cable mass

Cable weight is important for the installation, transport, manufacturing process, etc. In this section the masses of the treated cables are estimated (Table 3.8) using the material densities as listed in Table 3.9.

For transport and installation of the HTS cable, the weight without liquid nitrogen is of importance. The total transport weight of the single phase CD and WD cable is 44 kg/m and 21 kg/m, which is respectively 34 % and 72% lighter than that of XLPE cables, see Table 3.9. Since the HTS cables are lighter than XLPE cables, faster installation can be achieved and less heavy installation machinery can be used.

The total cable length between two cable joints is limited by the length which can be stored on a drum. With regards to the cable weight, the HTS CD cable has about the same weight as that of a single XLPE cable, whereas the WD cable is 16 kg lighter. The WD cable is therefore 56 % longer in length as compared to a single XLPE cable, assuming the same size of drum. This could be of particular advantage for water crossings, where the maximum XLPE cable length between joints is limited.

Table 3.8 Mass comparisons for CD, WD and two XLPE cables having 5 kA_{rms} maximum transport currents.

Component	CD		WD		two XLPE	
	Material	kg/m	Material	kg/m	Material	kg/m
Former	Stainless steel	1.1	Stainless steel	1	/	
Core	YBCO	0.1	YBCO	0.1	copper	44.8
Copper shunt layer	Copper	2.8	Copper	2.4	/	/
Cooling liquid	LN ₂	2.5	LN ₂	2	/	/
Dielectric	PPLP	17.7	XLPE	8.2	XLPE	17.8
Screen layer	Copper	4.9	Copper	3.7	copper	4.4
Cryostat	Stainless steel	11.4	Stainless steel	3.4	/	/
Protection layer	Polyethylene	3.8	Polyethylene	2.0	Polyethylene	7
Total operating weight (incl. cooling) liquid, kg/m	/	42	/	23	/	74
Total transport weight, kg/m	/	44	/	21	/	74

Table 3.9 Density of materials.

Materials	kg/m ³
Copper	8960
Stainless steel	7850
Aluminium	2702
YBCO	8920
LN ₂	808
Polyethylene	940
XLPE	950
PPLP	946

3.2.12 Thermal cycling

Inevitably, one has to cope with mechanical stresses that appear during thermal cycling in a HTS cable. It is of importance that the electrical insulation stays in good contact with its support tube at all times. To overcome unacceptable mechanical stresses, for example, during shrinkage or expansion, a pre-stressed layer of e.g. stainless steel supporting the extruded insulation can provide a solution.

The largest contraction is attributed to the stainless steel components when cooling down the cable. The expansion/contraction can be estimated using Equation 3.4.

$$l_2 = l_1[1 + \alpha(T_2 - T_1)] \quad \text{Eq. 3.4}$$

where, l_2 is the length after cooling down, l_1 is the length at room temperature, α is the expansion coefficient, and T_1 and T_2 are the temperature at room temperature and cryogenic temperature.

Based on the expansion coefficient of stainless steel 304 ($\alpha = 15 \times 10^{-6} \text{ K}^{-1}$) a 0.3 % contraction is found for the cable cooled from room temperature down to 77 K and is in agreement with [55]. This means that the cold part of the 34 km long cable will contract about 100 m. For shorter cable lengths, e.g. shrinkage of some meters can be compensated in the terminations that are fixed to a sliding rail, as indicated in Figure 3.5 and 3.6. However, for longer lengths the shrinkage must be compensated in a way that is independent on the cable length. One could think of making the parts to be cooled respectively longer (e.g., parts 2-4 for WD design, Figure 3.3) and laying them loose inside the cryostat, using the idea that worked fine in a 46 m long cryostat [17, 21].

3.3 General comparison of cables and OHL

To compare CD and WD HTS cables with conventional cables and OHLs we have summarised the most important advantages and disadvantages in Table 3.10 and expressed them in the radar plot shown in Figure 3.8. Each feature is evaluated qualitatively using a relative score, ranging from 1 to 4, wherein 1 is the highest and 4 is the lowest score. In Figure 3.8 it means that the closer the line is to the radar plot centre, the better the score.

To assess these scores a group of experts has been interviewed after which the average outcome has been fed back to the group [15]. Different solutions to solve technical hurdles that were indicated have been evaluated, compared with literature, [17], [31], [83], [84], after which final scores were assessed. Currently the transmission grid exists mainly of OHLs (> 95 %) and cables are used only where the use of OHLs is impossible. The transmission grid transformation from OHLs to cables into a grid that consists mainly of cables, is only possible when cables perform better than OHLs.

In Figure 3.9, the comparative scores are shown for the future HTS and the conventional cables and for the OHL. The HTS cable has to demonstrate superior performance to OHL in: reliability, power capacity, maturity, availability, failure rates, maintenance, time of repair, connection length and life expectancy [15]. Our study concludes that reliability of a transmission connection with OHLs alone is the highest, with cables in parallel to OHLs is close to that, and with cables alone is lower. Until the HTS features with respect to the OHLs are to be demonstrated, then we propose to use HTS cables in parallel to OHLs. This way the issues of HTS cables can be tolerated in the grid and these cables can separately be used as soon as they have their assets at the level of XLPE cables [21].

Table 3.10 Overview of the target criteria for HV single CD, WD cables in order to compete with the conventional cable and OHL.

nr	Specification of component	CD cable	WD cable	Cu Cable	Cu OHL
1	Public acceptance	1	1	3	4
2	Power capacity, GW	1	1	4	3
3	Maturity	4	4	2	1
4	Reliability*	1	1	2	1
5	Availability	2	2	3	1
6	Failure rates	2♥	2♥	4	1
7	Maintenance*	2	2	2	2
8	Time of repair*	2♥	2♥	3	1
9	Connection length	1	1	4	1
10	Initial investment cost	1	1	4	1
11	Total lifetime costs	1	1	4	3
12	Life expectancy	1	1	4	2
13	Rights of way	1	1	3	4
14	Efficiency	2	1	3	4
15	M-field pollution	1	1	2	4
16	Visual impact	1	1	2	4
17	Acoustic impact*	1	1	1	4
18	TV and radio interference	1	1	1	4
19	Electrocution risk*	1	1	1	4
20	Impact on aviation*	1	1	1	4
21	Impact on building planning*	1	1	2	4
22	Impact on flora/fauna*	1	1	2	4
23	Impact of weather*	1	1	2	4
24	Catastrophic event*	1	1	3	4

* Following comparison made by Realise grid [31]

♥ These are one of the most important target criteria from the specifications list. These targets have to be satisfied in order to let HTS cables compete with conventional cables and OHLs

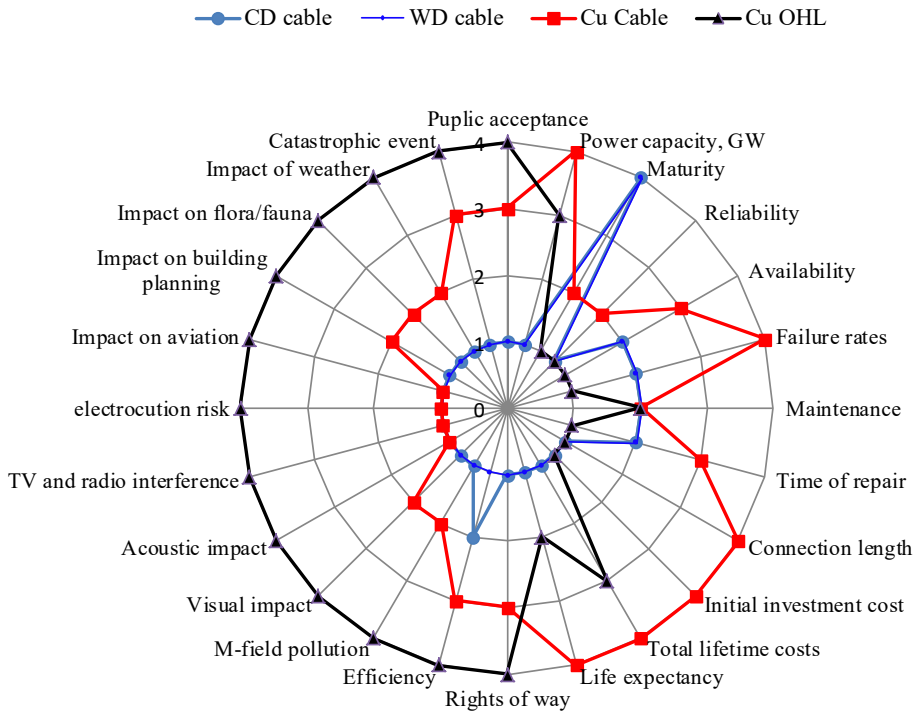


Figure 3.8 Comparison of characteristic of: CD cable, WD cable, Cu cable and Cu OHL.

3.4 AC Cable Activities

In this section the outlook will be given of recent promising HTS cable projects ongoing in Japan, US and Korea.

Figure 3.9 shows an overview of the activities in these countries which are deduced from their roadmaps. The activities are in line with the roadmap for the (E)HV grid evolution outlined in section 2.3.7.

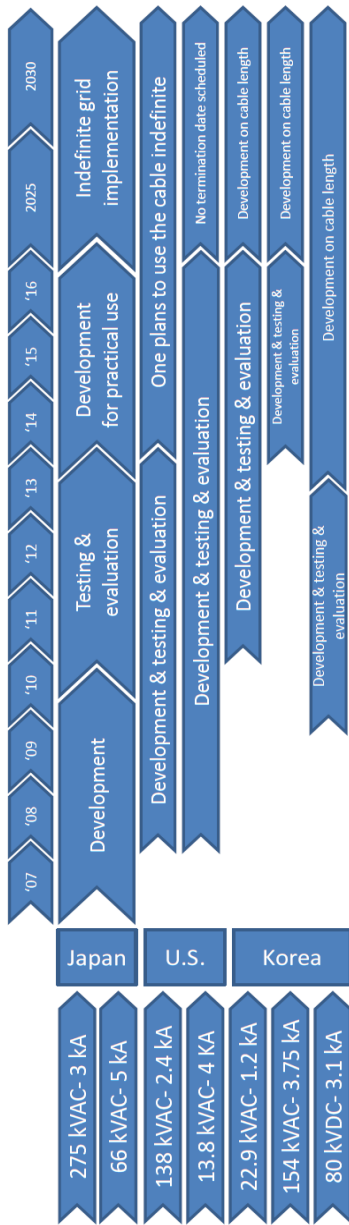


Figure 3.9, Overview of the recent HTS cable projects in Japan, US and Korea based on their HTS cable roadmaps.

Below, the HTS cable activities in these countries are discussed.

Japan Following the HTS cable roadmap of Japan, HTS cables at a voltage level of 66 and 275 kV AC are already developed for practical use and are expected to become integrated in their grid after 2020. The actual progress in developing 66 and 275 kV HTS cables follows the roadmap precisely according to information given in [62]. Tokyo Electric power Company (TEPCO) has successfully executed a one year-long electrical HTS cable endurance test that has been integrated in their electricity network between October 2012 and December 2013. The cable was connected to Asahi station, as part of the Yokohama project. The three phase cable with a length of 240 m and 66 kV / 200 MVA, is manufactured by Sumitomo and its cooling by Mayekawa [85].

US

US also has a HTS national roadmap, containing of three phases [86], see Figure 3.9. Phase 1 of the US roadmap is almost accomplished, however, some attention is needed for instance in the areas of acceleration of acceptance, critical technologies etc. In phase I, a 132 kV the LIPA cable (Chapter 2) was realized; in 2006 a 13.2 kV, 3 kA HTS cable link between a step-down transformer and the substation load (Columbus Triax project); in 2016 a 13.8 kV, 4 kA cable connection (Hydra project) between two substations will be commissioned [57]. The US roadmap is executed according to the plan (Tres Amigas project may be executed when it is unrealistic to use conventional cables).

Korea

A similar roadmap as that for Japan and US exists in Korea [87, 88]. A 154 kV HTS cable (1 km) was successfully type tested. An 80 kV HTS DC submarine cable (500 m) provides a parallel connection to the 154 kV AC cable for strengthening. Later in time Korea implements longer cable lengths [57].

3.5 Conclusions

In this chapter we have shown that it is technically possible to develop concepts of AC HTS transmission cable with adequate network specifications for the connection Krimpen-Geertruidenberg. Essential feature of the concepts is that such HTS cables are cost-competitive as compared to other options available to transmission system operator (conventional XLPE cable, OHL, etc.). Main parts of such cable system are: shielded and electrically insulated HTS cable core, cryostat, two terminations and two cooling stations at the cable ends

We have elaborated two such HTS cable designs, namely the cold dielectric (CD) cable and the warm dielectric (WD) cable.

First, the cold and the warm dielectrics HTS cable interior arrangements are explained resulting in the 266 mm and 144 mm outer cable diameters respectively. Comparison of laying arrangements of the designed HTS cables to that of conventional XLPE cables and of OHLs for 7 GVA capacity show that both designed HTS cables are very compact: OHLs, XLPE, HTS CD and WD cables require 80, 10, 1.8 and 1 m-wide ROW respectively.

The HTS core and shield specifications are explained for CD and WD cables: the required cable critical currents are derived providing acceptable AC losses in the cores and shields. Furthermore, the cable critical current is kept constant along the cable length despite changing temperature of the flow (this provides constant AC losses in the core along the cable length and saves 20-30% of the core costs).

Use for electrical insulation of novel dielectric materials (e.g., Tyvek-PE) results in more compact and more efficient CD cable design, while use of PLLP-C leads to more conservative design: cable is more bulky and less efficient. A WD HTS cable allows using conventional electrical insulation, such as XLPE with the advantage (over the CD cable) that dielectric losses are outside the cryostat.

More efficient semi-flexible cryostats are used in the design: for the CD cable the targeted heat leak of 0.5 W/m agrees well the near-term expectation (0.3 W/m) and for the WD cable the target of 0.1 W/m is within reach when improved thermal insulation is used.

Terminations enable a connection to the substations at both cable ends, are designed separately for CD and WD cables and provide the transition from high voltage to ground potential; interface from low to ambient temperature, take care of the cable shrinkage and expansion during a thermal cycle. As a result, the total heat leak of 1.5 kW per three-phase CD or WD termination is derived.

Hydraulic and thermal study of both HTS cables operated at 7.5 kA_{rms} resulted in two cooling stations at the cable ends and the following characteristics: for the CD cable the inlet and outlet temperatures and pressures of the go and return flows are 65 and 76.7 K, 15 and 7 bar; 65 and 77 K, 15 and 7 bar respectively at the mass flow rate of 1.16 kg/s. For the WD cable the inlet and outlet temperatures and pressures of the go and return flows are 65 and 77 K, 15 and 7 bar; 65 and 73 K, 15 and 7 bar respectively at the mass flow rate of 0.14 kg/s.

At n-1 redundancy for the CD HTS cable a cooling station of eight turbo Bryton cryocoolers (each able to remove 12 kW at 65 K) is sufficient at each cable end, for the WD HTS cable a cooling station of two such cryocoolers at each cable end is sufficient.

A study of the designed HTS cable systems reveals that the total losses (including the cooling penalty of 10) are: 5.5 and 12 kW/km for WD and CD cables respectively, as compared to 86 kW/km for conventional XLPE double cable per phase circuit of the same capacity.

Therefore, main conclusion of this chapter is that it is technically possible to develop a competitive (to other available options) concept of AC HTS transmission cable addressing the required network specifications of the connection.

Both developed HTS cables as compared to a conventional copper cable with the same rating have more compact arrangement, lower loss, less magnetic field pollution, less weight, allow faster installation, etc.

This makes HTS cables attractive for TSOs but require further demonstration of their capabilities in the real transmission grid. As the remaining challenges: reliability, power capacity, maturity, availability, failure rates, maintenance, time of repair, connection length and life expectancy will be properly addressed, HTS cables will replace OHLs in transmission grid.

Conclusions in detail

- Conventional transmission UGCs are only suitable for relatively short lengths (25 km at 380 kV) and are limited in power capacity;
- Conventional 380 kV cables use more than one cable per phase to obtain the power capacity;
- The HTS WD cable has its dielectric loss outside the cryostat leading to a better economics;
- Extruded insulation as used in conventional cables can be applied in the WD HTS cable;
- Aging of the dielectric is least pronounced for a CD HTS cable, less pronounced for a WD HTS cable and most pronounced for a conventional copper cable;
- The CD HTS cable cryostat is electrically insulated and allows faster repair as compared with the WD HTS cable;
- A CD trefoil cable needs only one cryostat and is therefore more compact than the three CD cables each placed in a separate cryostat;
- At present no HTS AC cable design for 380 kV system voltage exists;
- Challenges for HTS cables are the relatively high costs (of HTS tapes), distance between cooling stations, reliability maturity, availability, failure rates, maintenance, time of repair, and life expectancy;
- The outer dimension for the CD HTS cable 380 kV, 5 kA_{rms} is 266 mm, when needed, this dimension can be further reduced by using lower-loss HTS tapes in the cable core and by introducing intermediate cooling stations;

- The outer dimension of the WD HTS cable design can be equal to that of a conventional 380 kV cable (2500mm² core) and with double power capacity;
- The dielectric loss can be substantially reduced with Tyvek-PE insulation;
- Adjustment of the electrical insulation thickness allows HTS cable to operate close to SIL;
- An external cooling channel can be used as a “return” flow to increase the cooling capacity;
- With regards to the network specifications, HTS CD and WD cables with a 40 km distance between cooling stations can operate with an acceptable pressure drop;
- Using flexible cable parts only where needed, improves the HTS cable performance;
- The cable refrigeration system should be reliable, have long maintenance intervals, small footprint, high efficiency and low costs;
- A refrigeration system using the Brayton-cycle satisfies the requirements for a HTS cable system;
- Total losses for WD, CD single cable and XLPE double cable per phase arrangement (at 7.5 kA_{rms} for CD cable and 5kA_{rms} for WD and XLPE cables) are respectively 5.5, 12, and 84 W/m;
- Grading the HTS tape critical current with respect to the temperature distribution along the cable provides uniform AC losses in the cable core and is cost-effective;
- A suitable cryostat can be made for the CD and WD HTS cables using available thermal insulation materials;
- It is profitable to invest in a refrigeration system instead of using an open loop cooling system when operating longer than 1 and 5 years for the CD and WD systems respectively;
- The CD and WD cables have 28 % and 72 % lower mass in comparison with a conventional XLPE cable and HTS cables can be fabricated in longer length between joints as compared to that of the conventional XLPE copper cable.

4

HTS AC cable integration in the distribution network

In this chapter we present the possibilities to employ HTS cables in the distribution grid. The required grid power capacity is expected to grow over the coming years, in particular in cities. Consequently the maximum fault current, voltage fluctuations and AC losses will rise. Furthermore, the rise of distributed energy resources (DER) changes the operation of the distribution grid.

HTS technology could address changes in the distribution grid. In this chapter, most attractive ways to integrate HTS cables in the distribution grid are illustrated. Running HTS cable pilot projects in the distribution grid are discussed. Economic comparison with existing alternatives is made and ways are elaborated to make HTS cables economically viable.

4.1 Introduction

4.2 HTS distribution cables

4.3 Feasibility study for integrating a HTS cable into the distribution network

4.4 Discussion

4.5 Conclusions

4.1 Introduction

In the future more distributed energy resources (DER) in the electricity grid will arise, such as wind parks and solar panels. These energy sources integrated in the grid allow to use less large scale generation. Small and medium scale DER together with increasing large-scale renewable energy sources will supply a significant part of the energy demand. Besides, the introduction of hybrid and fully electric cars is expected to grow and households are requested to comply with CO₂ neutral electricity consumption. In the future, households are expected to generate their own electricity consumption and feed the excess to the grid. All these grid changes will lead to a change in the energy distribution such as: increasing power consumption, short circuit current, voltage fluctuations, reactive power flow and occupation of land, as illustrated in Figure 4.1.

HTS cables could contribute to a more efficient and flexible network operation. As shown in Chapter 2, HTS cables at transmission voltages can easily compete with conventional cables. However, for the same transmitted power in comparison to high voltage cables, the transport current in distribution cables is higher, hence the HTS distribution cable requires more HTS tapes. Since cost of HTS tape defines the HTS cable cost, it is challenging for HTS cables to economically compete with conventional cables at distribution voltages.

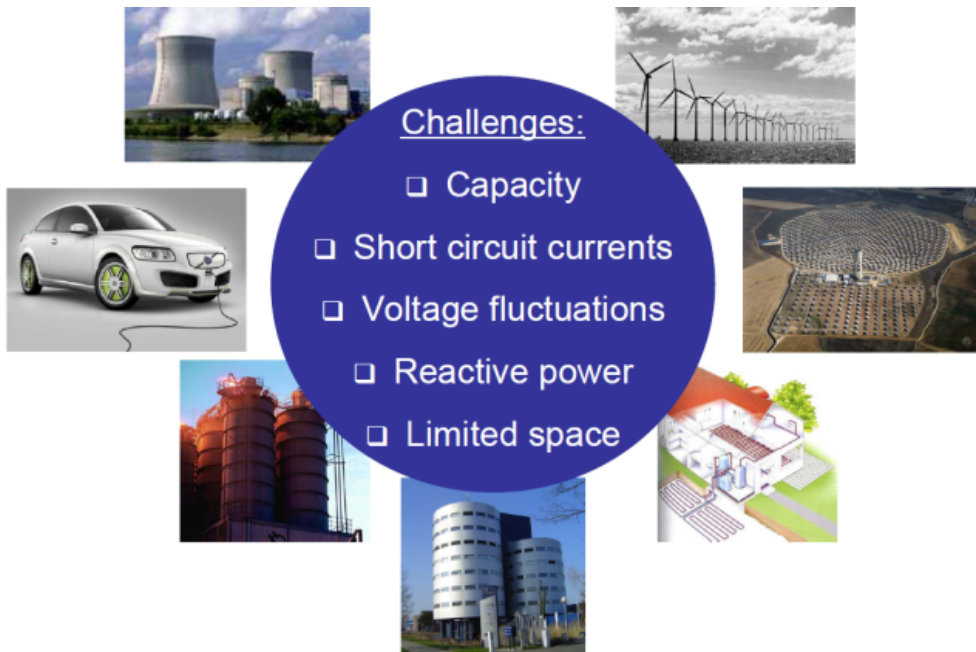


Figure 4.1, Challenges to overcome at distribution level [89] (Illustration courtesy of Alliander).

4.1.1 Changing existing Dutch distribution network

The Dutch low and medium voltage network is executed using only underground cables. As the Netherlands is a density populated country, distribution cables are typically 5-30 km in length, and the MV and LV voltage networks have the following voltages (arranged from higher to lower levels): 6 - 25 kV³ and 230 V and 400 V to residential areas.

After the deregulation of the electricity network, voltage levels up to 50 kV are under the courtesy of the DSOs (and above under the responsibility of TSO's). The high voltage network is connected through a MV substation from where the distribution network enters a city. The distribution network is developing mainly at sites where the expected loads will appear. By the year 2012 the total length of the medium voltage 6-25 kV distribution network measured about 100000 km. In areas where the load demand is relatively low, the network has mostly a radial structure, in which the power at one medium voltage node is supplied by at least 2 power transformers. In areas where the load is highly concentrated the network has a ring shape structure. The ring enables more power distribution connections with increased reliability. Feeder cables, of 10 or 20 kV depending on their transport capacity, supply the substations (usually ~several 100 MVA) and comply with the $n-1$ criteria. In dense load areas more feeder cables are connected to form a ring structure to increase the reliability. These ring shaped structures have more connection nodes which attributes to the higher possible fault current. It is expected that the number of rings will grow in the network to increase the power transfer flexibility. In this way a more meshed network is formed. Average lengths between substations and cables in 50-20 kV and 10 kV networks are respectively about 5-10 and 1 km. In all likelihood, the network control of the distribution grid will be mostly done by the grid itself. Coming years, more intelligence will be integrated in the grid using sensors to, for instance, control of the power distribution flow. This might lead to autonomous energy consumption of households providing the excess of electrical energy back to the grid.

The incentive is that 10 kV will be replaced by 20 kV (i.e. making the grid cheaper, more flexible, reliable, etc.) and adding DER - like wind and solar - connected to the grid. This DER can contribute to load balancing issues, of which local storage facilities are seen as a solution. In Figure 4.2, the future grid is visualised.

³ 25, 20, 12, 10, 6 kV

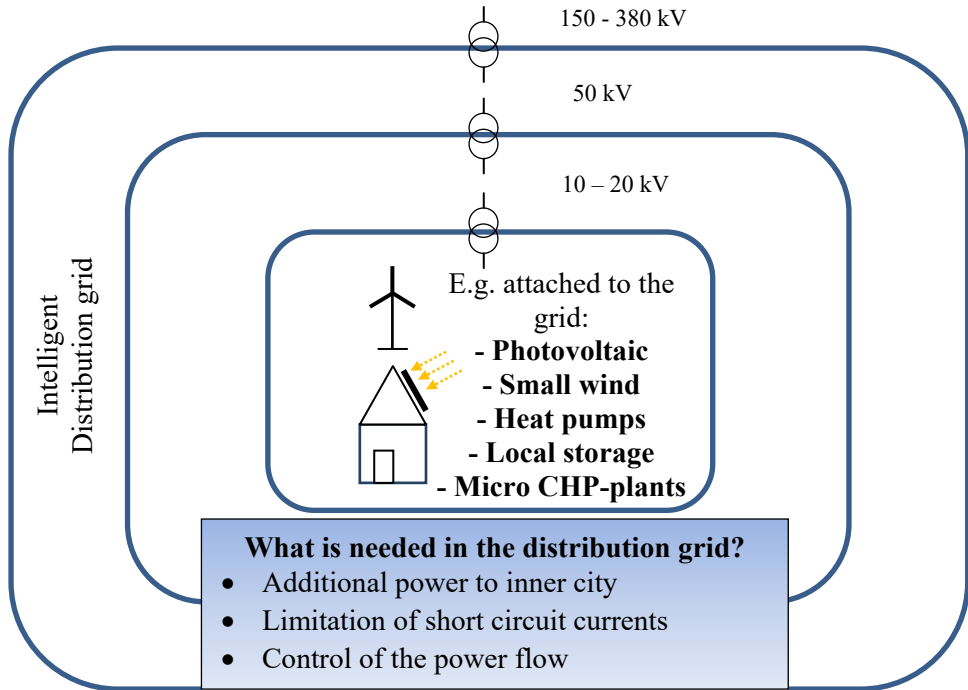


Figure 4.2 The change to an intelligent of the distribution grid.

4.2 HTS distribution cables

Applying HTS technology to the future grid enables the following advantages:

- Larger transport capacity; up to 10 times in comparison to conventional options;
- Lower AC losses; use of HTS tapes decrease the AC losses during electrical power transport, which lowers the lifetime cost;
- HTS tapes enable the use of lower transport voltages. This could lead to a cost reduction for transformers;
- Less reactive power; HTS cables produce remarkable less reactive power with respect to the active power flow;
- No thermal interaction; the cryogenic envelope in which the cable is enclosed leads to the absence of thermal interaction with its surrounding environment;
- No electromagnetic field; the concentric arrangement of cable phases cancels the electromagnetic field outside of the cable;
- Improved grid performance; as bidirectional flows are possible (Figure 4.2), HTS cable can prevent voltage problems in the MV grid due to its low reactance;

- Limited fault currents; the use of the second generation YBCO wire allows efficient fault current limitation.

In the next sections, two HTS cable projects in Amsterdam and Essen are discussed, of which the latter has been realized. For economic consensus the Amsterdam project is not continued before the realization phase. Thereafter, economic analysis and comparison of both are performed.

4.2.1 Dutch project

To demonstrate the high performance of the HTS cable technology in the life grid, the consortium of the Dutch distribution network operator (DSO) Alliander, Ultra™ (Joint Venture of Southwire and NKT Cables) and Delft University of Technology (TUD) formulated a R&D program to establish a 6 km FCL Triax® HTS cable in Alliander’s network. This HTS cable allows to meet the future power capacity by retrofitting one existing copper cable in the connection.

Three existing pipes are available to provide the electrical power connection to the city centre by two important 150 kV substations Hoogte Kadijk (HK) and Noord Klaprozenweg (NDK), as indicated in Figure 4.3. Currently, three gas pressurized cables (GPC) are located there in the steel ducts. These cables are, however, at the end of their lifetime. The GPC consists of three cores and provides a total power capacity of 300 MVA, see Figure 4.4. The projected maximum demand at HK is about 200 MVA. Under $n-1$ criterion, the connection operates just under its limit. Thus, when a fault occurs in the network during maintenance, the load could reach two times the rated level. To solve this problem, the existing cables need to be retrofitted by higher capacity cables. As mentioned before, the power demand is expected to grow, potentially leading to an even further capacity upgrade. One strives for an environment-friendly future grid and therefore the use of polluting oil and gas pressure cables must be prevented.

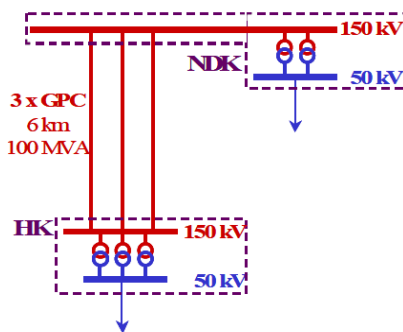


Figure 4.3 Existing grid structure [90].



Figure 4.4 Conventional cable [90].

(Courtesy Ultra® - A Southwire / nkt cables Joint Venture)

As the GPC's are not able to meet the power demand, and there is no space to expand the connection with an additional cable, an alternative is needed. A new type of XLPE cable, the "City Cable" (CC), is seen as a possible solution.

In comparison to the existing GPC, the CC doubles the power capacity to 200 MVA per cable. This capacity is sufficient for the near future, but might not be the case for the longer term.

Alternatively, a HTS power cable can be used as a third cable in parallel to the CCs. In Figure 4.5 the proposed future network between substation HK and NDK is shown. The specially designed HTS cable is connected in parallel to two CC, in order to provide $n-1$ criteria (see black line in Figure 4.5: when e.g., HTS cable fails, 200 MVA of nominal power capacity remains). The higher power capacity and lower loss of HTS cable allow operating at a lower voltage in comparison to conventional cables. Therefore the operation voltage for the HTS cable is 50 kV, resulting in 3 kA_{rms} transport current in each phase. The CC and HTS cable is shown in Figure 4.6 left, right. Moreover, the XLPE and HTS cables are seen as an environmental friendly replacement. The HTS cable design and advantages will be further discussed and elaborated in Chapter 5.

To connect the HTS cable to the 50 kV grid, the remaining issues to be solved at the system level, are:

- The power sharing in parallel circuits; large amount of reactive power flow as there is no voltage regulation at the 50 kV bus;
- The increase of the short circuit current through the installation of the HTS cable between the 50 kV substations;
- Unbalanced currents in the three phases due to the concentric phases leading to a current flow in the neutral [90].

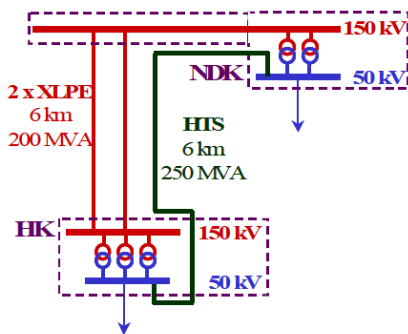


Figure 4.5 Grid structure with HTS cable [90].

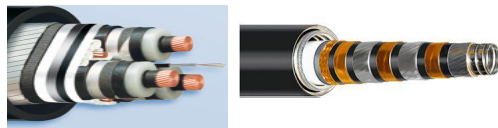


Figure 4.6 XLPE city cable (left), HTS cable (right) [91].

(Courtesy Ultera® - A Southwire / nkt cables Joint Venture)

In order to address the issues, the load flows and the losses in the existing and in the proposed grids are studied using programme “Vision”. The study is performed in Alliander’s network within the joint venture of the Amsterdam HTS project. The results give insight into the load flow and the expected grid losses.

The cable and transformer parameters and specifications used in the study are listed in Tables 4.1 and 4.2, respectively. The existing and proposed grid structures are depicted in Figures 4.7a and 4.7b, based on the networks shown in Figures 4.3 and 4.5.

Table 4.1 Cable parameters.

	HTS cable	City cable (CC)	GPC
I_{nom} , kA	2.9	0.665	0.338
R , m Ω /km	0.110	50	77.4
X , m Ω /km	8.796	106.8	138.7
C , μ F/km	2.2	0.231	0.2903
S , MVA	250	170	86

Table 4.2 Three phase transformer parameters.

	Transformer 1 (Tr1)	Transformer 2 (Tr2)	Transformer 3 (Tr3)
U_{nom} , kV	150/52.5/11	150/52.5/11.1	150/52.5/11
P_k , kW	232 /124/124	547/141/134	245/110/109
S_{nom} , MVA	100/70/30	100/100/30	100/70/30
P_{null} , kW	54	51	60

The three underground distribution cables (UGD) provide the power connection between station NDK and HK, see Figure 4.7a. For the proposed grid scenario (Figure 4.7b), two GPC cables are retrofitted by two 150 kV City Cables. The third cable could be retrofitted by the HTS cable connected at 50 kV, provided by the third 250 MVA transformer (Tr2) which is relocated to station NDK, see Figure 4.7b.

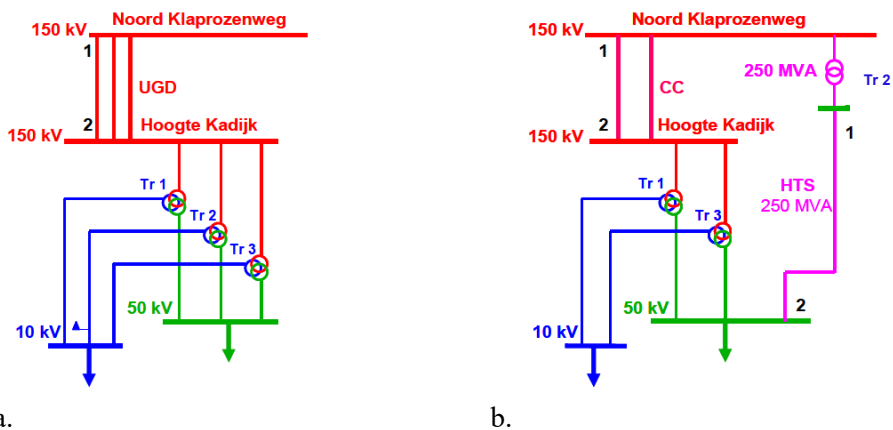


Figure 4.7 Grid structure for network study, where the red, green, blue solid lines, respectively represent 150 kV, 50 kV and 10 kV connections.

Table 4.3 Comparison of existing (3xUGD, 150kV) and proposed grid (including HTS cable: 2xUGD, 150 kV + HTS, 50 kV).

Criteria	Length, km	Option	Nb. of Circuit x Type	In kA	P1 MW	Q1* MVar	Q2 MVar	I2 kA	Loss kW	Loss MWh	Tot. Loss GWh
n-1	6.2	1	3xUGD	3x0.3	188	-49	-91	0.767	261	782	4.2
			3xTR1,2,3	-	-	-	-	-	792	3378	
		2	2xCC	2x0.7	75	4	-18	0.3	36	36	2.3
			1xHTS	1x2.9	112	-48	-60	1.4	89	709	
			1xTR2 2xTR1,3	- -	- -	- -	- -	- -	65 301	218 1237	

* load is calculated with $\cos \varphi = 0.98$

Assuming a load of 200 MVA at the 50 kV bus, the powers, currents and losses are calculated and the results are shown in Table 4.3 for the existing and the proposed situation, respectively. As the HTS cable is operating at a lower voltage (option 2), the transport current through the circuit is almost doubled as compared to the transport current in the two GPC in option 1. The reactive power flows, see Q1 and Q2 in Table 4.3, in the three gas pressurised cables in option 1 are in the same order of the reactive flows in the HTS cable in option 2. Therefore, no mitigation measures are required to regulate the voltage for this connection.

The total circuit losses for option 1 and 2, including the transformer losses for options 1 and 2, are 4.2 and 2.3 GWh, respectively. The losses are calculated assuming an operation time of 3000 hours/year for the conventional and for HTS cables. The continuous cryostat and termination losses (1 kW/ termination) are calculated assuming 8760 operational hours/year. In option 2, 112 and 75 MW is transported through the HTS cable and CCs, respectively. More power is directed via the HTS cable due to its lower impedance compared to the CCs. The AC losses of the single CC are 18 kW and of the HTS cable 89 kW, see Table 4.3. However the HTS cable in comparison to the CC has the advantage to operate at a lower voltage level, moreover it has three times higher power capacity. The 150/50 kV transformer in option 2 contributes only with 65 kW to the loss, which is on average about 200 kW lower than the average transformer loss in option 1.

The second generation HTS tape enables resistive fault current capability of the HTS cable. This advantage can be used to protect the grid against the increasing short circuit currents. The fault current limiting HTS cable has a core design accommodating the grid requirements as explained in more detail in Chapter 5.

A study of a fault current limiting functionality in the grid of Alliander is performed by Liandon and illustrated in Figure 4.8.

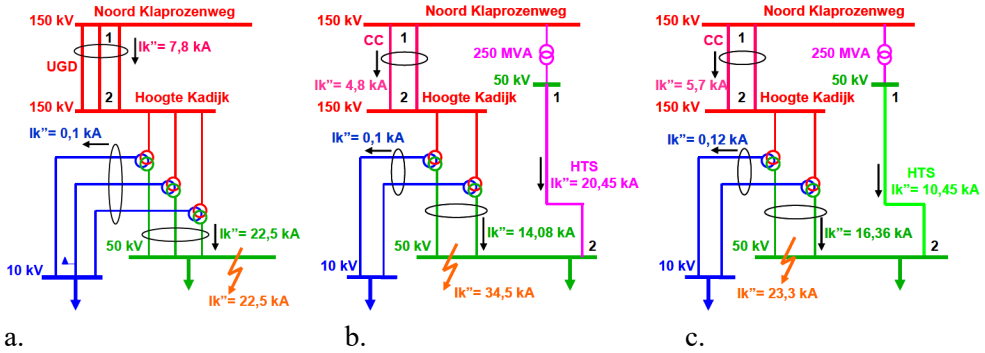


Figure 4.8 Subtransient short circuits currents in a) existing grid, b) upgraded grid without FCL and c) upgraded grid with FCL.

The fault current limiting capability study is explained in the following three scenarios (Figure 4.8a, b and c, respectively): 1) using the existing network, 2) using the upgraded network with HTS cable without fault current limiting capability and 3) the latter with fault current capability. The fault current limiting cable has a critical current of 10.5 kA, see Chapter 5. Short circuit currents are presented in Figure 8a, b and c, for scenarios 1, 2 and 3, respectively.

The results of the network study are listed in Table 4.4. Using the short circuit network powers, the sub-transient fault current I_k'' and peak fault current i_p at the 50 kV bus of HK are calculated, based on Equations 4.1 and 4.2 [35].

$$S_k'' = U_{nom} \cdot I_k'' \cdot \sqrt{3} \quad Eq. 4.1$$

where, S_k'' is the short circuit power, U_{nom} is the the nominal voltage.

$$i_p = \kappa \cdot \sqrt{2} \cdot I_k'' \quad Eq. 4.2$$

where, κ is a constant representing the networks R/X relation and I_k'' the subtransient fault current.

The subtransient fault current in the scenario 1 has the lowest value, namely 22.5 kA. The low impedance HTS cable (scenario 2) increases the subtransient current to 34.5 kA in comparison to the existing situation, see Table 4.4 and Figures 4.8a and 4.8b (the numbers in orange). Alternatively the fault current capability of the HTS cable (scenario 3, Figure 4.8c) reduces the subtransient fault current to 23.3 kA, see Table 4.4.

Table 4.4 Comparison of the short circuit results for conventional, HTS with and without FCL property for 50 kV bus at HK.

50 kV rail	Scenario 1 Conventional cable	Scenario 2 HTS cable <u>without</u> FCL	Scenario 3 HTS cable <u>with</u> FCL
Short circuit power, S_k'' , MVA	2047	3137	2114
Subtransient fault current, I_k'' , kA	22.5	34.5	23.3
Peak short circuit current ¹ i_p , kA	60	95	55.7

¹ peak short circuit current, where κ is 1.8, 1.9 and 1.7 for scenario 1, 2 and 3

The most excessive fault current for the system is the peak current, which rises inherently with the short circuit power. System calculations shown a short circuit peak limited to 55.7 kA in case of FCL integrated. This peak short circuit current is below the existing network limit, meaning that there is no need for heavier switchgear.

4.3 Feasibility study for integrating a HTS cable into the distribution network

The German utility company Rheinisch-Westfälische Elektrizitätswerke (RWE), Karlsruhe Institute of Technology (KIT) and cable manufacturing company (Nexans) begun a HTS cable project (similar to the Amsterdam project) named: “Ampacity”, to strengthen the distribution grid in the centre of Essen, Germany. The consortium received funding by the Ministry of Economics and Technology due to the innovative character of the project.

The majority of the electrical connections around Essen centre comprise 110 kV overhead lines, some 110 kV cables are also used. One of the alternatives is 10 kV connections. According to the consortium study, lowering the voltage enables reduced total investment costs and makes it easier to employ cables.

In Essen, the connections are powered by two parallel 40 MVA transformers enabling $n-1$ redundancy, see [90]. This connection has a length of one kilometer.

A 40 MVA connection comprised of 10 kV cables requires five parallel XLPE cables [90]. On the other hand, one HTS cable can easily transport this power.

As mentioned, the reliability of the HTS cable needs to be demonstrated, the Ampacity project is a large scale trial to show the ability of the system and is seen as an important step to more widespread HTS applications [93]. By running the Ampacity project successively for several years, Germany aims to attract more of such projects in Europe.

In order to limit fault currents the project has made the choice for an external fault current limiter and in the middle of the connection a joint is installed.

4.3.1 Ampacity project costs

To investigate the feasibility of a grid using HTS cables, the costs that are used as reference are presented in [93].

The investment and operating costs are determined for three grid scenarios (see [93]); 1) existing grid consisting of 110 kV, 2) grid upgrade with 10 kV conventional and 3) grid upgrade with 10 kV HTS cables. The presented investment and operating costs for scenario 1, 2 and 3 are about 76, 62 and 70 M€ and 27.2, 25.8, 23.7 M€, respectively

The main difference between scenario 2 and 3 is the 1 km cable section, that is made of conventional or HTS cable. Achieving the stated cost level is challenging, especially when compared to the cost of 13.5 M€/km for the Ampacity project [57].

Our conclusion is that at this moment the HTS distribution cable is economically not yet feasible. Therefore, all available cost saving options should be used in order to reduce the cable costs and to make HTS distribution cables feasible.

In the next section the costs for the HTS distribution cable for the Amsterdam grid will be estimated using the cost analysis procedure of Chapter 2, section 2.4.5 adjusted for distribution network requirements.

4.3.2 Estimation of the costs for Triax distribution cable in Dutch cable project

The 50 kV, 3 kA Triax HTS distribution cable is described in detail in Chapter 5. The costs of the cable are estimated using the method described in section 2.3.4. Assumed component costs are listed in Table 4.5.

Table 4.5 Assumed costs for HTS Triax distribution cable, in M€/km.

Triax cable cost components	Costs, M€/km
HTS tapes, (25 €/(kA·m))	0.70
HV insulation	0.03
Cryostat	0.22
Terminations (two sides, three phase)	0.06
Installation	0.13
Refrigeration	0.16
Vacuum system	0.05
Conductor components (10% of tape costs)	0.07
Conductor contingency (10% of tape costs)	0.07
Fabrication (5% of tape costs)	0.04
Total	1.53

The total cost comparison is based on the network options that are shown in section 4.2.1, namely:

- 1) three gas pressure cables (existing network situation);
- 2) two City Cables in parallel to one HTS triax cable.

For a connection length of 6 km, the costs for two above mentioned options are calculated and compared. We expect that when HTS power cables are applied at large scale in the transmission grid, a HTS tape cost of 25 €/ (kA·m) will become realistic (section 2.3.5). The listed laying costs are based on retrofitting the cable in an existing tube. The costs are deduced from the laying costs mentioned in Chapter 2 (the laying costs are reduced with factor five to 0.02 M€/km, as the cables are retrofitted, have a lower weight and comprise 3 phases in one cable).

As a result the total allowable costs for the HTS Triax cable for Amsterdam project are projected at 1.6 M€/km.

Assumptions for LGCC and the LGCC are 102 and 60 €/MWh, in a similar way as done in Chapter 2. The maintenance costs are assumed 10 % of the transmission HTS cable maintenance cost. The transformer investment costs are assumed 0.01 M€/MVA, which is a realistic assumption for a 100 MVA transformer. As both options 1 and 2 have three transformers, it has no influence on the total costs comparison.

The total life time costs of options 1 and 2.3 become comparable at the tape price of 19 €/ (kA·m).

Furthermore, a cost comparison is performed for the connection made of three existing parallel UGD cables (option 1), of existing connection with four parallel UGD cables (option 1.2), new connection with two City Cables parallel to the HTS cable (option 2), new connection without costs of cooling (option 2.2), new connection, with cost performance ratio (CPR) chosen that TLTC are the same as for option 1 (option 2.3), see Table 4.6.

Table 4.6 shows that total initial investment costs (TIVC) for options 1 and 2 are 11 and 20 M€, respectively and the total lifetime costs for options 1 and 2 are estimated to be 29 and 32 M€ respectively.

We can therefore conclude that initial investment costs of the proposed connection using HTS cable are higher than that of the existing connection since the costs of HTS cable are substantially higher. However, the TLTC for both options are comparable.

As stated above, it is expected that the HTS transmission cable will be integrated in the Dutch grid sooner than the HTS distribution cable. Therefore, we may assume that HTS transmission cables are already widely integrated when HTS distribution cable is still pending.

Table 4.6 Comparison of cable costs for UGD, HTS and XLPE cables for Amsterdam project.

Option*	Length, km	CPR, €/(kA·m)	Circuits: number & type	I_{nom} , kA	CC, M€/km	Cable IVC, M€	Trafo IVC, M€	LGCC, M€	TIVC, M€	MNC, M€	LELC, M€	DMC, M€	TLTC, M€
1	6		3xUGD + TR1,2,3	3 x 0.8	1.0	6	3	2	11	0.7	10	7.2	29
1.2			4xUGD + TR1,2,3	4 x 0.8	1.3	8	3	2	13	1.0	10	9.6	34
2	6		2xCity + TR1,3	2 x 0.96	1.0	6	2			0.5		4.8	32
		25	1xHTS + TR4	1 x 2.9	1.7	10	1	1	20	0.4	6	0.6	
2.2	6		2xCity + TR1,3	2 x 0.96	1.0	6	2			0.5		4.8	30
		25	1xHTS + TR4	1 x 2.9	1.4	8	1	1	18	0.4	6	0.6	
2.3	6		2xCity + TR1,3	2 x 0.96	1.0	6	2			0.5		4.8	29
		19	1xHTS + TR4	1 x 2.9	0.9	6	1	1	17	0.4	6	0.6	

*1 Existing network of three parallel cables

1.2 Existing network of four parallel UGD cables

2.1 New network with two City Cables parallel to HTS cable, assuming CPR of 25 €/(kA·m)

2.2 New network, without costs of cooling

2.3 New network, with CPR such that option 1 and 2 have equal TLTC

One of the possibilities is to let the HTS transmission system provide the cooling for the HTS distribution system. This option has similarities to the charged costs for transmitting electrical energy from the transmission grid via the distribution grid to the consumer.

By considering that costs for cooling are paid by the transmission system, the HTS cable investment costs, total investment costs and total lifetime costs are reduced to 8, 18 and 30 M€ respectively, see option 2.2 of Table 4.6. In option 2.2, the maintenance and dismantling costs are assumed equal to that of option 2. As a result, the costs for the HTS distribution cable are reduced, but remain significantly higher than those of the conventional cable. However, the TLTC are close to that of option 1 TLTC. Same TLTC for option 1 and 2.3 can be achieved when the HTS tape costs are reduced from 25 to 19 €/(kA·m), which corresponds to a HTS cable investment cost of 6 M€/km (option 2.3). Clearly, other benefits of HTS cables (section 4.2) such as higher capacity, retrofit, fault current limiting capability, no thermal

interaction, etc. can justify these higher costs and stimulate earlier use HTS distribution cables instead of conventional cables. For instance, the HTS cable in this scenario can offer about 33 % more power than the CCs, see Table 4.6.

The additional power benefit is not included in our cost evaluation, since in most cases it is more cost beneficial to lay an additional cable to achieve the power capacity. In order to compensate for the additional power capacity obtained in option 2 in comparison to option 1, it is fair to add one conventional cable in option 1 (option 1.2). Subsequently, the cable circuit investment costs for option 1 becomes 8 M€ instead of 6 M€ leading to 34 M€ TLTC. As a result, option 2 becomes competitive with option 1 with 2 M€ of TLTC savings.

Moreover, at a tape price of 35 €/ (kA·m) the TLTC for options 2 and 1.2 are the same.

We can conclude that when beneficial features of the HTS cable in comparison with conventional cables are valued, HTS cables can become competitive to conventional technologies in niche projects. And in case the price of the HTS tapes reduces due to e.g., HTS transmission cables implementation, wider integration of HTS distribution cables will follow.

Hence we have shown by means of the Amsterdam project example that more effort to reduce costs is needed for successful integration of HTS distribution cables.

The important incentive for early integration of HTS distribution cables is an optimal cooperation between the transmission and distribution operators.

4.4 Discussion

The Dutch HTS cable project presented in the previous section shows its technical ability to contribute to upgrading the future distribution grid by adding higher power capacity, lower losses and reduction of the fault currents.

Besides the reliability issue (requiring to install adequate mature cables in parallel for the time being), the relatively high cost of HTS cable compared to the conventional cable at present forms a bottleneck for integration of HTS cables in the distribution grid.

Investment costs analysis shows that it is currently difficult for the HTS distribution cable to compete economically with XLPE cable. However, we expect that integration of HTS transmission cables will enable deeper penetration of HTS distribution cables. When HTS transmission cables have shown their maturity and reliability, it will become economically beneficial to start integration of HTS distribution cables in the Dutch grid. This process can be accelerated by e.g., providing a cooling from the HTS transmission system to the distribution system. In case HTS transmission and distribution cables are implemented in the grid, a HTS transformer could provide the electrical termination in the cold area, resulting in an efficient connection. To conclude, more research and development effort focusing on the cost reduction of cable components is needed before HTS distribution cables can be widely integrated in the distribution grid.

4.5 Conclusions

In this chapter it is shown that as compared to a conventional cable, the HTS distribution cable provides more power transport capacity to the grid together with lower AC loss, consumes less reactive power, has no negative thermal interaction with the surrounding environment, has almost no external magnetic field, enables bidirectional flows, is more compact and provides intrinsic fault current limitation (the concept of such HTS cable is addressed in Chapter 5).

As an example, we identified a 6 km-long connection in the Alliander distribution network in Amsterdam, between two 150 kV substations Hoogte Kadijk and Noord Klaprozenweg, where HTS cable could demonstrate the above mentioned advantages. In this case, the future demand in higher power capacity of the connection can be met by retrofitting one of the existing aged copper cables with HTS cable.

A comparative network study of this connection is conducted for two available circuit options (1: three existing 150 kV conventional underground cables with total capacity of 300 MVA using three 150/50/10 kV transformers, and 2: two 150 kV citycables –CC with total capacity of 400 MVA- using two 150/50/10 kV transformers in parallel to one HTS cable with capacity of 250 MVA using one 150/50 kV transformer). The study shows that at delivered power of 200 MVA more power (112 MVA) flows via the HTS cable (due to its lower impedance) as compared to both CC (75 MVA), while the short circuit current for option 2 remains the same as in option 1 (peak below 60 kA) due to the intrinsic fault current limiting property of the HTS cable. The calculated (at the same delivered power of 200 MVA through the connection) losses for options 1 and 2 are: 4.2 and 2.3 GWh, respectively.

With the use of the triaxial HTS cable integrated in the distribution grid of Essen, Germany in 2014, the grid was strengthened and the technical abilities of HTS distribution cable were demonstrated.

To compare, the allowable investment costs of the Dutch triaxial HTS cable in the above example are estimated at 1.6 M€/km). Based on the studies performed in the Alliander network connection, the total initial investment costs and total lifetime costs for the existing and proposed Alliander network (option 1 or 2) are estimated to be 11 or 20 M€ and 29 or 32 M€ respectively. At the HTS tape price of 19 €/kA·m) the total lifetime costs of both options are the same.

We conclude that expansion of the grid with conventional CC is at present more cost effective and that integration of HTS distribution cables will only become feasible, when the price of HTS tape (and other HTS cable components) is reduced substantially. At this moment, HTS distribution cables are only suitable in niche applications, where their technical or environmental benefits prevail. Based on our assumption made we expect that HTS transmission cables will be integrated first, followed by HTS distribution cables as soon as the HTS tape price is acceptable and the cooling infrastructure for HTS transmission cables is sufficiently developed.

5

HTS AC distribution cable design (50 kV)

Based on the technical specifications discussed in Chapter 4, a concept of HTS distribution cable is explained. Targets to implement the HTS distribution cable in the Dutch grid are challenging, requiring a decline from today's levels of AC loss, lower cryostat heat leak and friction loss, a fault current limitation capability together with the transition to cheaper HTS tapes. The target feasibility is supported by theoretical studies, engineering and laboratory measurements.

- 5.1 State of the art
- 5.2 Concept and interior arrangement
- 5.3 Terminations
- 5.4 Temperature profiles
- 5.5 Cooling
- 5.6 Intrinsic fault current limiter
- 5.7 Electrical imbalance modeling
- 5.8 Conclusions

5.1 State of the art

Examples of medium voltage HTS AC cables are: 34.5 kV, 800 A Albany cable [97], 13.2 kV, 3 kA Columbus cable at American Electric Power's Bixby substation in Ohio, operated between 2006 and to 2012 [95] and 10 kV, 40 MVA Essen cable [22] (discussed in the previous chapter). The highest distribution voltage is met in Yokohama project: a 66 kV, 200 MVA, 240 m-long, 150 mm outer diameter cable is installed and operated for over one year at the Asahi substation, Yokohama [96]. All these cables are using a single cryogenic envelope and their cores were made with BSCCO tape. Furthermore, at the end of 2016, a 170 m-long, 13.8 kV, 4 kA triaxial cable in Manhattan will be commissioned. This cable uses 2G tapes in the core enabling a high capacity fault current limiting link between two substations in New York City [57].

5.2 Concept and interior arrangement

In this section, the concept and the interior arrangement of the 50 kV HTS distribution cable are explained for the Dutch superconducting medium voltage cable (DSMVC) project with the specifications derived in Chapter 4.

The HTS cable uses the cold dielectric design (see examples in Chapters 1 and 3) further discussed below. The distribution and transmission HTS cables are different in the way that the triaxial distribution cable has three phases arranged concentrically inside one cryostat [97]. This cable configuration is more compact, saves on the HTS tape length, costs, has lower outer magnetic field, etc.

Restrictions for the DSMVC are as follows [91]. The cable has to be installed in existing steel duct of 150 mm \varnothing over a six kilometer long length. Therefore the cable outer diameter is restricted to 139 mm. Moreover the cable must be capable of limiting the fault current within three AC cycles. And it has to recover from the fault without being switched off the grid. Furthermore, only two cooling stations are allowed (placed at the cable ends).

In Figure 1.3 an impression of such cable concept was shown. The cable itself consists of: the former, cable phases, electrical insulation, sheath and cryostat. The cable phases are wound onto a non-magnetic former. The phases and the neutral are electrically insulated from each other by the Cryoflex™, which is fully immersed in liquid nitrogen. Cryoflex™ operates in liquid nitrogen and therefore has better dielectric aging properties. The liquid nitrogen flow goes through the former and returns in the space between the cable sheath and the outer cryostat.

5.2.1 Design constraint for the HTS distribution cable

Design targets for a 6 km HTS triaxial cable for DSMVC project are [98]:

- AC core losses below 0.2 W/m/phase;
- Cryostat loss below 0.5 W/m;
- Cryostat pressure drop below 2 bar;
- Cooling penalty as low as possible in order to reduce the cooling losses;
- Maximum outer cable diameter of 139 mm in order to retrofit the cable in existing tube with an outer diameter of 150 mm;
- Limit a fault current within 60 ms to 4 kA_{rms};
- Acceptable neutral current.

5.2.2 HTS core

State of the art ways to reduce the AC loss of a HTS core (without a substantial increase of its costs) would result in the core losses of 1 W/m, which is not sufficient for the Amsterdam cable. Therefore, we studied and used alternatives.

In Figure 5.2 impressions of the tape arrangement around the cable former are presented. The left and right drawings indicate tape arrangements for 13 and 44 tapes respectively, placed around a former of the same diameter. One can see that narrower tapes fit better to the roundness of the former. As a result the magnetic field perpendicular to HTS tapes is reduced and the AC losses decline [23].

Alternatively a larger diameter of the core also results in a better fit of the tapes to the roundness of the former. Obviously, a larger core diameter for the same tape width leads to an increase in the number of parallel tapes around the core perimeter. This results in a higher critical current of the HTS core. Moreover, a larger core diameter gives smaller amplitude of the magnetic field (to which HTS tapes are exposed), which also leads to AC loss reduction. Reference [23] gives more details on the applied strategy to reduce the AC loss in HTS cable core.

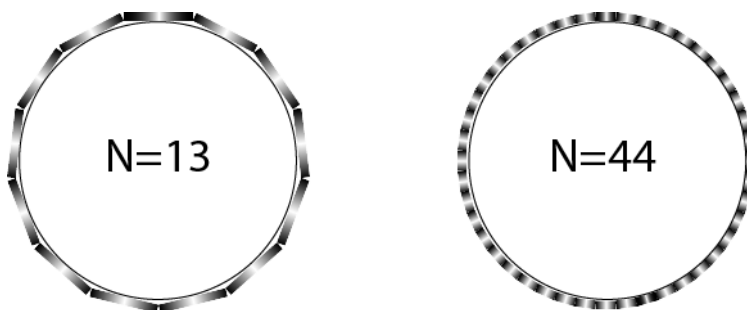


Figure 5.2 Arrangements of tapes around a same former size.

Three cable cores were manufactured using different strategies in order to reach the total cable loss target of 0.2 W/m using the AC loss reduction approach. The HTS cores were made by hand in order to get a better feeling of how to improve the arrangement. Three set-ups were investigated for tape widths of 6, 4 and 3 mm, which we referred to in this thesis as set-up 6, 4 and 3, respectively. So, each of the core samples were made with different tape widths to support the AC loss decline. Practical reasons limit HTS tape width to a minimum of 3 mm.

In case of the DSMVC the tape width is in fact fixed by the 3 mm limit and the former diameter is selected based on the maximum cable diameter allowing the cable installation in the existing cable conduit. The core is made of non-magnetic material to prevent eddy current loss. Care is taken to minimize the gaps between neighbour HTS tapes in each layer. Multiple HTS tape layers must be sufficiently insulated from each other minimizing coupling currents. The core manufacturing will be explained in more detail in the next section. The core losses for the 6 km cable could be further reduced by grading of HTS tapes as described in Chapter 3.

5.2.3 AC losses in HTS conductors

AC losses in a superconductor consist of three main components: hysteretic loss, coupling loss and eddy current loss [99]. Hysteretic loss occurs due to external magnetic field (direction, amplitude, frequency, shape, phase in respect to the phase of the transport current are important), and magnetic field of the transport current (frequency, amplitude and shape are important) through the superconductor. Magnetic flux penetrates into the superconductor and causes hysteretic loss. Coupling losses arise when within the superconductor a conducting path exists along with the e.m.f. induced for instance by changing magnetic field; therefore induced currents are created. Moreover, when phase layer inductances do not match, a coupling current can run through these individual layers and create additional loss. If tape layers in the same phase are not electrically separated by an insulation layer, point contacts are formed, which also contribute to the coupling loss. Subsequently coupling currents contribute to AC-loss to a large extent. The current distribution through the tapes becomes highly non-uniform when coupling currents are formed. Coupling currents may flow in the same or in opposite direction with respect to the transport current. Besides hysteresis and coupling losses, eddy current losses occur as a result of current induced in the normal metal stabilizers (copper, silver, etc.). Eddy current losses occur due to the transport current and external magnetic field. In YBCO superconductors the magnetic field component perpendicular to the broad side of the superconductor causes the highest AC-loss [99]. Compared to that, the magnetic field component parallel to the YBCO tape can be generally neglected since the YBCO thickness is typically about 1 μm . When the tapes do not exactly follow the concentric former and/or have gaps between them, the magnetic field will penetrate through the tapes longer edges resulting in additional AC-loss [100, 101].

5.2.4 Arrangement and manufacturing

Three HTS cable core conductor samples were prepared, Set-up 6, 4 and 3, to verify the reduced core AC losses explained in the previous section. An example lay-out of a core and the core ready for measurement is shown in Figures 5.3a and b. The commercial tapes SCS3050 from Superpower were used in this case. The tape consists of: 1 μm thick (RE)BCO layer; 2 μm thick silver over-layer 20 μm thick surround copper stabilizer and 50 micron Hastelloy substrate. No additional tape stabilizer was used which resulted in thin and flexible tapes.

The cable is built on a rigid glass-fibre reinforced plastic (FRP) former. This glass-fibre reinforced plastic is not magnetic and has no eddy current loss. To adjust the cylinder outside thickness, a thin layer of Tyvek is wound onto the outer side of the cylinder to meet the required diameter for the conductor layer and to prevent the tapes from buckling. In case of the Set-up 3, 44 tapes of approximately 3.30 metre length were spirally wound on the former making the first layer. Next, the second layer of 44 tapes was wound in opposite direction. The 1 μm thick YBCO layer in the HTS superconductor is not exactly located in the middle of the in total 100 micron thick tape. To reduce the distance between the YBCO layers, the first tape layer is faced radially outwards, the second YBCO layer is faced radially inwards. The cable conductor ends are soldered onto two massive copper contact tubes of 20 cm in length. The copper contacts fit very smoothly over the glass-fibre reinforced former and were not fixed to the former. In this way the free contraction of materials is allowed preventing the tapes to buckle when cooling down. The thickness of the copper contact tubes was approximately 5 mm and a mechanical stress cone prevented any mechanical stresses to the tapes and distributed the tapes equally over the tubes.

To measure the voltage drop correctly, the voltage taps (V1 and V2, see Figure 5.3b) were placed before tape transitions. These voltage taps are ring shaped and soldered almost perpendicular to all the tapes. Due to the ring shaped voltage taps all tapes (in the outer layer) are short circuited, therefore the voltage over each tape between the voltage taps is equal. The distance between the two voltage taps is 2.60 metre and they are at equal distance from the cable connection ends.

The winding angle of the outside layer can be easily seen in Figure 5.3a, indicated by the tape winding angle α . The core contains two HTS tape layers with opposite twist pitch, see Table 5.1, minimizing currents flowing in the created loops. Specifications of the HTS conductor are given in Table 5.1. The total conductor DC critical current I_c is not measured, but calculated from the individual tape critical currents of the tapes used, provided by the tape manufacturer. The available tapes were just enough for assembling the samples and therefore it was impossible to further improve the design by tape grading. More tape and cable specifications for the 3 mm model are shown in Table 5.1.

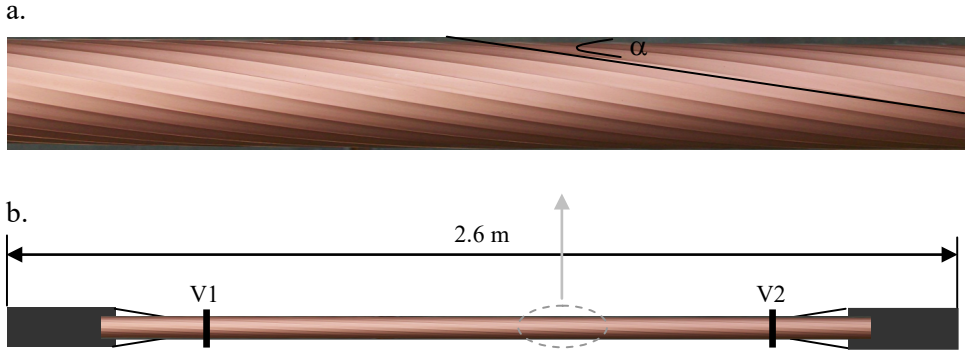


Figure 5.3 Photo of the Set-up 3 core with the pitch angle indicated (top), sketch of the cable with the current contacts and voltage taps (bottom).

Table 5.1 HTS single phase cable core model made with 3 mm tapes.

Cable conductor parameters	Layer 1	Layer 2
YBCO tape used:		
Manufacturer of tape	Superpower	
Tape width, mm	3	
Number of tapes in one layer	44	44
Total tape length, m	~140	~140
Calculated cable I_C , A at 77 K	3855	4114
Calculated n-value* @77K	25.49	25.17
Dimensions of cable:		
Former	Glass-fibre	
Inner diameter, mm	42.09	42.66
Outer diameter, mm	42.28	42.77
Cable length (between voltage taps), m	2.6	2.6
Average gap size between tapes, mm	0.05	0.05
Other characteristics:		
Twist pitch angle, degrees	-10.40	12.33
Twist pitch, mm	-720.50	610.40

* V-I transition slope to the normal state

5.2.5 Experimental setup

Set-up 3 was tested at 77 K in liquid nitrogen boiling at atmospheric pressure using a dedicated low voltage test facility of the Danish Technical University (DTU) [102]. AC-loss measurement of the single-phase conductor core was performed using the measurement set-up shown in Figure 5.4.

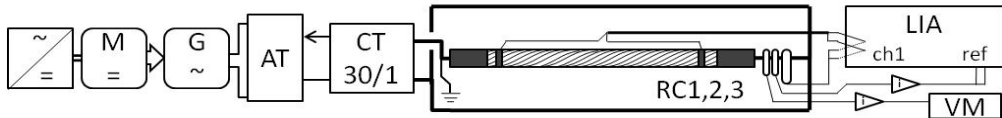


Figure 5.4 AC-loss measurement setup, where: \sim/\simeq is the AC/DC drive, M is the motor; G is the Generator; AT is the auto transformer; CT is the current transformer; RC the Rogowski coil; LIA is the lock in amplifier (enabling sensitive measures of voltage amplitude and phase angle); VM is the voltage measurement [102]. (Courtesy Dag Willén, nkt cables group a/s)

The measurement circuit is energized by an AC/DC drive to control a DC motor which is mechanically coupled to a generator. To exclude disturbance of the 50 Hz grid, the generator produced a voltage with a frequency between 59-61 Hz. The generator is connected to an autotransformer in series with a current transformer that provides AC current through the cable.

The (return) current leads were symmetrically arranged to prevent any asymmetrical magnetic distribution through the cable. One cable end was connected to earth potential.

The voltage was measured with two soldered voltage taps (see Figure 5.3) around the core circumference on a distance of 2.6 m from each other. Voltage leads connecting the voltage taps with the measurement equipment were spaced by spacing tubes, about 3 mm above the cable core in order to reduce interference. The voltage signal was measured at several transport current amplitudes by a lock-in-amplifier (LIA). The loss is calculated by the multiplication of this RMS loss voltage and RMS current through the cable.

As shown in Figure 5.4, three Rogowski coils were used during the measurement. Two Rogowski coils (RC1, RC2) were connected with an integrator amplifier (i) to measure RMS voltage and a stable input reference signal for the LIA. RC1 measured the current through the cable by using the voltmeter. To be absolutely sure no angle displacement occurs, a third Rogowski coil was used to measure the “raw” non-amplified signal with the exact phase of the current.

The voltage and current measurement was performed on the same LIA channel in order to measure the smallest phase shift possible between the voltage and current measurement as accurate as possible. Switching between the two signals was done either manually or by a programmable data-acquisition switch.

To summarise, the following measurement procedure was followed:

- 1) At first the RC3 was connected to the LIA to measure the 90 degree out of phase component of the current;

- 2) Thereafter the cable voltage leads were connected to the LIA, to measure the cable voltage;
- 3) Again RC3 was reconnected to make sure that the first harmonic of the raw Rogowski signal remained exactly 90 degree by adjusting the internal phase compensation of the LIA;
- 4) If more measurements were required, steps 1 to 3 were repeated.

The accuracy of the Rogowski coil to verify the currents phase angle of 90 degree was -0.003 mV for the real part of the signal at the selected amplification. To increase the sensitivity, an interpolation was made between two phase compensations. The 0.01 -degree step sensitivity reflects in a voltage of 0.003 mV. Some measurement points were close to this maximum step (0.003 , 0.006 , etc). Therefore, we decided to measure the positive and negative phase compensation for two points and interpolated both measures to obtain an increase in the sensitivity of the measurement.

To verify the test circuit, a preliminary DC current test at room temperature was done. The DC voltage measured was 4.1 mV at 1 A, a second test at 10 A measured 42 mV DC. The room temperature DC resistance was calculated to be 4.15 m Ω . After the DC test an AC current test was done with $113A_{\text{rms}}$ and the cables in-phase voltage was measured. Hence the AC resistance was calculated to be 4.3 m Ω , which was around 4% higher than the DC resistance. The similarity in AC and DC resistance revealed that the measurement setup connection could be approved.

5.2.6 Measurement results

In this section AC loss results of the cable sample are presented and compared to the numerical results calculated with a model made in the COMSOL program [100]. The sample critical current and n index (voltage-current relation) is deduced from Superpower manufacturer's measurements on each tape [23].

Our main result is that the measured AC loss for the sample shown in Table 5.1 amounts 0.115 W/m at a transport current of 3 kA $_{\text{rms}}$, frequency of 60.2 Hz and temperature 77.3 K [23]. The measurement is repeated several times and resulted in the same loss. Since the operating frequency of the DSMVC is 50 Hz, at 3 kA $_{\text{rms}}$ the calculated AC loss is 0.096 W/m as indicated in Table 5.2. The measured AC loss of the cable sample as function of the transport current amplitude (scaled by the critical current) is presented in Figure 5.5. Using the model [100] the AC losses calculated for the same conditions are in good agreement with the measurement [23]. The theoretical AC loss of the sample without magnetization currents (static loss, resulting from the static V-I curve) is also shown for reference by the black dashed line in Figure 5.5.

Table 5.2 Comparison of measured AC losses for a 3 kA-class YBCO cable [23].

Parameter	Set-up 3mm conductor	Furukawa conductor [65]
<u>AC loss at 3 kA_{rms}, 77 K and 50 Hz</u>		
Measured AC loss, W/m	0.096 [♣]	1.3
I_c , kA of the conductor (77 K, self-field)*	7.5*	4.7
Index n for the DC I-V curve of the cable	26*	-
Scaled transport current amplitude i^\blacklozenge	0.57	0.90
<u>Lowest AC loss at 3 kA_{rms} and 50 Hz</u>		
Measured lowest AC loss, W/m	0.096 [♣] (77 K)	0.235 (68.7 K)
I_c , kA of the conductor (self field)	7.5* (77 K)	9.2 (68.7K)
Scaled transport current amplitude i	0.57	0.46

* Estimated from the measured I_c and n of all individual tapes

♣ The loss of 0.115 W/m measured at 60.2 Hz, gives 0.096 W/m at 50 Hz

♠ $i = I_{tr0}/I_c$

As expected, at current amplitudes higher than $i > 0.8$, the calculated AC loss using the model approaches the static one [101] (resulting from the static V-I curve, the static losses account only for the contribution to the AC losses of DC I-V characteristic of the cable conductor at a sinusoidal transport current and the index $n = 26$ in this case, with all magnetization currents suppressed). For comparison the Furukawa cable specifications [103] are also indicated in Table 5.2. The Furukawa loss measured at 68.7 K was 0.235 W/m, at the total cable I_c that is factor 1.2 higher than the DSMVC project sample model.

Also Figure 5.5 shows the measurement results for Set-up 3, of which, the AC losses are indicated by the blue rhombs. The calculated AC losses indicated by the bold red line, are in good agreement with the measured one's. The respectively red and blue thinner solid lines represent the AC losses calculated for respectively 84 and 46 stand alone Norris tapes on a former [100].

One can see that in the Furukawa cable, due to the larger gaps between tapes AC loss agrees reasonably well with Norris theory (N=46), while in our cable (due to the incorporated loss reduction measures) actual measured AC loss is far below that predicted by Norris theory (N=84).

As a result, at 3 kA_{rms} (77 K, 50 Hz) AC loss in our cable is over 13 times lower than that in Furukawa cable, Table 5.2.

Additional confidence is gained by the positive validation of measurement results by Furukawa that were performed on a sample using the former diameter of 33.3 mm, comprising two layers of (in total of 61 tapes) 3 mm-wide YBCO tapes

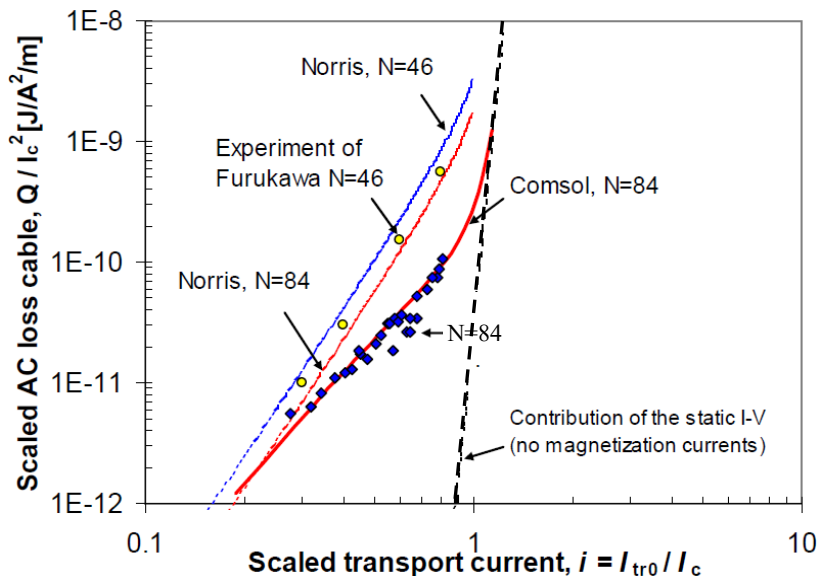


Figure 5.5, Ac loss measurement results [23]: the blue and the thinner red lines represent model of Norris (for $N=46$ and 84 tapes respectively), the yellow circles represent Furukawa experimental results ($N=46$), the thicker red line represents: Cmsol model result ($N=84$), the blue rhombs represent the experimental results ($N=84$), the dashed black line represents the static AC loss.

(with laser-trimmed 0.1 mm edges): at $3 \text{ kA}_{\text{rms}}$ the measured AC loss amounts 0.124 W/m at 60 Hz , 74.4 K , with I_c of 8150 A at this temperature and 6270 A at 77.3 K [103]. Note that from this data we calculated a loss in the Furukawa sample at 77.3 K , 50 Hz and $3 \text{ kA}_{\text{rms}}$ is 0.39 W/m , which is still 4 times higher than in our sample. This result is expected, since our sample has larger former diameter (1.3 times) and respectively lower amplitude of magnetic field acting on HTS tapes (both parallel and perpendicular components). In conclusion, our method using commercially available HTS tapes, is more practical (no tape modification needed, such as laser-trimmed edges) and results in lower AC losses as compared to the Furukawa approach.

Furthermore, in Table 5.3, Set-up 6 and Set-up 3 for the DSMVC project project (3, 4) are compared with two cable samples (1, 2) from the Entergy project, which were kindly provided by Ultera [104].

As for the DSMVC project cores, each of the Entergy cores is made of two layers, which were mounted onto the former with proper selected twist pitch and minimized gaps to equalize current distribution in the layers. The AC loss results depending on the transport current for the samples 1 to 4 are specified in Table 5.3 and are also shown in Figure 5.6. In conclusion we see an increasing loss for increasing P_{AC} , for all samples according to our expectations. Furthermore, lowest loss is shown for Set-up 3, according to the high critical current, tape width, gap size, former material, etc.

Table 5.3 Measurement results of HTS models: 3, 4, 6 mm core models (frequency 60.2 Hz).

	Sample 1	Sample 2	Sample 3 (Set-up 6)	Sample 4 (Set-up 3)
Project	Entergy/ New Orleans	Entergy/ New Orleans	Alliander/ Dutch project	Alliander/ Dutch project
Diameter [mm]	60	60	42	42
Former	Stainless- steel	Stainless- steel	Glass-fiber	Glass-fiber
ΣI_c (tape, 77 K)	6000	5500	9100	7500
HTS tape width, [mm]	6	4	6	3
Gap size, g_m [mm]	0.8	1.4	0.05	0.05
P_{AC} @ 1.0 kA _{rms} [W/m]	0.12+-10%	0.12+-10%	0.05+-20%	0.01+-100%
P_{AC} @ 2.0 kA _{rms} [W/m]	0.52+-10%	0.55+-10%	0.26+-20%	0.04+-100%
P_{AC} @ 3.0 kA _{rms} [W/m]	1.40+-10%	1.60+-10%	0.65+-20%	0.11+-100%
P_{AC} @ 4.0 kA _{rms} [W/m]	n/a	n/a	1.50+-20%	0.25+-100%

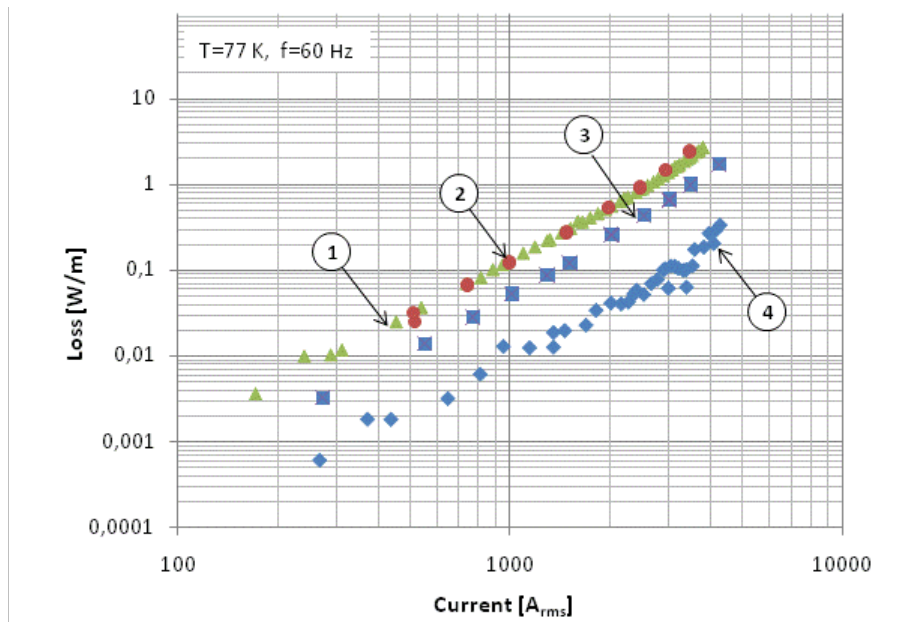


Figure 5.6, Measured at 77K and 60 Hz AC losses vs I_{rms} in four different cable samples made from 2G superconductors from Super Power Inc. The samples are different in terms of diameter, D , tape-width, w , and gap size, g . These parameters are, in mm, 1) 60/6/0.8; 2) 60/4/1.4; 3) 42/6/0.05; 4) 42/3/0.05 for $D/w/g$ respectively. Further construction parameters of samples 1-4 are given in Table 5.3. (Courtesy Ultera® - A Southwire / nkt cables Joint Venture)

5.2.7 Electrical insulation

The characteristic electric field strength of a HTS AC cable is explained in Chapter 3. The insulation thickness for the DSMVC project is based on the peak stress that normally occurs at the surface of the cable in accordance to the IEC 60840 [105].

For the required thickness of Cryoflex between the phases the peak electric stress has to be known. Usually the peak stress is selected to be one third of the working stress for safety reasons. The required thickness for the electrical insulation, t_{ins} can be described by the following formula [75]:

$$t_{ins} = R_1 \left(e^{\frac{V}{E_m \cdot R_1}} - 1 \right) \quad \text{Eq. 5.1}$$

where R_1 is the outer core radius, V conductor voltage, E_m the peak stress.

For the selected peak stress and the outer core radius of 40 kV/mm and 42.76/2 mm respectively, this results in an insulation thickness of 1 mm.

The 40 kV/mm stress is deduced from the breakdown results for 1 mm PPLP insulation [106].

A new test cable for type testing the electrical insulation is developed, using finite element calculations in order to calculate the electric field distributions in the sample. Based on the calculations we made a new electrical test sample to perform an electrical type test program according to IEC 60840. The test program successfully passed the electrical tests for $U_0 = 50$ kV in the appropriate test facility [107]. The new test sample design is described in more detail in Appendix B.

Recommended test scheme for HTS cables system is listed in Appendix B. More information on HTS cable test requirements can be found in Cigré brochure 538 [108].

5.2.8 Cryostat and hydraulics

To acquire HTS cable applications with longer distance between cooling stations, a reliable cryostat with low pressure drop and low friction factor is essential. In order to address this problem, we designed, manufactured and tested a special low-friction cryostat, as explained below.

The friction factor depends on several factors such as Reynolds number, corrugation height, corrugation length, pitch etc. [109]. The setup and the experimental procedure of measuring the pressure drop and friction factor of a 47 m long cryostat containing a HTS model cable are described in [68].

The total pressure drop in a conduit is:

$$\Delta p = f \rho w^2 L / (2D_h) \quad \text{Eq. 5.2}$$

where, f is the friction factor, ρ is the fluid density, w is fluid velocity defined as $G/(\rho F_c)$, L is tube length, D_h is hydraulic diameter of the tube defined as $4F_c/P_w$, F_c is cross-sectional area of the flow, P_w , wetted perimeter of the flow.

For classical straight rigid pipes with a certain wall roughness, the friction factor can be extracted from the Moody's chart [109]. HTS cables usually have more complex geometry and a better estimate of the friction factor can be achieved using expressions as in [110, 111, 112]. Here, one measured the friction factor (f) of the annulus between the cable outer surface with diameter D_c and the inner cryostat wall with diameter D_i . In this case, the hydraulic diameter is given by $D_h = D_i - D_c$.

The hydraulic circuit for testing the cryostat is explained in Figure 5.7. The 47 m long cryostat consists of three straight sections made from smooth tubes and two flexible sections made of corrugated tubes.

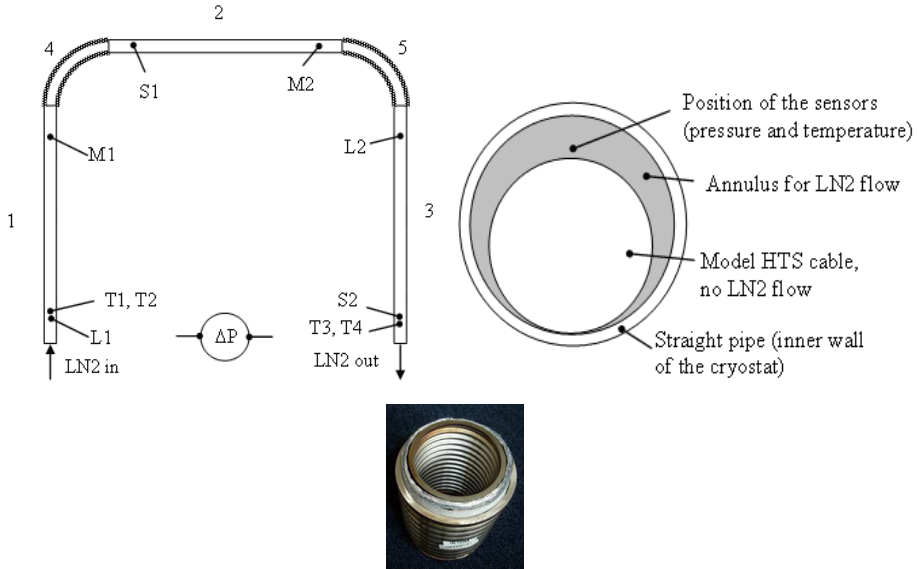


Figure 5.7 Left top: schematic representation of hydraulic circuit for testing the cryostat: 1, 2 and 3 are the three straight sections (each 12.5 m long); 4 and 5 are the two flexible sections, (each 4.5 m-long); labels of the points are also shown where the capillary tubes probe the pressure in the flow of liquid nitrogen (L1,L2;S1,S2;M1,M2) and where the temperatures are measured: T1, T2 (inlet of the cryostat, two measures averaged to increase accuracy) and T3, T4 (outlet of the cryostat). Right top: The differential pressure meter can be connected to any of the capillary tubes via a manifold (not shown in the figure). Right: Hydraulic

cross-sectional view of the model cryostat (straight sections). Centre below: cryostat used in the measurement without the dummy cable.

A dummy HTS cable was inserted into the cryostat (Figure 5.7 right). Liquid nitrogen was circulated in the annulus between the dummy cable surface, and the inner cryostat surface, Figure 5.7, right. Each straight section was 12.5 m long, with 0.100 m inner diameter and roughness 0.1 mm. Each corrugated section was 4.5 m long, with 0.098 m inner diameter, with the corrugation depth and corrugation length 3 mm and 3 mm respectively. The outer diameter of the dummy cable was 0.081 m and its length was equal to that of the cryostat. Calculated hydraulic diameters for the straight and the corrugated sections are 0.019 m and 0.017 m respectively. As shown in Figure 5.7, left, the corrugated sections were 90 degrees bent. The cable dummy had welded end caps at the ends to prevent the LN₂ from flowing inside the cable dummy/model.

A photograph of the complete setup for hydraulic test of the cryostat is given in Figure 5.8. The setup consists of the cryostat, with the insert HTS cable, the cooling machine, the vacuum pumps, the connecting tubes, the capillary pipes, wires, cables, measurement instruments and data acquisition system.

Four precision thermometers PT100 were mounted in the nitrogen flow inside the cryostat (points T1, T2, T3 and T4, see Figure 5.7 and connected to the multi-channel temperature measurement system MIT 8.15 (MIT 8.15 [113])). Six capillary tube probes were mounted in the flow (points L1, M1, S1, M2, L2 and S2, see Figure 5.7) to measure the pressure drop along the cryostat. The absolute pressure and the flow rate were measured using precision differential pressure meter Emerson 3051S1CD2A* (± 200 mbar; 0.025% span accuracy) at the flow entrance (outside the cryostat by the cooling machine, see Figures 5.7 and 5.8). The capillary pipes probing the flow pressure were placed inside the dummy cable and fed through the cryostat ends and connected to the manifold at room temperature. Using the manifold, any two capillary pipes could be connected for precision differential pressure measurements. In each measurement, we swapped two capillary tubes connections to the differential meter in order to eliminate any offsets. Care was taken to place the setup horizontally to avoid pressure differentials due to height differences.

5.2.9 Measurement results

We calculated the average friction factor for the straight and the flexible sections from the measured pressure drop, the mass flow rate, the temperature, the pressure, assuming the weighted average hydraulic diameter of $D_h=0.0186$ m by using Equation 5.2, see Figure 5.9. The dots are the measured points, and the line is the linear fit with Equation 5.3. The two main results are depicted in Figure 5.9: the pressure drop increases linearly with the flow rate and the measured friction coefficient decreases from 0.095 to 0.05 linearly with the Reynolds number

increasing from 4500 to 11500, as formulated by Equation 5.3. A similar decrease was measured in [112].

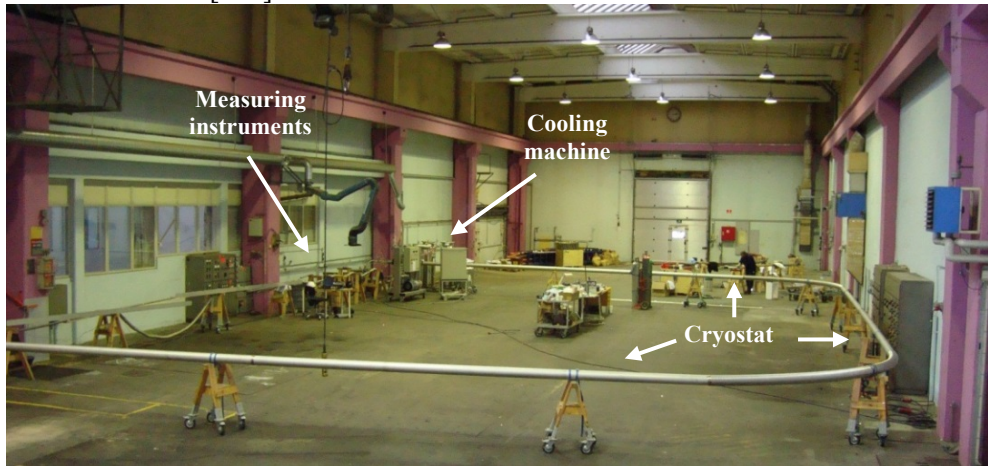


Figure 5.8 Photo of the 47 m-long cryostat for hydraulic testing.

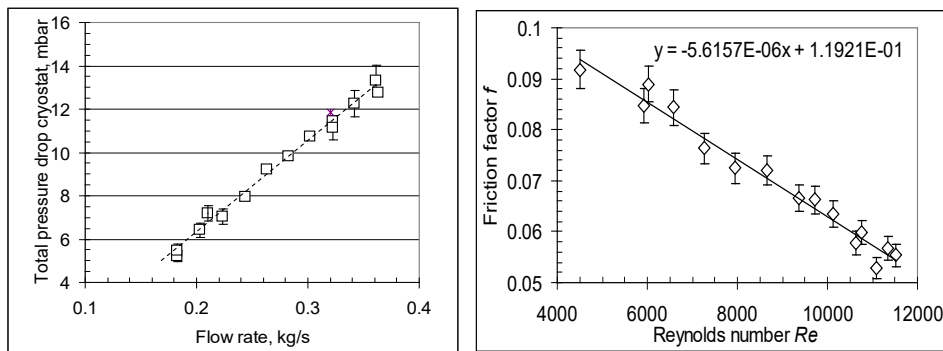


Figure 5.9 Left: measured dependence of the total pressure drop across the cryostat length versus the mass flow rate (the temperature and the pressure varied from 68 to 82 K and from 0.8 bar to 1.5 bar); right: friction factor of the cryostat versus the Re number.

$$f = 0.1192 - 5.616 \cdot 10^{-6} \text{ Re} \quad \text{Eq. 5.3}$$

It is clear from Figure 5.9, left that the measured total pressure drop along the cryostat is 11 mbar at the mass flow rate of 0.3 kg/s and when extrapolated to 0.4 kg/s, gives 15 mbar. The pressure drop goes with the square of the flow rate as shown in Figure 5.9 left. This indicates a decreasing friction factor for higher flow rates. For the cryostat of the same dimensions made entirely with corrugated pipes, the friction factor of 0.1 and pressure drops of 20 mbar and 40 mbar would be expected for same flow rates 0.3 and 0.4 kg/s respectively [111]. Based on the measurement results, the extrapolated pressure drop over the 6 km long Dutch HTS

cable (made with alternating rigid and flexible sections) is below 2 bar (for 0.3 kg/s and 0.4 kg/s, 68 K), which is an acceptable figure.

5.3 Terminations

Figure 5.10 shows the example terminations for the HTS distribution cable installed in Manhattan, New York. As mentioned, the Manhattan cable is also triaxial, linking two substations continuously with each other. Two terminations are shown enabling a three phase electrical connection to the cable. A single termination provides a three phase connection to the core. As shown in the picture, above the Ultera logo the “go” and “return” cooling connections are located, providing the cooling to the cable. Since this termination is for the 13.8 kV triaxial Manhattan cable, the termination for the DSMVC project shall be upgraded to 50 kV. The upgrade shall be associated with an increase of the electrical insulation distance in the termination, which is about proportional to the voltage increase and results mainly in an increase in height. The total length of such termination is 5 meters.

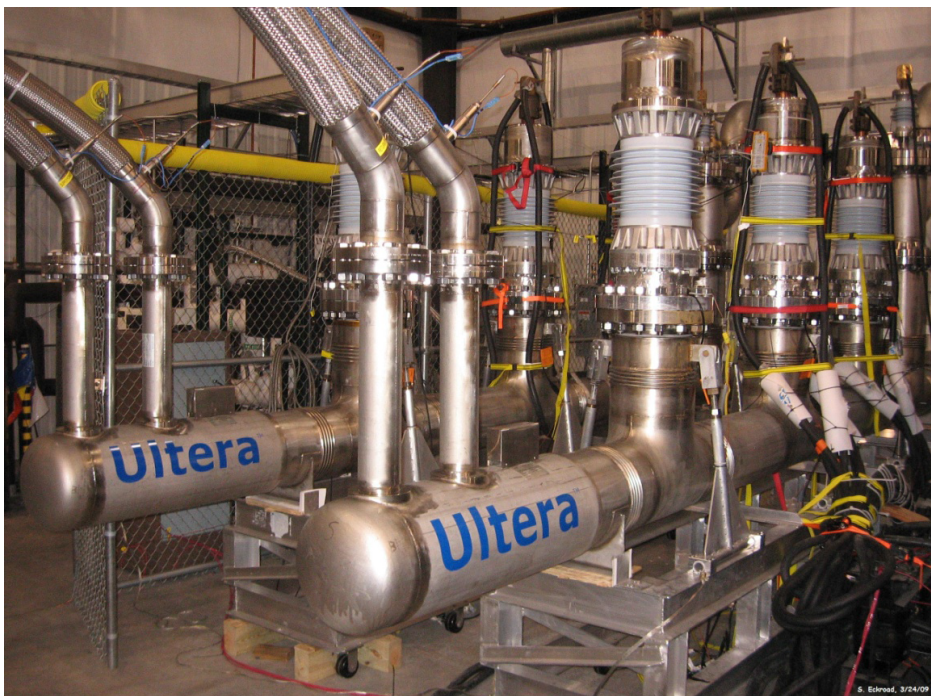


*Figure 5.10 Photo of the HTS distribution cable terminations used for the Manhattan cable which would be similar for the DSMVC cable [15, 57].
(Courtesy Ultera® - A Southwire / nkt cables Joint Venture)*

5.4 Temperature profiles

In Figure 5.11, calculated temperature profiles inside the DSMVC are shown under steady state operation assuming 0.5 W/m and 0.2 W/m cryostat and AC loss, respectively. The profiles are independent of the nitrogen flow, only the absolute temperature changes, see figure below. The results are shown for the cable (a) and for both terminations (b, c). In Figure 5.11a, the temperature distribution with respect to the cable length is shown, and in Figure 5.11b and 5.11c the temperature distribution in the terminations. The cable friction coefficients used in the simulation are 0.04 and 0.08 for the former and annulus, respectively. More input parameters and assumptions are presented in [114].

The results in Figure 5.11 show that it is possible to keep the temperatures within the limits over the 6 km length, between two cooling stations installed at both cable ends. Further investigation shows that the allowed maximum core AC loss for an assumed cryostat loss of 0.5 kW/km is 0.85 kW/km. In case the cryostat loss is 1.5 kW/km, the allowed AC loss is 0.55 kW/km.

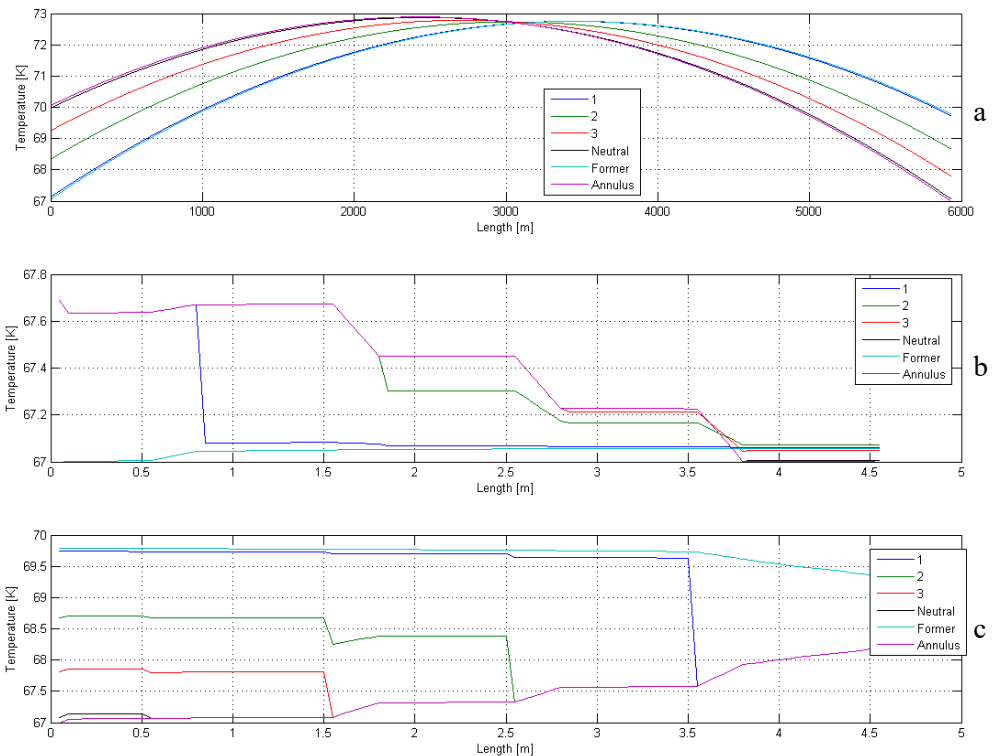


Figure 5.11 Temperature profiles in cable (a) and in terminations left (b) and right (c) [90, 114]. (Courtesy Ultera® - A Southwire / nkt cables Joint Venture)

5.5 Cooling

Currently, cooling has to be provided by cooling stations in the distribution grid. Particularly for pilot projects refrigeration systems would be the most convenient option. In this way experience is gathered with the cooling systems.

In this subsection the options for using available cooling stations are discussed. The total cooling power needed for the 6 km long distribution cable is about 8 kW. This calculation is based on a 6 km long connection containing of 2 terminations, cable and cryostat with a loss of respectively, 3, 0.5 and 0.35 kW/km.

Estimated footprint of the cooling system is therefore 50 m² (Figure 5.13). Most of the footprint contains cryocoolers, backup system with nitrogen vessel and communication equipment as sketched in Figure 5.12 left. A Stirling engine of 4 kW cooling power is presented in Figure 5.13. Two such cooling systems on both sides of the HTS cable is sufficient, see Figure 5.12, this excludes any redundancy for the cooling system.

The terminations, as shown in Figure 5.10, are cooled separately from the cable since they require a substantial part of the cooling power. In this way the overall cooling system is more efficient.

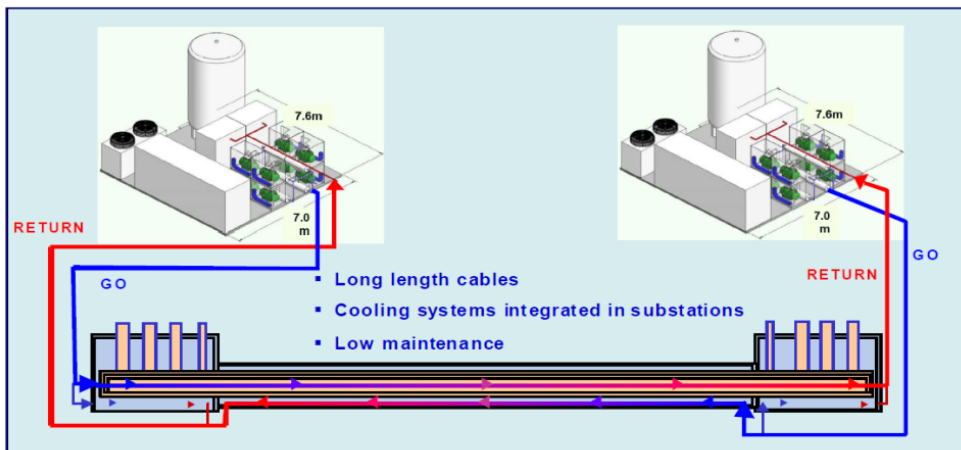


Figure 5.12 Illustration of the cooling system with two cooling stations at the cable ends connected to the inlet (go) and outlet (return) of the cryostat and the terminations being cooled separately [90, 115].



Figure 5.13 Cooling system refrigerator with 4 kW cooling power [90].

5.6 Intrinsic fault current limiter

The excellent fault current limiting characteristics of HTS cables provide the opportunity to upgrade existing distribution networks and to integrate dispersed generation or distributed energy resources (DER) and renewables in an efficient and flexible way as mentioned in Chapter 4.

During the fault, power dissipated in the non-linear resistance will increase the cable temperature. The cable is specially designed to limit the fault before the first circuit breaker opens.

The latest generation of HTS cables has improved non-linear voltage-current characteristics. This means the cable impedance is considerably low during normal operation and it increases if the operating current exceeds the cable I_c , see Figure 5.14. HTS cables with the intrinsic voltage-current characteristic behave intelligently adapting their impedance to the short circuit conditions in the network. As a conclusion, HTS cable with the intrinsic voltage-current characteristic help to obtain a stable grid voltage, furthermore it provides the option to limit short circuit currents.

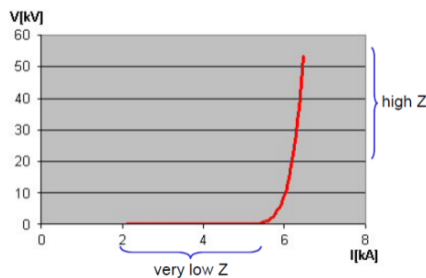


Figure 5.14 Voltage-current characteristics of FCL HTS cable, during normal operation the impedance is very low and if a fault occurs it has the intrinsic ability to increase the impedance rapidly [90, 115].

The FCL modelling of the DSMVC shows that the cable is capable to limit the fault current in compliance with the grid protection management [116]. The model uses the following DSMVC targets; AC loss: 0.3 W/m/phase, cryostat loss: 0.6 W/m and a friction coefficient of 0.08. For the DSMVC a steady state current of 4 kA_{rms} will trigger no current limitation and will keep the heat development in the cable core at reasonable level. The DSMVC will stay in operation during the fault current limiting state. The limited current and temperature modelling results are shown in Figure 5.15a and b, respectively [90]. Figure 5.15a, indicates a maximum current of 15.2 kA_{rms} in the first cycle, which is in accordance with the limiting constrains of the network. After 4-6 current cycles (60 ms) the current is limited to 4 kA_{rms}, which is the allowed let through current. Thermal modelling in Figure 5.15b shows a maximum temperature of about 130 K for the innermost phase 1 at about 3.5 km from the cable end.

In conclusion, the DSMVC has the capability to limit a maximum fault current to about 15 kA within the first cycle. However, as the cable stays in operation during the fault, the 4 kA let through current heats up the cable towards 130 K at maximum, see Figure 5.15 b. More investigation is needed to update the design to prevent excessive heating up the tapes in order to meet the first protection system time (450 ms). As the cable warms up to 130 K in the middle, it is challenging not to overheat the cable at the first protection. An alternative way is to switch the cable from the network, and switch back to the grid when the cable sufficiently cooled down.

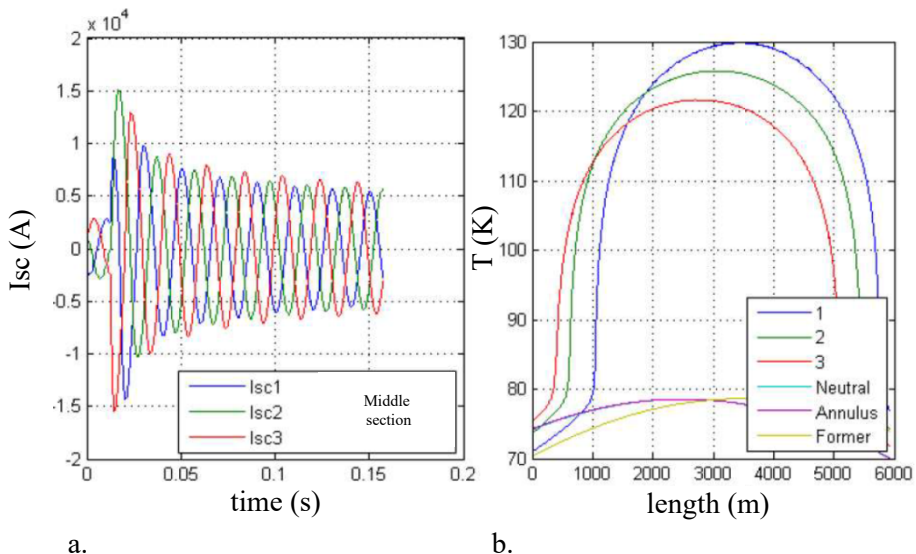


Figure 5.15 Calculated three phase short circuit cable length (x-axis: time in second, y-axis: current to earth, a) and calculated temperature in the cryostat (x-axis: cable length in m, y-axis: temperature in K; (b) [98]. (Courtesy Ultera® - A Southwire / nkt cables Joint Venture)

5.7 Electrical imbalance modeling

Cable phase current optimization is obtained by adjusting twist pitch length for each cable phase. By varying the twist pitch length the cable phase inductance changes, hence magnetic fields penetrating through the other phase tapes will change the phase impedance and cable current distribution. Practical constraints (manufacturing, bending ability) limit winding angles to approximately 12 degrees. Figures 5.16 and 5.17 indicate the effect on the phase and mutual inductance in case of the winding pitch angle is varied from 0 to 53 degree.

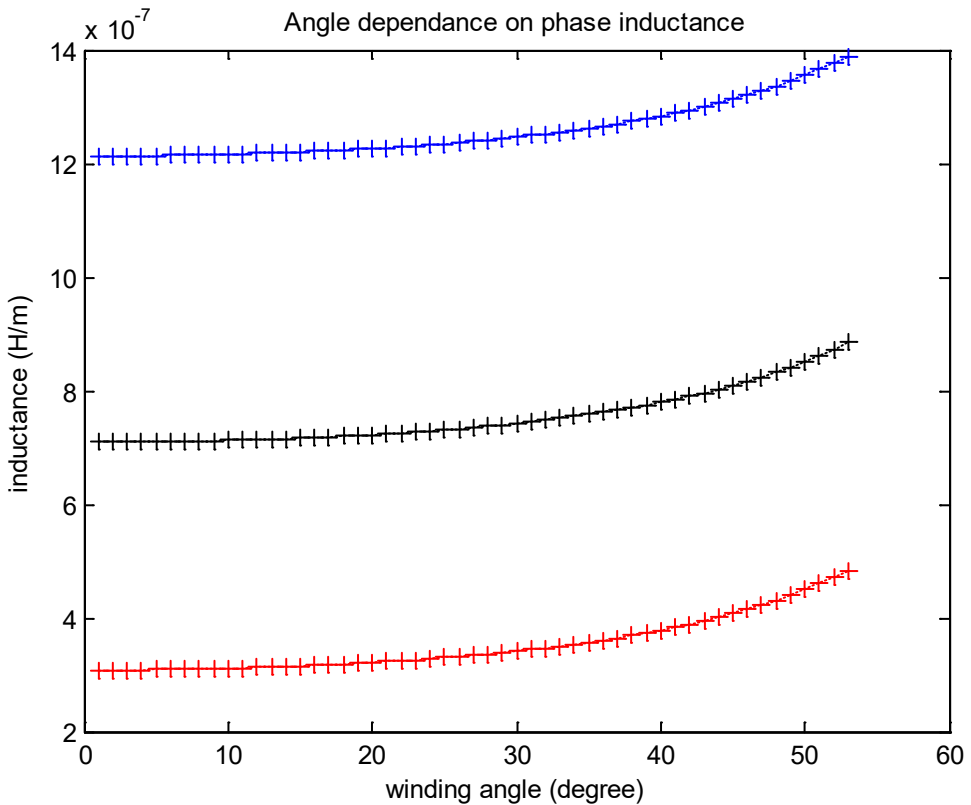


Figure 5.16 Phase inductances with respect to the winding angle for innermost phase (red), middle phase (black) and most outer phase (blue).

In case of more HTS layers per phase the inductances can be lumped to one inductance since the individual winding angles of the individual layers are selected such that the inductances are similar. In this way the phase currents are equally divided through the layers.

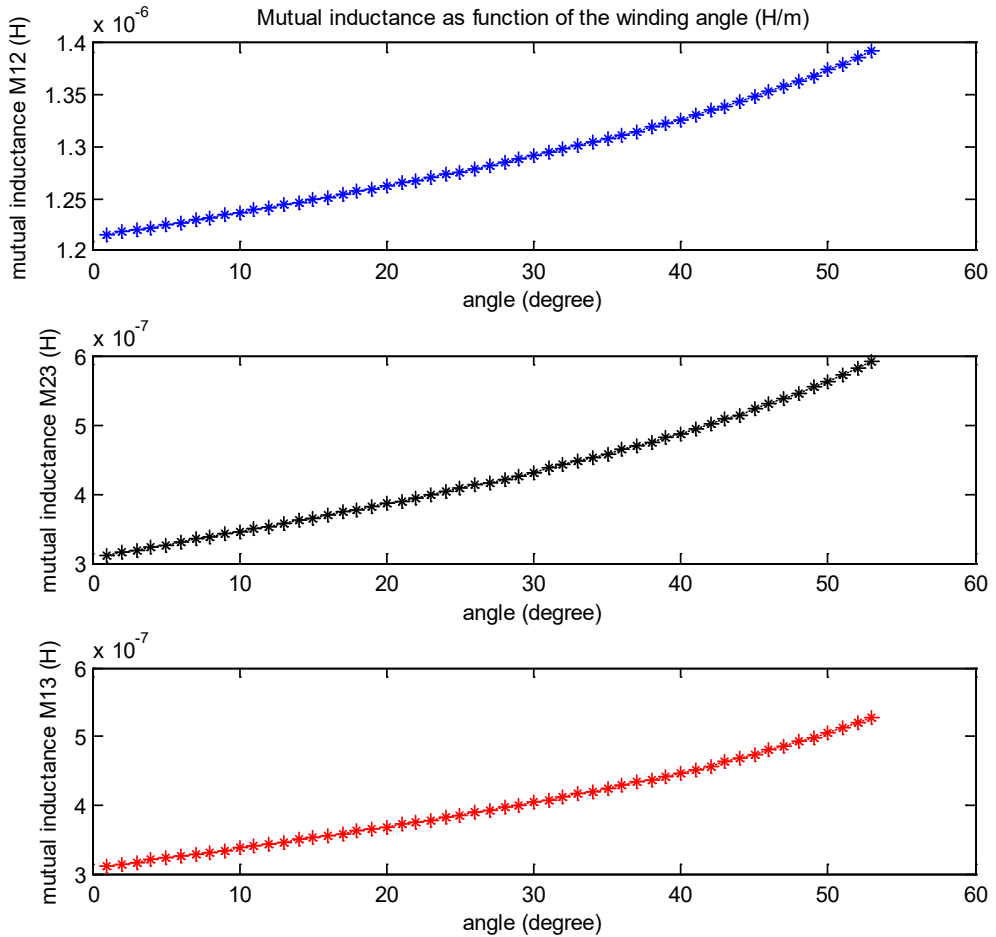


Figure 5.17 Mutual inductance for innermost phase (red), middle phase (black) and most outer phase (blue).

In practice the pitch angle of each phase is determined on the maximum allowable phase current imbalance and the tape costs since a short winding pitch needs more tapes.

Equations to calculate the cable parameters, such as the inductance and capacitance are shown in [75, 117]. As the core is built in a concentric way, the phase currents are not balanced. The amount of imbalance can be found by determining the current in the neutral. The steady state grid performance of the DSMVC is simulated using a distributed π line equivalent [105], wherein the line capacitance is assumed as two capacitances in the pi legs that are half the line capacitance, and the line impedance is represented as a resistance and inductance in series between

the legs. A nominal π equivalent is representative for a cable length in km and an approximately 3000/frequency in Hz [105].

In order to investigate the phase currents imbalance and if phase transposition is needed, the imbalance is investigated by adding the three vector phase currents. By doing so, the current in the neutral of the cable is estimated based on the cable characteristics as shown in Table 5.4. The imbalance is only attributed to the cable, because in a life grid configuration, terminations, earthing method, etc. will have a large influence on the neutral current.

A model to calculate the neutral current is entered in Matlab Simulink™ program to simulate the neutral current by connecting a 3 phase source to the DSMVC and to the other cable end a three phase a star load. The star neutral point load is directly connected to the cable wherein the current is measured in the cable mid-section and the other side of the DSMVC neutral is earthed to ground. The model is in agreement with the results presented in [75].

A neutral current of 220 A is simulated in the DSMVC. The current is within 10 % of the phase currents, see Figure 5.18. We can conclude that the neutral can be made of copper conductor since such a current will have low impact on the neutral AC loss. As mentioned, due to the cable configuration in the actual grid, the current in the neutral when installed in the grid is expected to be lower. However, the neutral must withstand a short circuit current, which corresponds to a required thickness.

Alternatively, if needed the neutral current can be declined by selecting twist pitches in such a way that an inductively balanced DSMVC is achieved. Using the analytical method as presented in [118], twist pitches for the DSMVC are determined.

Twist pitches for each cable section are equal for phases a and b (TP_a , TP_b and TP_c), Table 5.5. As expected, for the most outer phase the twist pitches are opposite to each other, namely -192 and 192 mm. As a result the phase inductance and mutual inductances are equal and 0.1557 and 0.0312 mH/km, respectively. As a result the neutral current drops to about 10 A, see Figure 5.19.

This is a good alternative to the more complicated phase transposition. The neutral current reduction shows to be in good agreement with results presented in [119].

In case of a fully balanced cable the capacitances are made equal in magnitude, by selecting the insulation thickness. This result in slightly larger inductances, namely 0.1564 and 0.0410 mH/km for self and mutual inductance respectively, see Table 5.6.

Table 5.5 Electrical parameters for inductively balanced Dutch triaxial HTS cable: 50 kV, 250 MVA, 3 kA and 6 km.

Twist pitch section 1 [m]	Twist pitch section 2 [m]	Self inductance [mH/km]	Mutual inductance [mH/km]	Capacitance [μ F/km]
$TP_a = 0.236$	$TP_a = 0.236$	$L_a = 0,1557$	$M_{ab} = 0.0312$	$C_{ab} = 0,725$
$TP_b = -0.191$	$TP_b = -0.191$	$L_b = 0,1557$	$M_{bc} = 0.0312$	$C_{bc} = 0,910$
$TP_c = -0.192$	$TP_c = 0.192$	$L_c = 0,1557$	$M_{ca} = 0.0312$	$C_c = 1,09$

Table 5.6 Electrical parameters for inductively and capacitive balanced Dutch triaxial HTS cable: 50 kV, 250 MVA, 3 kA and 6 km.

Twist pitch section 1 [m]	Twist pitch section 2 [m]	Self inductance [mH/km]	Mutual inductance [mH/km]	Capacitance [μ F/km]
TP _a = 0.226	TP _a = 0,226	L _a = 0,1564	M _{ab} = 0.0410	C _{ab} = 0,725
TP _b = -0.188	TP _b = -0,188	L _b = 0,1564	M _{bc} = 0.0410	C _{bc} = 0,725
TP _c = -0.185	TP _c = 0,185	L _c = 0,1564	M _{ca} = 0.0410	C _c = 0,725

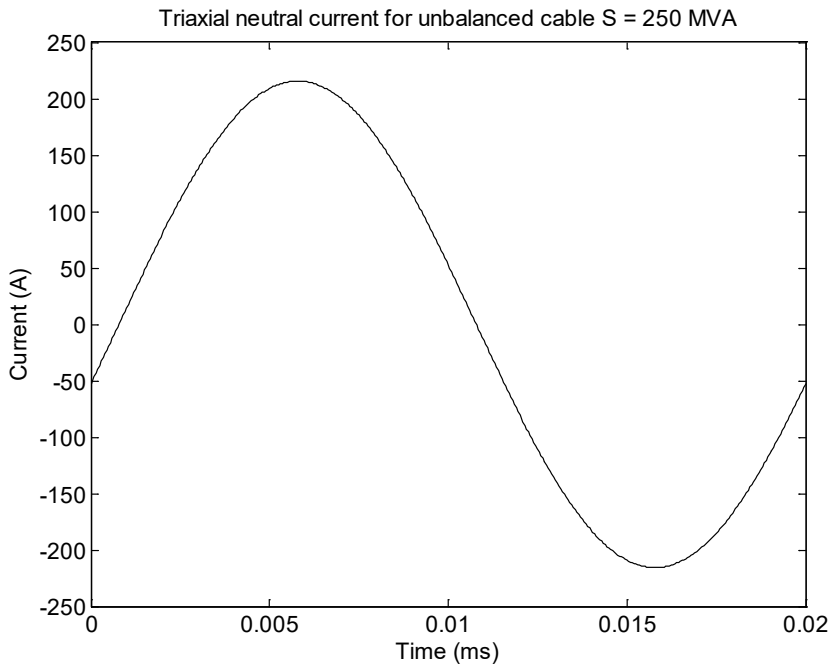


Figure 5.18 Neutral current for unbalanced cable.

Since the cable phases are inductively balanced for the 6 km cable, capacitance imbalance affects the steady state phase currents. The steady state phase currents I_a , I_b and I_c shows an imbalance for a 10 km length of respectively: 1.87%, 0.13%, 2.55% and the cable voltage drops ($U_a=U_b=U_c$) by 2.8%.

As a result, the neutral current amplitude in the cable is about 10 A, see Figure 5.19. In order to reduce the effect, the cable capacitances can be further balanced by adding an external capacitance and/or by changing the electrical insulating thicknesses in the cable.

For a fully balanced DSMVC (phase inductances and capacitances are balanced), the insulation thicknesses are:

- between the cable former and the most inner phase 4.62 mm;
- between the most inner phase and the middle phase 5.91 mm;
- between the middle phase and the most outer phase 7.21 mm.

The increase in insulation thickness for the middle and most outer phases is respectively, 28% and 56%, as compared to the inductively balanced cable.

Increasing the insulation thickness is allowed since the HTS cable insulation has no significant temperature gradient and therefore the increase of insulation thickness has lower risk as compared to the conventional cable.

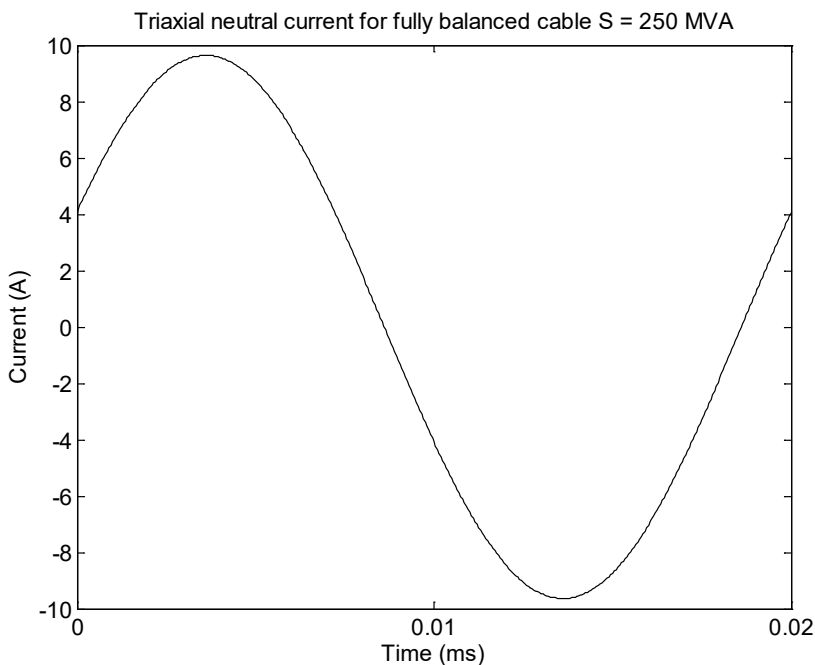


Figure 5.19 Neutral current for a balanced cable.

5.8 Conclusions

In this chapter a concept cable is elaborated according to the network specifications for a network location identified in Chapter 4. The cable specifications comply with the targets, are confirmed analytically and some by practical measurements. Our main conclusion is that it is technically possible to design such HTS cable. Furthermore, the low cable impedance and the intrinsic fault current limiting

property make such HTS cable very promising to help solving future grid issues and enable integration of more dispersed generation and distributed energy resources.

The targets for designed distribution cable (139 mm max outer diameter) are: 0.2 W/m for AC loss in the core and 0.5 W/m cryostat heat leak.

The AC loss target for the Amsterdam cable core is met by using narrow HTS tapes with a high critical current, a large diameter core, arranging the tapes on the former with almost no gaps, electrically insulating HTS core layers from each other, etc. In order to verify the AC loss reduction strategy, several HTS cable core samples are prepared and investigated. The lowest measured in the HTS core AC loss is 0.096 W/m at 3 kA_{rms}, 77 K, and 50 Hz for the 3 meter long Set-up 3 model. The measured value of AC loss was confirmed in a similar experiment conducted independently at Furukawa.

The pressure drops of 20 mbar and 40 mbar at the flow rate of 0.3 and 0.4 kg/s, respectively are measured in the developed 47 m-long, dedicated low-friction cryostat setup. Extrapolation of the obtained experimental results show that in the 6 km-long cryostat of the Dutch distribution cable (made the same way, with alternating rigid and flexible sections) the pressure drop is below 2 bar, which is acceptable figure.

According to the conducted heat balance analysis of the HTS cable it is possible to keep the temperature profile along the cable below 73 K, which occurs in the middle of the cable. Based on the thermal modelling, up to 0.85 W/m of total AC losses are allowed in the three-phase cable core assuming a cryostat loss of 0.5 W/m.

Based on the same design, the cooling station at each cable end requires a capacity of 4 kW and has a footprint of 50 m².

The low cable impedance makes it easier to integrate dispersed generation and distributed energy resources due to the ability to attract the load flow.

The designed cable has the ability to limit a fault current to 4 kA_{rms} let trough current within 4-6 cycles, with the heat up of the core tapes to a maximum of about 130 K occurring approximately in the mid-section of the cable.

Due to the concentric arrangement of the cable phases, a neutral current of 10 % of the phase current is estimated. By selecting proper twist pitches the current in the cable neutral is reduced substantially, which only require a sectioned the most outer phase layers.

6

HTS HVDC cables and Outlook

In this chapter we illustrate possibilities to use HTS DC cables. In the coming years the number of DC links is expected to grow. As compared to AC, DC links do not suffer from the capacitive current, enabling long distance transport without the need of compensation. Optional applications are power links at sea or interconnections. Moreover, DC connections on land are becoming more attractive. Therefore, in this chapter we address how HTS DC cables could contribute to the future grid and identify a suitable location to introduce a HTS DC cable connection in the Dutch grid. Finally, a concept of such cable is elaborated.

- 6.1 Introduction
- 6.2 HTS DC cable
- 6.3 HTS HVDC interconnection example
- 6.4 HTS HVDC case study
- 6.5 Concept and interior arrangement of HTS cable
- 6.6 Outlook for DC HTS cables
- 6.7 Conclusions

6.1 Introduction

Several large projects and initiatives: North Sea wind power [120], Desertec [121], European Supergrid [122], Offshoregrid [123], etc. show a need for large amounts of electrical power to be transported over long distances in the future. This could contribute to a low carbon economy. For example, Norway had approximately 28 GW of hydropower in 2010 [124]. In the future it is expected that Norway will extend its hydropower capacity. Such a storage facility would be the solution to the variable generation sources such as wind and solar, which will be widely used in the future. At this moment Norway has an annual potential of 84 TWh hydropower storage [124]. Storing energy in the reservoirs is attractive during the night, when the energy demand is low.

As mentioned before, the strategic position of the Netherlands within Europe and its flat landscape makes it very attractive to take the lead in transmitting bulk electrical power throughout Europe. One can think of the potential of sustainable electrical energy that can be harvested e.g. with wind parks, geothermal energy and concentrated solar energy and transported by HTS lines. Recently, a conventional HVDC land cable between the Netherlands and Germany to strengthen the connection is proposed by TenneT [125]. This could be one piece of the puzzle towards a “supergrid” or electric roundabout in Europe, making possible to transport high powers.

6.2 HTS DC cable

In comparison to AC cable, HVDC cable does not carry reactive current, this enables longer lengths without compensation. Besides, the core resistance is lower since there is no skin effect in the core. To operate a DC network, DC terminals are required and they are relatively expensive due to the high converter costs. Therefore at a circuit length there is an economic point where the DC is more economical than an AC. The main advantage of a HTS DC cable compared to the conventional HVDC cable is the lower core loss and the ability to transport about ten to twenty times more electrical power. The DC core has a less complicated design in comparison to the AC core, as no changing magnetic field penetrates through the HTS tapes. Moreover in the steady state there is no dielectric loss. Therefore the main cable loss is attributed to the cryostat. As a result less cooling is required for the DC cable than for the AC cable, enabling longer lengths more easily.

At this moment the maximum power capacity of a DC connection is limited by the DC circuit breaker (CB) current. Special solution is needed because at DC there is no zero current crossing as in AC transmission.

Of interest for future HTS DC cable are connections to wind parks (>100 km) and on land certain parts of the AC grid, that need more transport capacity.

Historically the development of the electricity grid is driven by industrialization to create a national network to connect load demands. Since there is a growing demand and international trade for electrical energy, more electrical energy exchange between countries occurs. In particular DC connections between the Netherlands, UK, Norway and Germany. Interconnections enable an increased security of supply and the use of sustainable energy i.e. the NorNed, BritNed, NorGer connections.

Technically the hydropower resources in Norway can be increased to 33-35 GW without serious impact to nature [124]. With the currently available capacity, about 5 to 7 GW could be utilized for power sharing between countries. It is known from the experience, that NorNed connection is profitable and a good way to store electrical energy. Besides Norway, Iceland has geothermal energy as a sustainable resource. A high capacity connection made to Iceland or via Norway or U.K is also a future possibility.

Technically, only HVDC is capable to transmit well over a GW electrical power (≥ 3 GW). Overviews of Europe's HVDC connections that are installed and will be realized within the coming years are given in [126]. Currently, the interconnections like BritNed and NorNed consists of a cable with a nominal transport capacity of respectively 1 (see Table 6.1) and 0.6 GW. Upgrading such a connection will result in additional parallel cables. For instance, the available 5 GW in Norway results in minimum of 5 to 9 parallel submarine cables for transportation to The Netherlands, without redundancy accounted. This will increase the availability of the connection but at a substantial increase in costs, laying costs in particular. From the security of supply perspective, it would be realistic to assume that the off-shore grid will have the same n -criteria as the transmission grid on land. Therefore, a ring structure is proposed [127]. Sharing of electrical power and connecting off-shore renewables will become easier via a ring structure using a multi-terminal network philosophy. A HTS DC cable could provide the required capacity for such a ring.

6.3 HTS HVDC interconnection example

In this thesis a case study is performed for a HVDC HTS subsea link. For this exercise we used the requirements as for BritNed, which nicely connects the Netherlands and United Kingdom with a depth small enough to avoid cooling problems. The BritNed connection with conventional cable was made and commissioned in 2011 to share the electrical energy between the United Kingdom and The Netherlands.

The United Kingdom is progressive on wind energy, has the idea to make a connection with Iceland and/or Norway. Therefore the Netherlands has the opportunity to provide an electrical power corridor to the rest of Europe.

The connection between UK and The Netherlands provides the following advantages [128]:

- Greater security of supply in Great Britain and The Netherlands;
- Increased diversity of supply enables integration of electricity generated by wind farms;
- Greater interconnection to achieve a common European market;
- Open access to all market participants providing greater import and export opportunities.

It can be expected that in the future more links to UK and or Norway are needed, as previously discussed. Therefore we have identified BritNed as a possible connection to be strengthened using HTS submarine cable that will serve as an example for other interconnections.

Specifications of the existing BritNed cable are given in Table 6.1 below.

As the route of the cable has a water depth of 30 to 50 m, no serious cooling problem due to the height difference is expected. Moreover, at both ends of the cable liquefied natural gas plants are located which could help with cooling.

The applications of HTS HVDC cables offer the following main advantages:

- High power capacity making additional cables unnecessary;
- Ability to further increase the power capacity of the cable by upgrading HTS core with better tapes;
- Negligible DC resistance (the residual loss contribution is mainly due to the cryostat).
- Enabling high power capacity connection with Voltage Source Converter voltage (VSC) levels;

Table 6.1 BritNed cable specifications.

Convertor stations locations	Isle of Grain (UK), Eemshaven (the Netherlands)
Voltage, kV	± 450 DC
Cable power capacity, GW	1 and 1.2 in overloading situations
Weight, kg/m	44
Length sea cable, km	250
Water depth	30-50
Length land cable, km	7 (NL) and 2 (UK)
Maximum sea depth, m	30
Conductor sizes submarine cable (SM), mm ²	2 x 1430
Conductor material (SM)	Copper
Cable configuration (SM)	Bi-polar, bundled
Insulation type (SM)	Mass impregnated
Cable mechanical integrity	Double armour

- Thermally independent of its surrounding and no external magnetic field [73];
- Close spacing of the poles without losing power capacity, since the cables are thermally independent of each other.

Voltage source convertors are currently limited in their maximum voltage output and therefore limit bulk power transmission. Hence, HVDC interconnections for bulk power transmission are normally based on Current Source Convertors (CSC). HTS cables enable a powerful link using VSC. VSC and CSC are compared in Table 6.2 [129, 130].

Table 6.2 Comparison of the VSC and CSC.

	VSC	CSC
Voltage rating	<450 kV	>450, <800 kV
Losses	High	Low
Bidirectional operation	Yes	Depends
Reactive power control	Yes	No
Largest cable system	400 MW	1.4 GW
Largest cable project	800 MW	3 GW
Convertor Size	Small	Large
XLPE cable	Yes	Depends
Filters	Small	Large
Black-start	Yes	No
Multi-terminal	Yes	Difficult
Transformer	normal type	Special type
Reactive power compensation	No need	required
Footprint, m	120x60x22	200x120x20

Table 6.2 shows that VSC possesses certain advantages in comparison to CSC. One major advantage compared to the CSC is that VSC is capable to start up after shut down.

Especially, transition to DC connections on land, the ability of black-start is an important issue. Losing a high power capacity connection can be harmful for the security of supply, hence the power should be connected back to the grid as soon as possible.

As the power capacity of conventional HVDC cable is presently limited to approximately 2 GW at 600 kV [131], a bulk power link (>3 GW) will require multiple cables in parallel. HTS cables can increase their power easily by adding additional tapes to the core without any significant compromise to the cable design. Theoretically, HTS HVDC cables could transmit several tens of GW (up to 10-20 times more than conventional HVDC cables). Applications depend on the commercially available CBs and on the strength of the receiving network. Recently, the electrical power industry has developed a high voltage DC hybrid CB

to enable the development of future grid capacities [132]. These switches might be usable for high capacity HTS connections as well.

6.4 State of art commercial HTS HVDC cable

Nexans presented a HVDC HTS cable concept [73], which included terminations. They also have tested successfully a 200 kV HTS DC cable sample of several meters length in 2010. The type test program also included 360 kV for a short time [133]. Based on this, our expectation is that sufficiently long HTS DC cable will be commercially available in future, assuming that sufficient research and development is in place.

Our estimates show that the HTS cable of concept A, as referred in Table 3, is not directly applicable to strengthen the BritNed connection, as such cable would require many cooling stations at sea, which is impractical. It gives a good impression about the level of manufacturing capabilities available today.

In the next section we will present our vision for an improved HTS cable concept enabling power transport over a distance of 260 km with just two cooling stations at the cable ends.

6.5 Concept and interior arrangement of HTS DC cable

A complete HTS DC cable system includes the HTS cable in the cryostat, terminations, two cooling stations at the cable ends, control and protection units. Assumed is that the cable will be made without any joints, which is addressed later, however if an accident occurs a repair joint will be necessary. With the proper research and development, such a joint can be developed [54]. The cable dimensions are mainly determined by dimensions of the cooling channel. For simplicity only one pole (positive and negative pole) of the bipolar cable system will be elaborated in this chapter because the other pole is identical. The main difference is the opposite cooling flow in the cooling channels of the cable.

6.5.1 HTS DC cable

For the connection we derived our so-called concept C from two commercially existing design concepts, referred to as design concepts A and B (Table 6.3).

Concept A has a positive and negative pole that has a current capacity of 4 kA. The outer dimension of this cable is 190 mm, which includes a 5 mm protection layer. The concept B is a high current density core with a good mechanical property. With proper electrical insulation and screening an attractive HTS core can be made.

Table 6.3 Cable concepts.

Design concept	
A	Nexans conceptual cable design [73]
B	Corc™ HTS core [134]
C	Our design

Cooling stations at sea are expensive and must therefore be prevented. The distance between cooling stations is 5 km for concept A [73], resulting in 104 (52 per pole) terminations, which substantially increases the cooling power. Furthermore, the concept C uses an improved MLI in the cryostat to decrease the cryostat heat leak [135].

Each pole of the HTS cable has the following interior design, see Figure 6.1 and 6.2: starting from the inside, the former with HTS layers (1), electrical insulation with semiconducting layer (2), a copper stabiliser/screen (3) on top, the cooling channel (“go or return”) (4), MLI placed within the cryostat inner and outer wall (5, 6), and the protective layer (7) as most outer layer of the cable.

Cooling channel is used for the “go” or “return” flow (depending on the pole), which is in one of the two poles, of pressurised liquid nitrogen and it hosts the transport current carrying layers of the cable phase that are made semi-transparent for the coolant;

The concept B cable consists of a flexible former over which the HTS tapes are mounted and provides mechanical support for current carrying layers;

- The electrical insulation separates the core from ground in accordance with the maximum field stress;
- The screen on top of the insulation keeps the radial electric field controlled;
- The cryostat thermally isolates the cable from the ambient environment and it hosts layers of MLI and spacing material in high vacuum;
- Finally, the cable is surrounded by extruded protection layer placed over the cryostat.

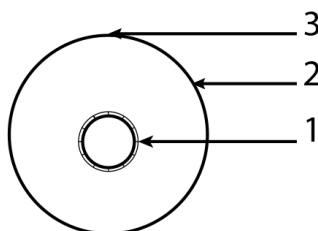


Figure 6.1 HTS single core design, where 1 is former with HTS tapes, 2 is electrical insulation with semiconductor layer, 3 is copper stabiliser/screen.

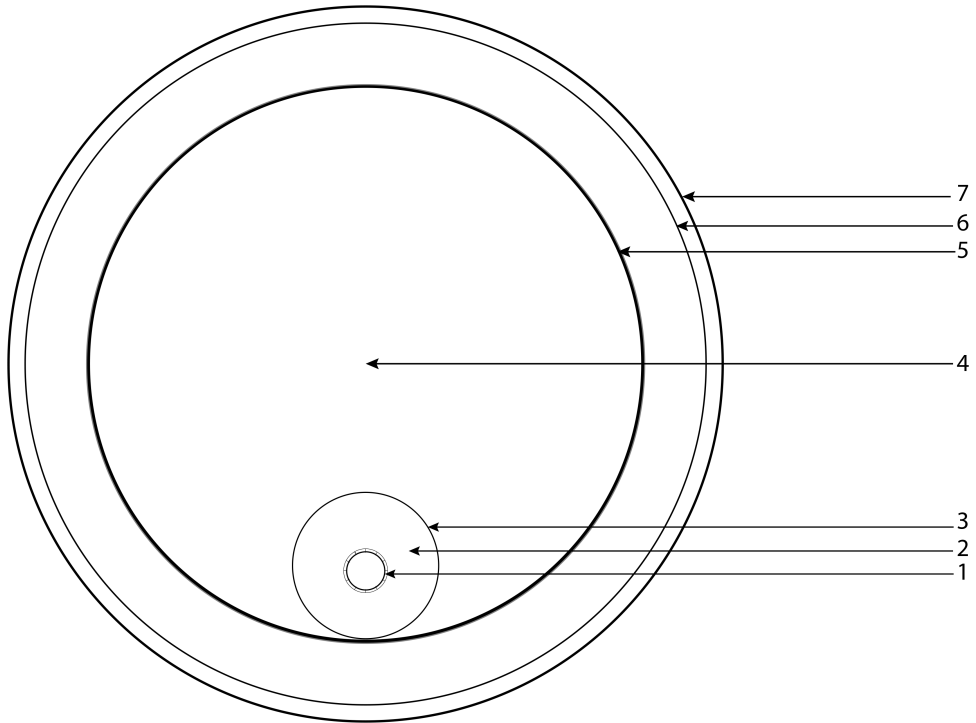


Figure 6.2 One pole of HTS HVDC ± 450 kV cable cross-section (concept C connection).

To note, that the concept B cable has a small cooling diameter (channel 4). In Figure 6.2, the small inner core channel is optional.

As mentioned before, the concept C cable consists of the components numbered from 1 to 7 as indicated in Table 6.3. The insulated core outer dimension is 42 mm. The electrical insulation, PPLP type, is firmly fitted to the copper stabilizer with a thickness of 15 mm. This results in average field strength of 30 kV/mm in the insulation, which is in accordance with the maximum allowable field stress [15]. In comparison to conventional HVDC cables, the insulation temperature remains in the HTS cable relatively constant, and is thus independent on the load connected. Besides, aging of the insulation is less pronounced due to its low operating temperature. Therefore the electrical field strength varies negligibly because the conductivity remains stable. The MLI is of the self-pumped type allowing more layers in the cryostat and therefore reducing the cryostat heat load [135]. A cryostat thickness of 20 mm is assumed in the concept.

Table 6.4 Core specification for HTS HVDC concept C.

Part Nb.	Parameters	Concept C single cable for bi-polar system
	Voltage level, kV	450
	Transport current, kA	4
	Cooling distance, km	260
1	Core pole outer diameter incl. 1 mm insulation screen, mm *	12
2	Insulation PPLP outer diameter, mm	42
3	Copper screen outer diameter, mm	44
4	Cooling channel, mm ²	19600
5	Inner cryostat wall outer diameter, mm	164
6	Outer cryostat wall outer diameter, mm	205
7	Protection layer outer diameter, mm	215

* core dimension based on [134]

The cryostat inner wall diameter is determined by the required coolant flow that removes the heat load in the cooling. The heat loads for both concept A and C are listed in Table 6.5.

Concept C has a slightly larger diameter (215 mm), according to the hydraulics presented in the next section, in comparison to the concept A cable (190 mm). The 25 mm larger diameter for the concept C cable is not expected to change the e.g. cable transport and laying.

To enable a transmission length of 260 km, the concept A cable requires as explained before, 104 terminations and 52 cooling stations. Concept C is made for 260 km with just two cooling stations on the ends. The cable is for 85 % made of rigid parts enabling less friction for the cooling. The oil and gas industry shows the feasibility of installing pipes at sea, by special pipe laying vessels.

The costs of the concept A cable are substantially higher due to the additional cooling stations at sea. Therefore cooling stations at sea must be avoided. For future needs, the transport power of 2 GW can be increased by upgrading the HTS wire with higher tape I_C or by adding additional tapes or additional concept B cables.

Table 6.5 Sources of loss for HVDC HTS 4 kA cable (concept A and C).

Losses accounted in a bi-polar cable system	Concept A	Concept C
Thermal loss single termination (0.45 W/kA), kW	0.18	0.18
No-load single termination loss, kW	0.16	0.16
Total termination losses, kW	35	3
Cryostat loss per cable, W/m	0.45	0.17
Total cryostat loss, kW	234	86
Total loss @ 77 K, kW	269	88
Total loss @ 273 K*, kW	3367	1104

*cooling penalty of 12.5 W/W is assumed

The option to use multiple concept B's in the cable is treated further below in this section.

In the presented comparison the HTS cable joints are assumed to operate with negligible loss [73]. However, in practice, few joints will be necessary to connect maximum production cable lengths together. Or in case of a cable failure, the cable is cut and repaired using repair joints. Joints are critical parts in the cable system, they decrease the reliability and must be avoided. The termination heat loads are assumed to be directly intercepted at the cooling stations, and do not limit the maximum cable length. The resulting cable system losses for two pole bipolar system are listed in Table 6.5.

The termination (current dependent and no load) heat losses for concept A and concept C are both assumed 0.18 kW and 0.16 kW respectively per termination. This result in the total termination losses of 35 kW and 3 kW for concept A and concept C, see Table 6.5. As mentioned, termination losses are assumed directly removed by the cooling system, hence they do not contribute to the cooling channel heat load but influence the amount of cooling power significantly and make the cooling costs higher.

The tape losses are not affected by frequency dependent losses as compared to the AC HTS cables and are assumed negligible. The main loss contribution is the cryostat heat losses, which also determine the pressure drop in the cable. The cryostat losses for the concept A are 0.45 W/m. The cryostat losses of concept C are more challenging. As shown in the Table, 0.16 W/m is required. Amongst other improvements the cryostat losses of 0.16 W/m can be achieved implying a cryostat thermal conductivity of 0.00003 W/m-K. Such a thermal conductivity can be obtained, for instance, using self-pumped MLI as described in [135]. As a result, the total system losses (including the cooling penalty of 12.5) at 77 K and 273 K

for concept A and concept C design are respectively, 269 (3367) kW and 88 (1104) kW. Therefore the total losses in the concept C are a factor 3 lower.

Estimates show that concept C cable weighs 13 kg/m without LN₂, The bipolar system therefore has a total weight of 26 kg/m. Based on the total weight capacity on a laying vessel, which is typically 7000 tonnes [136] and assuming sufficient loading capacity on the factory turntables, it allows to store the complete bipolar cables on the laying vessel. Hence, no subsea joint is required in the HTS cable system assuming that the total cable length can be manufactured in the factory and loaded onto the laying vessel.

Concept C cable allows increasing substantially the power capacity by a small modification to its design. For instance, as illustrated in Figure 6.3, the core is replaced by a four-concept B cores. Hydraulic calculations show that the outer cable diameter, comprising the new core, increases to 258 mm. The 20 % larger cable diameter in comparison to the cable with one concept B cable leads to a 4 times higher power capacity (4x7.5 kA instead of 1x7.5 kA).

The new cable design with the 4 CORC core (concept C), will use a profile or filler holding the concept B cables in their position and are hold together by e.g. a binding tape or bedding (semi-conductive).

There are several options to arrange the poles (“plus” and “minus”) in the profile, of which, the main options are:

- All positive or negative poles;
- Two positive (upper left and upper right, see Figure 6.3) and two negative (lower left and lower right, see Figure 6.3);
- Two positive (upper left and lower right, see Figure 6.3) and two negative (upper right and lower left, see Figure 6.3);

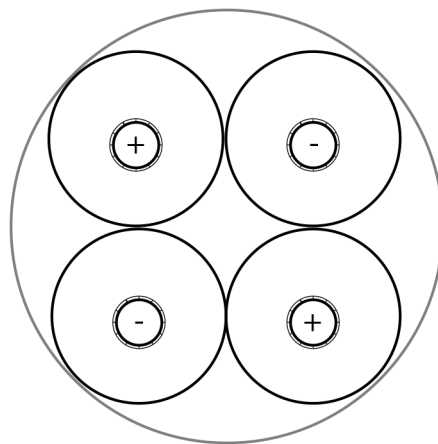


Figure 6.3 Four concept B cable core to upgrade the power capacity (concept C).

The option where the core contains all positive or negative poles obviously requires two cables in order to form the electric loop. A disadvantage of this option is that the whole connection is lost if a problem occurs in one of the cables. In this configuration the magnetic field exposure is similar to its alternatives. If the spacing between both poles the cables is decreased, the magnetic corridor minimises.

If the core has two positive and negative poles (concept C), the cable has a bi-pole configuration. Here, the connections can run on one concept C cable. However, its cooling needs a return in this case. Since a second concept C is expensive a cooling return pipe is optional. Having two of such cables increases redundancy of the system. Furthermore, the positive and negative cores in the concept C partly compensate for the external the magnetic field, where the best configuration for minimising external magnetic field is where the plus and negative pole are located on each diagonal, see Figure 6.3.

6.5.2 Hydraulics of HTS DC cable

The cooling system compensates the system losses where the heat is removed by the flow of liquid nitrogen. Hydraulic parameters for the concept A and concept C are listed in Table 6.6. As mentioned previously, the concept A cable has two cooling channels, across which, the cryostat heat load is divided. Therefore in Table 6.6, each channel is represented by one column that is attributed with half the cryostat heat load. Concept C has a core with a very small outer diameter in comparison with the concept A and makes a design with only one cooling channel feasible. The parameters for the concept A and Concept C are calculated for a 260 km length.

A significant difference between concept A and concept C is in the cross-section of the cooling channel. Herewith the required cable length can be obtained. The flexible sections of concept C have a friction factor of 0.2 and the smooth section of concept C 0.015. Due to the difference in cooling channel cross-sections the friction factor for the inner and outer cooling channel of the concept A design are equal to 0.3 in comparison to the 0.2 of the concept C cable.

As a result, concept A is limited to a length of 33 km for a similar pressure drop as that of concept C (5.5 and 6 for the inner and outer channel of concept A and 5 for the inner channel of concept C). Concept A would therefore require multiple cooling stations at sea, which is unpractical, see Table 6.6 (calculated as explained in section 5.2.8). In contrast to that, the total pressure drop of the full connection length is 5 atm for concept C and is acceptable for a submarine cable. Results of this study show that a HTS cable connection with a 4 to 7.5 kA current capacity between UK and the Netherlands is technically possible using CSC or VSC technology (if VSC becomes available at 450 kV).

Table 6.6 Hydraulics for HTS HVDC concept A and concept C (260 km and cooling stations).

Cooling parameters	Concept A		Concept C
Cooling channel	inner	outer	inner
Heat invasion, W/m	0.225	0.225	0.17
T _{in} , K	65	65	65
T _{out} , K	77	77	77
Mass flow rate, kg/s	3.11	3.11	1.8
Cross-sectional area of flow, cm ²	39	56	196
Friction coefficient smooth sections (for concept A design length is 0)	0	0	0.015
Friction coefficient bellows sections	0.3	0.3	0.2
Total pressure drop, atm	5.5	6	5
Length, km	33	33	206
Pump power, W/m	6x10 ⁻³	7x10 ⁻³	4x10 ⁻³
Required cooling LN ₂ , L/s	0.3	0.3	2

However, before that HTS cables must become mature, reliable and economically sound technology. Therefore active research and development of HTS cables and grids with integrated HTS cables is needed in the period to 2020 aiming at longer and more efficient cables, joints, terminations, etc. At the technology level care must be taken that the HTS tape price is acceptable; that HTS cable core is efficient and cheap; that HV insulation is adequate; that cryostats are adequate (reliable, easy maintenance; low heat leak, low price); that cooling is efficient and reliable; that testing facilities and standards are in place.

To benchmark HTS cables around the world, the next section gives an outlook for HTS cables.

6.6 Outlook for DC HTS cables

Figure 6.4 shows the potential for HTS cables and other HTS grid components. With the focus on HTS cables we see that around 2016 to 2025, the HTS cable market penetration is estimated to increase to 45 %. As explained in Chapters 2 and 3, HTS transmission cables can compete economically with conventional transmission cables already today.

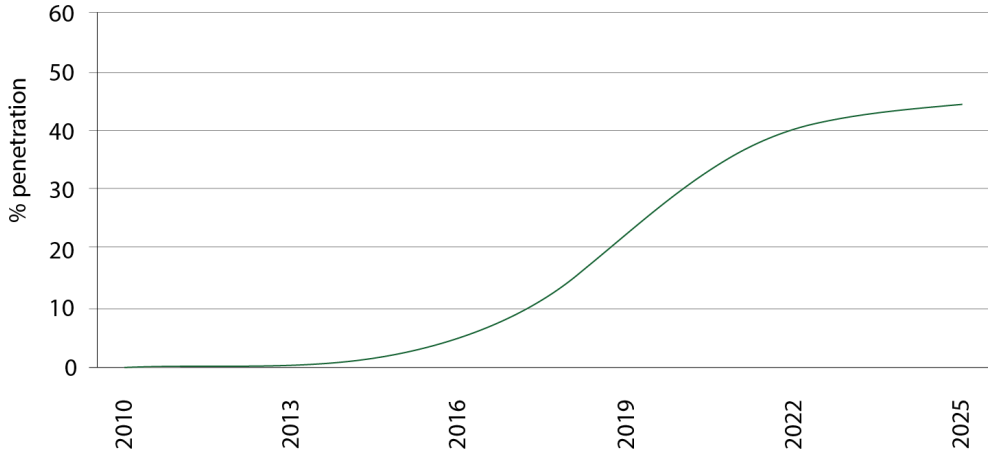


Figure 6.4 HTS component market penetration curve [136].

In regards with the results obtained in this thesis and based on the recent HTS DC cable activities around the world, we have summarised below outstanding HTS cable projects initiatives around the world.

- Korea has a HVDC cable incorporated in their roadmap, see Figure 3.10. The 80 kV cable has a length of 500 m, capable to transport 60 MVA. The cable will be installed in on Jeju island grid of KEPCO.
- China has made a HTS DC cable connection energizing an aluminium plant from a nearby substation where the AC/DC rectifier is located. This commercial cable is in operation since 2011 and has a length of 360 m. It has a rated voltage of 1.3 kV with a power capacity of 13 MW [57].
- Tres Amigas is an initiative to connect three US AC grids using convertor technology and powerful DC links [137]. This enables the share of renewable power between the networks. As the link has reached a power demand of 3 GW and predicts to grow to 5 GW, the plans are to replace one conventional DC Bus with a superconducting cable.
- A HTS HVDC conceptual design is made by EPRI [46] to function effectively in the power grid. The cable system is intended to achieve 10 GW power capacity, using 100 kA current en 100 kV voltage.

6.7 Conclusions

HTS HVDC cable enables bulk electrical power transport at high capacity and over long lengths. The cable power capacity can reach dozens of GW and is limited by the available DC circuit breakers. To compare, present capacity of conventional cable and OHL is limited to 3 and 7 GW respectively.

Such HTS cables are identified as a good option to increase the power capacity of the interconnections, e.g. NorNed, NorGer, BritNed. The expected advantages are: lower costs, lower ROW, lower loss and no need to use multiple cables or OHLs in parallel. Cooling stations at sea are avoided as the designed HTS cable has just two cooling stations placed onshore and spaced by 260 km.

At the cable design level, the HTS HVDC core has negligible electric losses and simpler design as compared to the HTS AC core. Close spacing of the DC cores is possible without decrease of the cable power capacity. A HTS screen results in no external magnetic field produced by the DC cores.

At technology level we assumed in our study that the HTS tape price is acceptable; that HTS cable core is efficient and cheap; that HV insulation is proper; that cryostats are adequate (reliable, easy maintenance; low heat leak, low price); that cooling is efficient and reliable; that testing facilities and standards are in place. In fact, these challenges must be properly addressed before HTS HVDC cables will mature.

Based on the current maturity of the HTS cable components we expect that sufficiently long HTS DC cable will be commercially available within 5-10 years, assuming that sufficient research and development is in place.

7

Conclusions and recommendations

In this thesis the feasibility to integrate HTS cables in the grid, as an alternative for conventional cables, has been investigated. Promising locations in the Dutch transmission and distribution grid for HTS cables have been identified and appropriate cable concepts for these network locations have been elaborated.

In this chapter the main conclusions and recommendations for further research are outlined.

- 7.1 Main results of the study
- 7.2 Conclusions per chapter
- 7.3 Opportunities for further research

7.1 Main results of the study

- Based on our techno-economic analysis HTS cables offer the most competitive solution in transmission grids. Introduction of such cables will reduce HTS tape price, which in turn will stimulate further applications.
- Conceptual designs of competitive HTS AC and DC transmission cables are formulated along with that for HTS AC distribution cable. Novel designs allow for much longer length between cooling stations.
- Our experimental research has shown that HTS cable core losses may be reduced by a factor 10 (down to 0.11 W/m/phase at 3 kA_{rms}, 77 K, 50 Hz).
- Dedicated low friction cable cryostat was developed and successfully tested for 47 meters length. Patented multi-layer thermal insulation improves the cable cryostat heat leak from 1 W/m to 0.1 W/m.

Since the Netherlands is a relatively small country long-distance HVDC connections are mostly outside the country (interconnections), while inside the country Dutch electrical network uses mainly AC connections. For this reason our study focused mainly on AC superconducting cables with less attention paid to DC, (even though HTS DC technology is simpler than AC).

In the following sections we recall the conclusions per chapter in technical detail and summarize conclusions in general (*Italic*).

7.2 Conclusions per chapter

7.2.1 Introduction

In the first chapter practical superconductors are reviewed, YBCO coated tape is selected as the most suitable HTS conductor for HTS cables. Worldwide there are many HTS power cable projects started, running or completed. It is a general consensus that HTS power cable technology is on the way from demonstration to commercialization making it possible to study integration of HTS cable into Dutch transmission and distribution grids.

7.2.2 HTS AC cables in the power transmission network

In this chapter, we identified the bottlenecks in the future Dutch 380 kV grid using energy scenarios of TenneT. Of these, the connection Krimpen-Geertruidenberg is selected as the most promising for integration of HTS cable. Using the network

study for this 7 GVA, 33.7 km long connection comprised of OHLs, or XLPE or HTS cables, or their combinations, we derived required transmission parameters for this connection. Load flows are compared for available transmission options (option 1- OHLs, 2- OHLs and HTS cables in parallel; 3- OHLs, HTS cable and FACTS, 4- OHLs and XLPE cables in parallel, 5- HTS cables, 6- XLPE cables). Due to use of cables in parallel with OHLs, reliability of the connection is preserved; furthermore, most of the load current flows in cables (due to their lower impedance), therefore connection losses are reduced and magnetic emission from OHLs is diminished. Comparison of the transmission characteristics shows that the cable length is limited not so much by the charging current, but rather by the voltage at the cable open end (Ferranti effect). While for the XLPE cable the limit is 33 km, for the proposed HTS cable it is 270 km, which is acceptable for most of applications in a country such as the Netherlands. In-grid case study shows that expected maximum voltages for HTS cable present no obstacle for the electrical insulation management (are within 1.05 of the nominal voltage).

Currently, to fulfill the requirements for integration of HTS cables into the grid, their competitive to OHL technical performance on aspects such as reliability, power capacity, maturity, availability, failure rates, maintenance, time of repair, connection length and life expectancy has still to be demonstrated in operational conditions. Meanwhile, our proposal is to use HTS cables in parallel to OHL's, in which case reliability of the grid remains uncompromised. This way the issues of HTS cables can be tolerated in the grid and HTS cables alone (without parallel OHL's) can be used as soon as their assets are at least at the level of XLPE cables. At present, the reliability of transmission by OHL is the highest. The reliability of the hybrid connection (comprised of HTS cables in parallel to OHL) is close to that, while for HTS cables only, the reliability is generally lower (the same is true for XLPE cables). We conducted an economical comparison of available transmission options for redundancy n-1. From economic point of view the hybrid HTS connection for the identified transmission connection Krimpen-Geertruidenberg (option 3 or 2) is cost efficient compared with the hybrid conventional connection (option 4) at current HTS tape price ratings ranging between 356 to 283 (192 to 137) €/ (kA·m) and below. And, it makes sense to select option 3 (or 2) instead of the OHL upgrade (option 1), at the HTS tape price from 241 to 103 (122 to 48) €/ (kA·m) and below. These tape prices are expected to be reached within 3 to 12 years. This allows to start expansion of the Dutch grid underground in a cost competitive way. A roadmap for the Dutch transmission grid evolution is made using three scenarios. We concluded that HTS cable routing can be selected on the need, e.g. shortest distance therefore total length of future transmission grid can be substantially reduced, while keeping redundancy unchanged. This is used in the long term scenario for optimising the transmission routes. Moreover HTS cables allow undergrounding the Dutch transmission grid for more or less the same investment.

7.2.3 HTS 400 kV AC transmission cable design

In this chapter we have shown that it is technically possible to develop concepts of AC HTS transmission cable with adequate network specifications for the connection Krimpen-Geertruidenberg. Essential feature of the concepts is that such HTS cables are cost-competitive as compared to other options available to transmission system operator (conventional XLPE cable, OHL, etc.). Main parts of such cable system are: shielded and electrically insulated HTS cable core, cryostat, two terminations and two cooling stations at the cable ends. First, the cold and the warm dielectrics HTS cable interior arrangements are explained resulting in the 266 mm and 144 mm outer cable diameters respectively. Comparison of laying arrangements of the designed HTS cables to that of conventional XLPE cables and of OHLs for 7 GVA capacity show that both designed HTS cables are very compact: OHLs, XLPE, HTS CD and WD cables require 80, 10, 1.8 and 1 m-wide ROW respectively. The HTS core and shield specifications are explained for CD and WD cables: the required cable critical currents are derived providing acceptable AC losses in the cores and shields. Furthermore, the cable critical current is kept constant along the cable length despite changing temperature of the flow (this provides constant AC losses in the core along the cable length and saves 20-30% of the core costs). Use for electrical insulation of novel dielectric materials (e.g., Tyvek-PE) results in more compact and more efficient CD cable design, while use of PLLP-C leads to more conservative design: cable is more bulky and less efficient. A WD HTS cable allows using conventional electrical insulation, such as XLPE with the advantage (over the CD cable) that dielectric losses are outside the cryostat. More efficient semi-flexible cryostats are used in the design: for the CD cable the targeted heat leak of 0.5 W/m agrees well the near-term expectation (0.3 W/m) and for the WD cable the target of 0.1 W/m is within reach when improved thermal insulation is used. Terminations enable a connection to the substations at both cable ends, are designed separately for CD and WD cables and provide the transition from high voltage to ground potential; interface from low to ambient temperature, take care of the cable shrinkage and expansion during a thermal cycle. As a result, the total heat leak of 1.5 kW per three-phase CD or WD termination is derived. Hydraulic and thermal study of both HTS cables operated at 7.5 kA_{rms} resulted in two cooling stations at the cable ends and the following characteristics: for the CD cable the inlet and outlet temperatures and pressures of the go and return flows are 65 and 76.7 K, 15 and 7 bar; 65 and 77 K, 15 and 7 bar respectively at the mass flow rate of 1.16 kg/s. For the WD cable the inlet and outlet temperatures and pressures of the go and return flows are 65 and 77 K, 15 and 7 bar; 65 and 73 K, 15 and 7 bar respectively at the mass flow rate of 0.14 kg/s. At n-1 redundancy for the CD HTS cable a cooling station of eight turbo Bryton cryocoolers (each able to remove 12 kW at 65 K) is sufficient at each cable end, for the WD HTS cable a cooling station of two such cryocoolers at each cable end is sufficient. A study of the designed HTS cable systems reveals that the total losses (including the cooling penalty of 10) are: 5.5 and 12 kW/km for WD and CD

cables respectively, as compared to 86 kW/km for conventional XLPE double cable per phase circuit of the same capacity. Therefore, main conclusion of this chapter is that it is technically possible to develop a competitive (to other available options) concept of AC HTS transmission cable addressing the required network specifications of the connection. Both developed HTS cables as compared to a conventional copper cable with the same rating have more compact arrangement, lower loss, less magnetic field pollution, less weight, allow faster installation, etc. This makes HTS cables attractive for TSOs but require further demonstration of their capabilities in the real transmission grid. As the remaining challenges: reliability, power capacity, maturity, availability, failure rates, maintenance, time of repair, connection length and life expectancy will be properly addressed, HTS cables will replace OHLs in transmission grid.

We elaborated for the connection two novel cables, warm and cold dielectric designs, based on realistic cable dimensions and with two cooling stations at both cable ends. So far no such cable is commercial available at 380 kV. Main advantages of these cables in comparison with conventional solutions are: higher power capacity, drastic increase of the distance between two cooling stations (from the current 1 to possibly 35 km), compact, lighter, reduced losses and magnetic fields, independent on soil properties, faster installation, better screen the magnetic field, lower losses, aging of electrical insulation, lower mass and enable longer lengths between joints. A warm or cold cable design is selected based on the needs such as: trench width, magnetic field pollution, repair time, familiarity of design (extruded insulation), manufacturing easiness, time of repair, use of three phases in a single cryostat, etc. New advances can make HTS cables even more attractive: better ReBCO tapes, electrical insulation and cryostats, more efficient cooling using a cold from liquefied natural gas and gas-driven compressors at the cable cooling stations; the latter contributing to a climate in nearby buildings (with heat pumps fed by cable cooling losses), etc. Therefore we concluded that HTS cables become attractive for TSO's, although more research is required to demonstrate the benefits of such a HTS cable and its capability in the real transmission grid.

7.2.4 Integration of HTS AC cable in the distribution network

In this chapter it is shown that as compared to a conventional cable, the HTS distribution cable provides more power transport capacity to the grid together with lower AC loss, consumes less reactive power, has no negative thermal interaction with the surrounding environment, has almost no external magnetic field, enables bidirectional flows, is more compact and provides intrinsic fault current limitation (the concept of such HTS cable is addressed in chapter 5). As an example, we identified a 6 km-long connection in the Alliander distribution network in Amsterdam, between two 150 kV substations Hoogte Kadijk and Noord Klaprozenweg, where HTS cable could demonstrate the above mentioned

advantages. In this case, the future demand in higher power capacity of the connection can be met by retrofitting one of the existing aged copper cables with HTS cable. A comparative network study of this connection is conducted for two available circuit options (1: three existing 150 kV conventional underground cables with total capacity of 300 MVA using three 150/50/10 kV transformers, and 2: two 150 kV City Cables –CC with total capacity of 400 MVA- using two 150/50/10 kV transformers in parallel to one HTS cable with capacity of 250 MVA using one 150/50 kV transformer). The study shows that at delivered power of 200 MVA more power (112 MVA) flows via the HTS cable (due to its lower impedance) as compared to both CC (75 MVA), while the short circuit current for option 2 remains the same as in option 1 (peak below 60 kA) due to the intrinsic fault current limiting property of the HTS cable. The calculated (at the same delivered power of 200 MVA through the connection) losses for options 1 and 2 are: 4.2 and 2.3 GWh, respectively. With the use of the triaxial HTS cable integrated in the distribution grid of Essen, Germany in 2014, the grid was strengthened and the technical abilities of HTS distribution cable were demonstrated. Our study shows that allowable HTS cable investment costs for the Ampacity grid should be at 0.75 M€/km in order to compete economically with a conventional cable grid. To compare, the allowable investment costs of the Dutch triaxial HTS cable in the above example are estimated at 1.6 M€/km). Based on the studies performed in the Alliander network connection, the total initial investment costs and total lifetime costs for the existing and proposed Alliander network (option 1 or 2) are estimated to be 11 or 20 M€ and 29 or 32 M€ respectively. At the HTS tape price of 19 €/kA·m the total lifetime costs of both options are the same. We conclude that expansion of the grid with conventional CC is at present more cost effective and that integration of HTS distribution cables will only become feasible, when the price of HTS tape (and other HTS cable components) is reduced substantially. At this moment, HTS distribution cables are only suitable in niche applications, where their technical or environmental benefits prevail. We therefore expect that HTS transmission cables will be integrated first, followed by HTS distribution cables as soon as the HTS tape price is acceptable and the cooling infrastructure for HTS transmission cables is sufficiently developed.

As compared to a conventional distribution cable, a HTS cable provides more power transport capacity to the grid together with lower AC loss, consumes less reactive power, has no negative thermal interaction with the surrounding environment, has almost no external magnetic field, enables bidirectional flows, is more compact and provides fault current limitation. In order to study this in more detail, we identified a 6 km long connection in the Alliander distribution network in Amsterdam, between two 150 kV substations Hoogte Kadijk and Noord Klaprozenweg, where HTS cable could demonstrate the above mentioned advantages. In this case, the future higher power capacity of the connection can be met by retrofitting one of the existing aged copper cables with HTS cable. Such

retrofitted connection strengthened with a triaxial HTS cable confirmed its benefits, but economic analysis showed that at distribution voltage levels it is impossible yet to achieve competitive cost for HTS cables as compared to conventional cables due to the currently higher component costs. As example, the cryostat alone is more expensive than a conventional distribution cable and hence the other HTS cable benefits must be included to justify the higher cost. This allows at present only niche application for HTS cables, where their technical or environmental benefits prevail. We conclude that HTS transmission cables will be integrated first, followed by HTS distribution cables.

7.2.5 HTS AC distribution cable design

In this chapter a concept cable is elaborated according to the network specifications for a location identified in Chapter 4. The cable specifications comply with the targets, are confirmed analytically and some by practical measurements. Our main conclusion is that it is technically possible to design such HTS cable. Furthermore, the low cable impedance, the intrinsic fault current limiting property make such HTS cable very promising to help solving future grid issues and enable integration of more dispersed generation and distributed energy resources. The targets for designed distribution cable (139 mm max outer diameter) are: 0.2 W/m for AC loss in the core and 0.5 W/m cryostat heat leak. The AC loss target for the Amsterdam cable core is met by using narrow HTS tapes with a high critical current, a large diameter core, arranging the tapes on the former with almost no gaps, electrically insulating HTS core layers from each other, etc. In order to verify the AC loss reduction strategy, several HTS cable core samples are prepared and investigated. The lowest measured in the HTS core AC loss is 0.096 W/m at 3 kA_{rms}, 77 K, and 50 Hz for the 3 meter long Set-up 3 model. The measured value of the AC loss was confirmed in a similar experiment conducted independently at Furukawa. The pressure drops of 20 mbar and 40 mbar at the flow rate of 0.3 and 0.4 kg/s, respectively are measured in the developed 47 m-long, dedicated low-friction cryostat setup. Extrapolation of the obtained experimental results show that in the 6 km-long cryostat of the Dutch distribution cable (made the same way, with alternating rigid and flexible sections) the pressure drop is below 2 bar, which is acceptable figure. According to the conducted heat balance analysis of the HTS cable it is possible to keep the temperature profile along the cable below 73 K, which occurs in the middle of the cable. Based on the thermal modelling, up to 0.85 W/m of total AC losses are allowed in the three-phase cable core assuming a cryostat loss of 0.5 W/m. Based on the same design, the cooling station at each cable end requires a capacity of 4 kW and has a footprint of 50 m². The low cable impedance makes it easier to integrate dispersed generation and distributed energy resources due to the ability to attract the load flow. The designed cable has the ability to limit a fault current to 4 kA_{rms} let trough current within 4-6 cycles, with the heat up of the core tapes to a maximum of about 130 K occurring approximately in the mid-section of the cable. Due to the concentric arrangement

of the cable phases, a neutral current of 10 % of the phase current is estimated. By selecting proper twist pitches the current in the cable neutral is reduced substantially, which only require a sectioned the most outer phase layers.

A HTS triaxial distribution cable concept and interior arrangement have been advised, satisfying the Alliander challenging network specifications discussed in Chapter 4. We designed a cable core (addressing the challenging constrains) which uses good quality narrow YBCO tapes arranged with minimized gaps in electrically insulated layers, optimised twist pitches and diameters. This resulted in a measured single phase AC loss of 0.096 W/m at 3 kA_{rms}, 77 K and 50 Hz, well below the loss target (0.2 W/m). The designed and tested cable cryostat has low friction and low pressure drop, enabling the required distance between two cooling stations of 6 km. The 16 mm thick layers of PPLP electrical insulation met the electrical requirements. Modelling the fault current behaviour of the cable shows a current limitation to 4 kA_{rms} let through current within 4-6 cycles (from a prospective 15 kA peak current). The cable system can be cooled by two 4 kW refrigerators, each with a footprint of 50 m².

7.2.6 HTS HVDC cables and outlook

HTS HVDC cable enables bulk electrical power transport at high capacity and over long lengths. The cable power capacity can reach dozens of GW and is limited by the available DC circuit breakers. To compare, present capacity of conventional cable and OHL is limited to 3 and 7 GW respectively. Such HTS cables are identified as a good option to increase the power capacity of the interconnections, e.g. NorNed, NorGer, BritNed. The expected advantages are: lower costs, lower ROW, lower loss and no need to use multiple cables or OHLs in parallel. Cooling stations at sea are avoided as the designed HTS cable has just two cooling stations placed onshore and spaced by 260 km. At the cable design level, the HTS HVDC core has negligible electric losses and simpler design as compared to the HTS AC core. Close spacing of the DC cores is possible without decrease of the cable power capacity. A HTS screen results in no external magnetic field produced by the DC cores. At technology level we assumed in our study that the HTS tape price is acceptable; that HTS cable core is efficient and cheap; that HV insulation is proper; that cryostats are adequate (reliable, easy maintenance; low heat leak, low price); that cooling is efficient and reliable; that testing facilities and standards are in place. In fact, these challenges must be properly addressed before HTS HVDC cables will mature. Based on the current maturity of the HTS cable components we expect that sufficiently long HTS DC cable will be commercially available within 5-10 years, assuming that sufficient research and development is in place.

As compared to known alternatives, HTS HVDC cable offers the following advantages: higher power capacity (about ten to twenty times more electrical power limited only by the circuit breaker), ability to increase the cable power

capacity by upgrading the HTS core with better tapes, negligible DC resistance (the main loss is in the cryostat), enabling high power capacity connection using Voltage Source Convertors (VSC) and Line-commutated convertors (LCC), thermal independence of its surrounding and no external magnetic field, close spacing of the poles without losing power capacity, since the cables are thermally independent of each other, lower weight, less pronounced aging of the insulation and the electric stress is independent of the load. The Dutch HVDC connections are typically used offshore, e.g. interconnectors (such as BritNed, NorNed, NorGer), connections to wind farms (~100 km) and a future trend is foreseen to use HVDC systems on-land. Also several large international future projects and initiatives o.a. North Sea wind power, Desertec, European Supergrid, Offshoregrid, etc. need large amounts of electrical power to be transported over long distances in the future. On these locations HTS DC cables can be integrated. To illustrate our approach, we identified as prominent location the 260 km BritNed connection for upgrade its power transfer capacity (from 1 to about 3 – 10 GW) and to improve security of supply by adding this new parallel HTS DC cable. With due regard to the derived BritNed network specifications, a HTS DC cable concept is elaborated including a comparison with a DC cable concept. The HTS concept has advantages such as, higher power capacity with negligible DC resistance, thermal independence of its surrounding and no external magnetic field. Supposed by upgrading the BritNed connection will result in the advantages as mentioned above. Furthermore, we evaluated the recent worldwide HTS cables activities aiming for wide integration into grids between year 2020 and 2030. In our roadmap we consider cable projects, currently completed or being implemented: in Japan operating at 275 and 66 kV AC, US 138 kV AC and Korea 22.9 and 154 kV AC, 80 kV DC.

7.3 Opportunities for further research

Our investigation has shown that HTS cables are economically viable primarily in the transmission grid. We advise a demonstration project in order to show their advantages. During the finalization of the thesis a 150 kV HTS AC cable demonstration project was started, initiated by TenneT and TUDelft. The purpose of this project is to demonstrate the technology level in Dutch transmission grid and thus to make a first step towards HTS AC cables at 380 kV.

To our opinion, on a shorter term, current focus of the research on AC HTS cables has to move from distribution to transmission voltage levels. More research is needed for the introduction of (E)HV HTS cables such as thermal and electrical designs, system interaction issues, better HTS tapes, etc. as follows from chapters 2-3. Integration of HTS AC transmission cables into the grids on a longer run will decrease HTS prices and so will make AC distribution cables economically

competitive. Competitive design concepts of such cables are described in chapters 4-5 and those can provide a basis for further research and development.

As compared to DC, AC HTS cables are more developed at present. However, on a longer-term DC HTS cables have better potential offering for instance lower losses in conductors and dielectrics but at the same time require major improvement on maturity, reliability and economy calling for a sound research and development aiming at longer cables and longer distance between cooling stations, better joints and more reliable terminations. Furthermore, larger countries are in demand for HVDC cables already. Therefore, long-term research must elaborate DC HTS cable using the design concept outlined in Chapter 6.

Since properties of YBCO (ReBCO) tapes define many of HTS cable characteristics, it is important to further increase the engineering current density (primarily by increasing the superconductor to total fill factor, e.g., making thicker ReBCO layers of good quality) and to further optimize the AC losses in HTS tapes without increase of their price as well as in a cable core. Basic research for further tape improvements and for discovering new superconducting materials relevant for power applications should continue.

At the technology level, common to all HTS power cables system designs we recommend the following:

- To introduce sufficient length of HTS cables in the transmission grid since it is shown to be a cost efficient solution compared with conventional solutions (e.g. example Krimpen-Geertruidenberg). This will lead to a drop in the HTS tape price enabling wider integration, finally also in the distribution grid.
- In order to develop a successful HTS cable system, the following key issues should be further to be addressed in the studies:
 - Further reduction of the cooling penalty;
 - Simpler and more compact cooling systems with longer lifetime;
 - Cheaper cryostats, with improved efficiency using e.g., novel multilayer thermal - insulation and spacers;
 - Electrical insulation with reduced AC loss for AC cables and manageable space charges for DC cables.

Appendix A

Conventional OHL and cable

In Figures A.1a and A.1b, a schematic (left) and a photo (right) are presented of cross-sections for an OHL wire and a high voltage cable (220 kV), respectively. The OHL is composed of properly arranged three layers of aluminium wire with the core of reinforced steel wire to enhance its mechanical strength, Figure A.1a. This wire bundle has an outer diameter of about 28 mm (assuming a 620 mm² conductor cross-section).

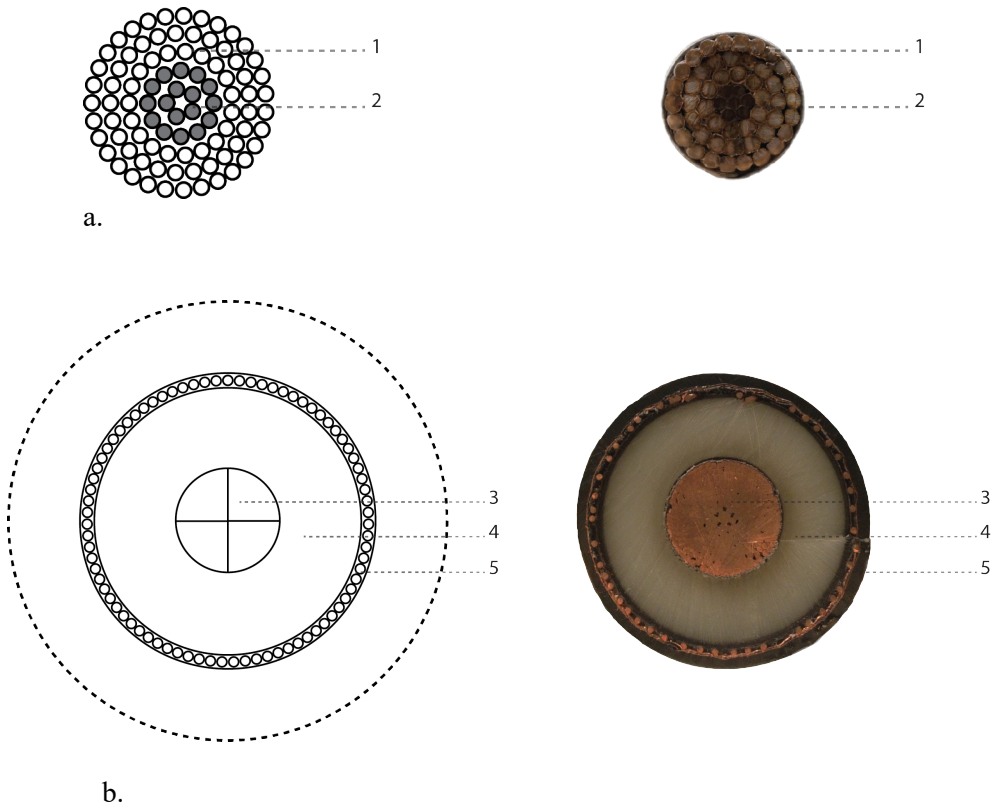


Figure A.1 schematic cross section of OHL conductor: 1-reinforced steel wire and 2 aluminium conductor (a) and of UGC conductor (b): 1-aluminum wire, 2-steel reinforcement wire, 3-cable core, 4-insulation and 5 cable shield.

The HV underground cable (UGC, 380 kV phase to phase in this case) is made of a copper core (approximately 80 mm outer diameter depending on the type of core configuration, 2.5 kA in this case) that is electrically insulated by a plastic (XLPE) extruded insulation (approximately 25 mm thickness) being in good connection with the core wherein the electric field is controlled, see Figure A.1b. A drawback is the thermal resistivity of the insulation and the dielectric loss its producing. One needs to optimise the cable loss to safely operate it and to prevent early aging.

The dashed circle in Figure A.1b (left) indicates the invisible outer dimension of the cable. The invisible distance is typically 700 mm, as recommended by [138]. The cable transport capacity is limited when another cable placed within the indicated area due to the proximity and skin effect, i.e. electromagnetic effects, yielding an uneven current distribution in the conductor that decreases the inductance and gives rise to the core resistance. In Randstad project, UGC's (about 2.5 kA_{rms}, 380 kV each) are typically spaced 750 mm from each other assuming a soil resistivity of 0.5 Km/W [26].

The losses in such cable occur mainly in the core and in the electrical insulation. Typically, the loss for a single 380kV cable (2500mm²) operating at nominal current is 41 W/m/phase ($I_{tr_rms} = 1320$ A). The loss is proportional to the transport current amplitude, thus when one cable per phase with a larger cross-section is selected, the loss will be about factor 4 larger. The dielectric insulation loss for a 380 kV single cable is about 1 W/m, see Table 3.6. It is clear from above that at full load the core loss has dominant effect on thermal aging of the cable electrical insulation.

The insulation condition often defines the remaining lifetime of a cable. Aging of insulation is attributed to stresses e.g., mechanical, temperature and voltage. Insulation is designed in such way that the cable will operate safely for 30 to 40 years. To reach such service life a maximum cable stress comprising XLPE insulation has a typical stress of 14 kV/mm is recommended by IEC 60287. In [3] a maximum operating stress between 7 and 16 kV/mm is described. In a single phase cable, the highest field strength is found at the conductor core surface. In practice, the maximum design stress is 12 kV/mm for 380 kV XLPE cables.

Laying arrangements define the maximum power capability and mechanical considerations, e.g., close cable spacing, laying depth, its surrounding. Conventional cables are often laid by: direct burial (flat, trefoil), in ducts, banks and galleries [138]. When direct buried in flat configuration is used, conventional cable operates close to its maximum transport capacity [26].

Direct buried cables are laid within the trench without any protection. However the heat removal depends on the soil type and is inherent to the maximum transport power. The heat removal can be increased using backfills in the trench, see Figure A.2. Conduit and ducts provide additional mechanical protection e.g. concrete enclosure and ducts prevent a prolonged period of civil works. The ducts are installed at first after which the cables are pulled in.

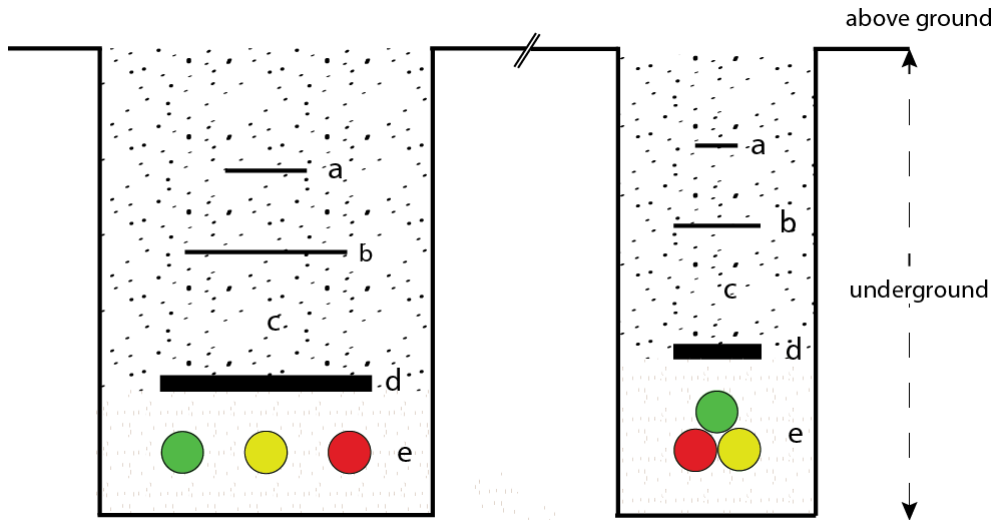


Figure A.2 Typical trench for flat (left) and trefoil (right) formation [138]: a warning layer, b warning grid, c backfill, d concrete layer, e good thermal property layer (e.g. fine sand).

When more circuits are planned in one area, it can be attractive to use a gallery. A gallery can house several cables in a limited space since its produced heat can be easily removed. Other advantages are: easy replacement and maintenance or repair. The disadvantage of a gallery is that the investment costs are high as compared to the other options.

In Figure A.2 left and right a typical trench for a cable circuit in flat and trefoil configuration is shown. The cable is surrounded by a highly thermal conductive material (e) with on top of that: a concrete cover, backfill, warning grid and a warning tape. As shown, the trefoil cable formation is more compact, which makes the trench smaller than that of the flat configuration, see Figure A.2. Moreover the trench materials for the flat and trefoil configuration are identical.

The depth of such a trench is typically 1.5 m, with a typical width for flat configuration of 11 m enabling a transmission power of 4-5 GVA, 400 kV [34], see Figure A.3.

In our study we assume a 5 kA transport current for each XLPE circuit with the arrangement as shown in Figure A.3 following [26].

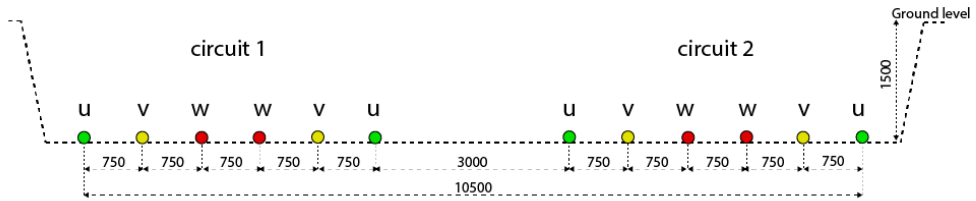


Figure A.3 Laying arrangement for three single phase cables (measures are in mm).

To summarise the technical and social merits for the OHL and the UGC connection (assuming 380 kV, 5 kA) a comparison is made between the most important properties in Table A.1.

Table A.1 comparison of properties for OHL and conventional cables at 380kV and nominal power of $5kA_{rms}$.

Property at 380 kV, 5 kA	OHL	Conventional UGC
Electric losses	+++	++
Reactive compensation	+	+++
Heat removal	+++	+
Connection length (>50 km and <200 km, >1GW)	+++	+
External magnetic field	+++	++
Visual pollution	+++	+
ROW	+++	+
Maturity of technology (400 kV)	+++	++
Weather issues	+++	+
Repair time	+	+++
Investment costs	+	+++

+++ high; ++ medium; + low, where high is beneficial and low is a disadvantage property.

The results from Table 1 show that UGCs compared to OHLs are only suitable for relatively short lengths and need special treatment to remove the produced heat. This is why the cable trench consists of several individual layers with a good thermal conductivity. Warning layers in the trench prevent excavation damages. The excavation work of such a trench contributes substantially to cable investment costs. This is the main reason that the investment costs for UGCs are higher than that of the OHLs. Moreover, a failure in the UGC is more difficult to locate and access compared to the OHL. On the other hand, the visual pollution of OHLs are vanished and the right of way is more compact for UGCs as compared to the OHLs. The compactness of the UGC trench results in a reduction of the magnetic field pollution. Issues to be resolved to allow significant UGC cable lengths in the

extra high voltage grid are: the need for reactive compensation, the long repair time, the high failure rate, the maturity and the high investment costs. Currently undergrounding in the EHV grid is only considered in the following scenarios where OHLs are not an option [33]: densely populated areas, areas where land is unavailable or consensus for overhead lines is difficult to obtain, river, sea and other natural obstacles, areas where land has outstanding natural historic or environmental significance and areas where land value must be maintained for future urban expansion and rural development.

Appendix B

Sample of electrical insulation for type testing

Within the DSMVC project consortium, a revised test sample was made as part of the type test for the 50 kV Dutch cable insulation.

The test facility [107] operates at its limit when testing a 50 kV_{rms} sample. A revised test sample was made which had no metal parts on the outside. In order to make this possible, the stress cone was made thicker to obtain low radial and tangential field strengths. Maximum field strengths in the stresscone are set to be 40 kV/mm and 1.5 to 2 kV/mm in radial and tangential direction, respectively. Field strengths are further optimized by adjustment of the ground tube.

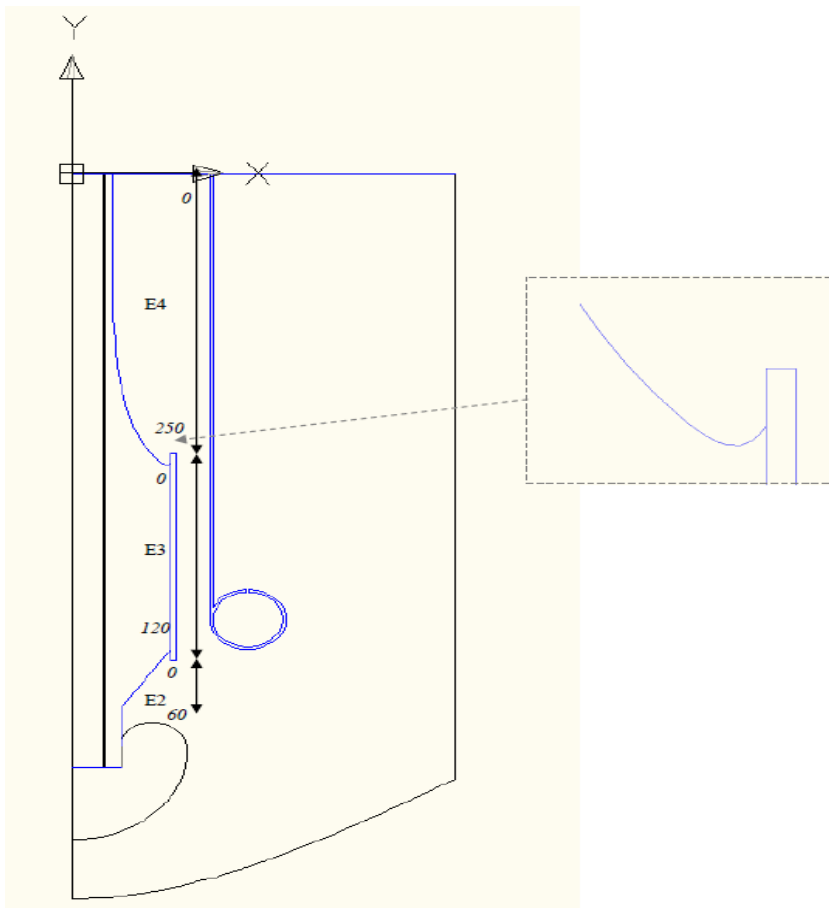


Figure B.1 drawing of the sample

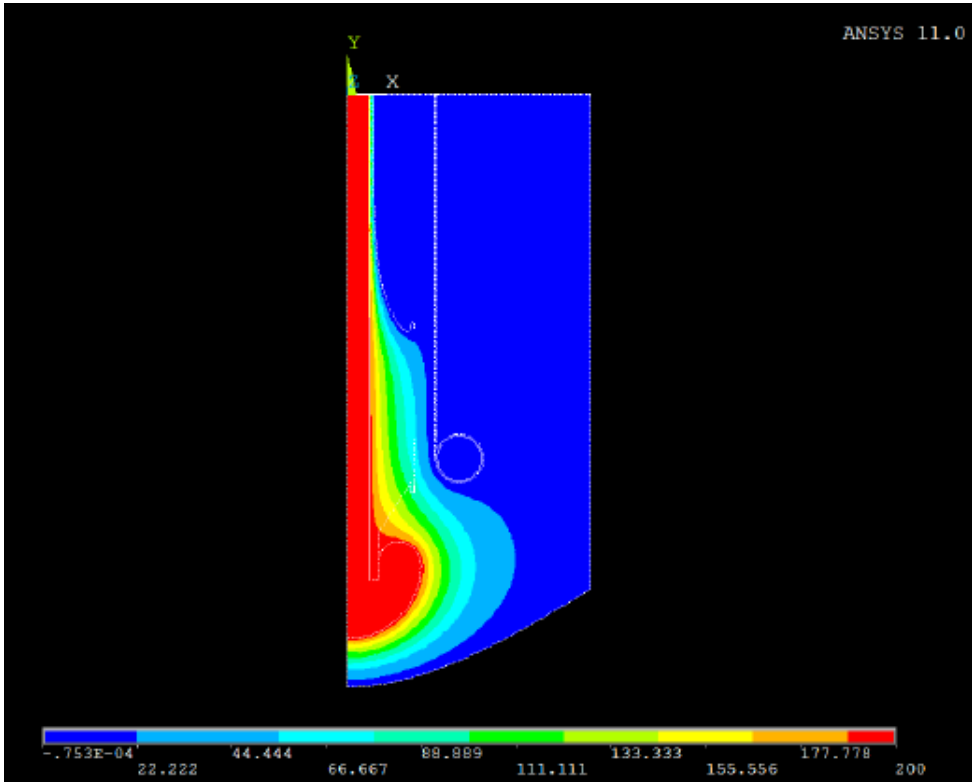


Figure B.2 drawing of the potential plot

Finite element calculation

In Figure B.1 and B2, the symmetric model is shown which represents one fourth of the total sample. The electric field strengths are calculated along section E2, E3 and E4.

Most important is the point, which connects E4 and E3. This point is also enlarged in Figures B.3 and B4.

Below, the graphs of the electric field strengths deduced along E4, E3 and E2 are given. The electric field strength for tangential, x and y direction are presented in blue, red and black, respectively and are within the expectations.

We can conclude that the maximum field stresses are below 2 kV/mm and therefore satisfies the maximum field requirement in the stress cone.

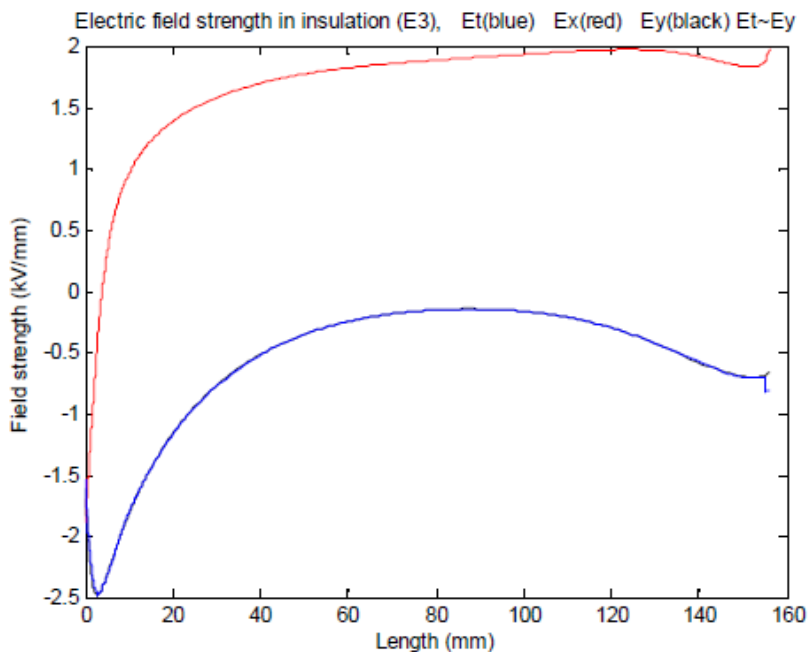
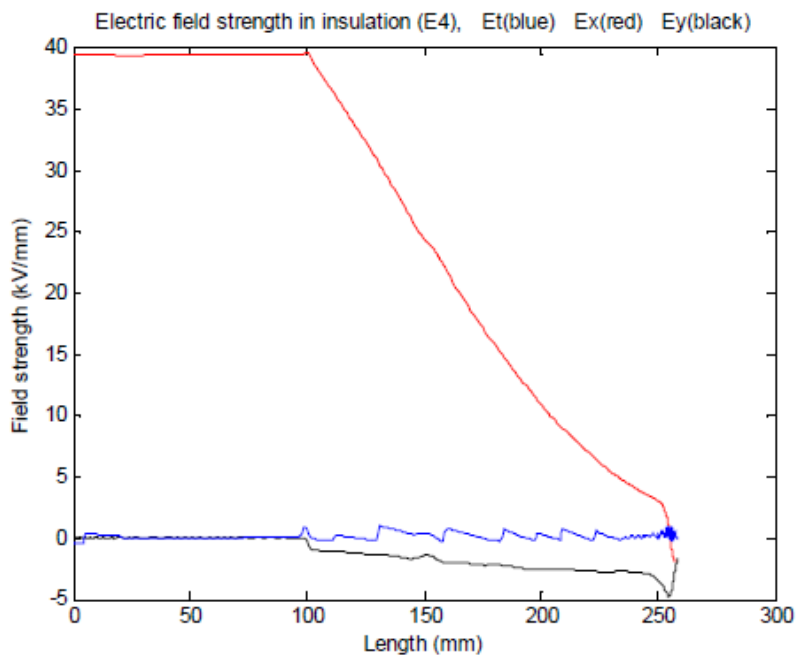


Figure B.3 Field strength along section E4 (top) and middle field strength along E3 (bottom)

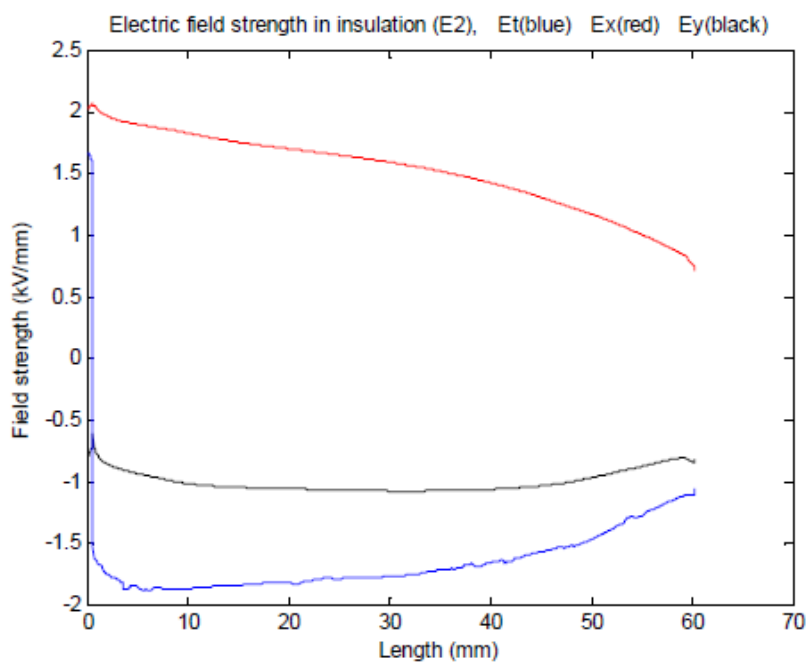


Figure B.4 Field strength along E2.

Appendix C

System test requirements

The general triaxial HTS cable design is available from NKT cables, however for the DSMVC project a new design is needed. Additional tests are required to verify a reliable operation throughout its operational lifetime. No IEC high voltage test standard is yet made wherein a recommend a test program is described in order to expect a successful quality over the cable operational lifetime. This is a very important issue since the reliability of a new cable should at least be similar to its alternatives. Therefore, in this Appendix we present a recommended test program to prevent failures in the cable at an early stage. Because a new cable design involves type testing, recommendation type tests are included. To finally qualify the HTS cable, it requires tests at different cable temperatures, electrical stress in the insulation and cable currents.

Based on the experience of succeeded HTS cable projects [107, 139] and using IEC standards [105, 140] and Cigré brochure [108], a recommended test scheme is developed. Since the cable operates at 50 kV, the cable dielectric needs special attention. Proposed is to take a step by step approach and test the insulation first on a short cable piece. In this way the required insulation thickness can be determined and a design fault can be found at an early stage.

A step by step program according to IEC 60840 and related to superconducting aspects are indicated in Table C.1. The test loop length should be at least 10 meter and the free length between accessories should be at least 5 meter, as stated in IEC 60840 and Cigré brochure 538.

Table C.1 Recommended DSMVC project test program.

Step	Test loop
1	10 m single core cable + two single core terminations
2	10 m single core cable + two single core terminations + one single core joint
3	10 m triax cable + two single core terminations
4	10 m triax cable + two single core terminations + one triax joint

1. Type testing on cable and accessories
2. Routine testing on cable and accessories
3. Long term test

We propose to combine the type and routine tests into one program especially selected for the DSMVC cable. The type test program has to be performed in the sequence as stated in the IEC standard. A summary of type and routine tests according to the IEC 60840 are listed in Table C.2 below.

In addition to the type and routine test, an after laying test is proposed. The after laying test verifies the quality of the DSMVC after installation and is also included in Table C.2.

According to IEC60840 the value U_0 for the determination of the test voltages is specified by a test voltage defined by Table C.2 of IEC60840. In the IEC standard clause 8.4 is written that if the rated voltage is not close to the values in the table, the value of U_0 on which the test voltages are based shall be the rated value. Corresponding to the DSMVC this corresponds to $50 \text{ kV}_{\text{rms}}$.

The U_0 proposed for the DSMVC dielectric tests is U_0 . However the manufacture or user may decide to increase U_0 to $72.5 \text{ kV}_{\text{rms}}$. The higher value for U_0 gives extra margin, but will lead to a more expensive cable design.

As the cable is of the triaxial type, the electrical insulation is stressed from two phases. Therefore test voltages for the inner two phases have to be multiplied by 1.73 as recommended in Cigré brochure 538.

Table C.2 Proposed combination of routine and type test based on IEC and Ultra-requirements.

Sequence	Test type $U_0 = 50 \text{ kV}$	Voltage level	Duration	Ref. Standard/comments
1	Withstand, $1.0 \times U$	50 kV_{rms}	1 h	Ultra standard test
2	Conditioning at $1.75 \times U_0$ Partial discharge at $1.5 \times U_0$	88 kV_{rms} 75 kV_{rms}	10 s 0.5 h	IEC 60885-3/IEEE-48-1996 Sensitivity 5 pC or better Routine test/Type test
3	Withstand, $2.5 \times U_0$	125 kV_{rms}	30 min	Frequency 50-60 Hz Routine test

4	Conditioning at $1.75 \times U_0$ Partial discharge at $1.5 \times U_0$	88 kVrms 75 kVrms	10 s 0.5 h	IEC 60885-3/IEEE-48-1996 Sensitivity 10 pC or better Routine test
5	Tan δ , U_0	50 kVrms	30 min	Type test
6	Impulse test (BIL), +10/-10	325 kVdc	1.0-1.5 μ s/ 50+/-5 μ s	IEC 60230 ICEA S-94-649-2000/IEEE 48-1996 Type test
7	Withstand, $2.5 \times U_0$	125 kVrms	15 min	Frequency 50-60 Hz Type test
8	Conditioning at $1.75 \times U_0$ Partial discharge at $1.5 \times U_0$	88 kVrms 75 kVrms	10 s 0.5 h	IEC 60885-3/IEEE-48-1996 Ultra standard test
9	$1.0 \times U_0$ $1.75 \times U_0$	50 kVrms 88 kVrms	With ~20 impulse voltage steps	After laying test performed with e.g. OWTS System <50 pC new cable Depending on PD inception the ratio above U_0 will be taken into consideration. ($1.2U_0$ - $1.75U_0$) Max PD in comparison with paper-oil insulated cable, breakdown strengths of LN ₂ and Cryoflex are higher than paper-oil 50 damped AC impulses are equivalent to withstand voltage test

Sequence	Pre-condition tests	T[K]	V[kV]	C[kA]	Comments
1	Leakage test	-	-	-	Determine if the cryostat is leakage free
2	Drying of cable	-	-	-	Warm LN ₂ flow to degas the cable and to create a small temperature gradient
3	Critical current measurement of each conductor phase	77	/	DC	I _c = 1 μV/cm
Additional tests					
4	Conditioning test; varying the LN ₂ pressure 1 to 5 bar with the LN ₂ pressure pump	~67-77	U ₀	3	Measurements: Pd, Tan δ, ΔP, ΔT, LN ₂ flow rate LN ₂ consumption in L/min and kW
5	Conditioning test; Overload current test, ~30% overload for 24 hours	~67-77	U ₀	3 + 30%	Test duration ~ 24h, Measurements: Pd, Tan δ, ΔP, ΔT, LN ₂ flow rate LN ₂ consumption in L/min and kW
6	Conditioning test; Overload current test, ~67% overload for 1 hour	77	U ₀	3 + 67%	Test duration ~ 1h, Measurements: Pd, Tan δ, ΔP, ΔT, LN ₂ flow rate LN ₂ consumption in L/min and kW
8	Quench test, section of cable in normal state	77	U ₀	1-3	Measurements: Pd, Tan δ, ΔP, ΔT, LN ₂ flow rate LN ₂ consumption in L/min and kW

7	Fault current test; Ik'' =21kA, Ip = 57kA Protection: Tp1 = 120 ms, Tp2 = 4250 ms	77	U ₀	Ik''=21 Ip= 57	Cable will limit the fault current to Ik'' =4-10kA, Ip = 10-23kA, Measurements: Pd, Tan δ, ΔP, ΔT, LN ₂ flow rate LN ₂ consumption in L/min and kW
---	--	----	----------------	-------------------	--

Additional tests that are proposed to ensure the quality of the superconductive cable system. Additional tests regarding overloads are included in the program for verification of the cable quality during this operational condition.

To investigate the behaviour of the system in case the LN₂ pressure is varied during nominal currents, it may result in a thermal runaway. Over current tests are proposed to investigate the current limiting behavior and temperature variations. Proposed is to repeat the critical current measurement after the short circuit tests to investigate if the cables critical current is not changed due to over current testing. Pre-conditional tests are added to verify the cable condition before the cable test system is attributed to the test program.

Bibliography

References

- [1] David Larbalestier, et. al., *High- T_c superconductor materials for electric power applications*, Nature, vol. 414, November 2001.
- [2] US department of Energy, *Basic research needs for superconductivity - Report on the Basic Energy Sciences Workshop on Superconductivity -*, May 8-11, 2006.
- [3] Chevtchenko O. A., *On the application of high- T_c superconductors in power coils and transformers*, PhD thesis, University of Twente, 2002.
- [4] V. Matias, R.H. Hammond, *YBCO Superconductor Wire based on IBAD-Textured Templates and RCE of YBCO: Process Economics*, Proc. of Physics, vol. 36, pp. 1440–1444, 2012.
- [5] D.W. Hazelton, *2G HTS Conductors at SuperPower*, Low Temperature High Field Superconductor Workshop 2012 (LTHFSWS2012), Napa, CA, November 6, 2012.
- [6] R. M. Scanlan, A. P. Malozemoff, and D. C. Larbalestier, *Superconducting Materials for Large Scale Applications*, Proc. of IEEE, vol. 92, no. 10, Oct. 2004, pp. 1639-1654.
- [7] G. Grasso, *MgB₂ ten years later: present state and perspectives for superconducting wires* (presentation), IASS Workshop, Transporting Tens of Gigawatts of green power to the market, Potsdam, May, 2011.
- [8] V. V. Kostyuk et. al., *Experimental Hybrid Power Transmission Line with Liquid Hydrogen and MgB₂Based Superconducting Cable*, ISSN 1060-7850, Technical Physics Letters, vol. 38, no. 3, pp. 279–282, 2012.
- [9] S. Choi, et. al., *AC loss in MgB₂ superconducting wires at various operating temperatures*, IEEE transactions on applied superconductivity, vol. 21, no. 32011.
- [10] A. Poncet and V. Parma, *Series-produced helium II cryostats for the LHC magnets: technical choices, industrialization, costs*, Adv. In

- Cryogenic Engineering, CEC, ed. by J. G. Weisend II, vol. 53, pp. 739-746, 2008.
- [11] M. Gouge, *Flexible Cryostats for Superconducting Cables: Reliability and Lifetime Issues*, DoE 2006 Wire Development Workshop, Session VII, February 2006.
- [12] M.A. Green, *The costs of helium refrigerators and coolers for superconducting devices as a function of cooling at 4 K*, Advances in cryogenic engineering: transactions of the cryogenic engineering conference, AIP conference proceedings 985, 872 vol. 53, 2008.
- [13] T. R. Strobridge, *Refrigeration for superconducting and cryogenic systems*, IEEE Trans. on Nuclear Science, vol. 16, N3, pp. 1104-1108, 1969.
- [14] John S. Engelhardt, Steven A. Boggs, *Room temperature dielectric HTSC cable*, patent number: US6262375 B1, September 1992 <http://www.google.nl/patents/US6262375?hl=nl>.
- [15] SuperNet project EOSLT07050, years 2008-2014, *Evolutionary path for the integration of superconducting components in electricity networks of 2030*, funded by Dutch RVO, 28 February 2014, www.rvo.nl.
- [16] TenneT: *Vision 2030*, TenneT's long-term vision of the 380-kV and 220-kV elements of the Netherlands' national electricity transmission grid, February 2008, Arnhem, The Netherlands, www.tennet.nl.
- [17] Wilfried Breuer, Presentation: HVDC - Innovative Technology for smart grids and super grids, re-launch press event Maasvlakte, Siemens, March 31, 2011, http://www.ptd.siemens.de/Presentation_BritNed_Breuer.pdf consulted 2016.
- [18] Ministry of Economic Affairs, Agriculture and Innovation, Energy report, June 2011, <https://www.government.nl/documents/reports/2011/11/01/energy-report-2011> consulted 2016.
- [19] ECN, Energie-Nederland, Netbeheer-Nederland, Energie Trends 2012, November 2012, <https://www.ecn.nl/docs/library/report/2012/b12005.pdf> consulted 2016.
- [20] Energie-Netbeheer Nederland, Energy in the Netherlands, August 2011, <http://www.windunie.nl/Documents/Energie-in-Nederland-2011rapport.pdf> consulted 2016.

- [21] R. Zuijderduin, O. Chevtchenko, J. Smit, G. Aanhaanen, and R. Ross, *Strengthening future electricity grid of the Netherlands by integration of HTS transmission cables*, Journal of Physics conference series, vol. 507, part 3, 2014.
- [22] M. Stemmler, et al., *AmpaCity – Installation of advanced superconducting 10 kV system in city center replaced conventional 110 kV cables*, applied superconductivity and electromagnetic devices, Beijing China, October 2013.
- [23] O. Chevtchenko, et al., *Low AC loss in a 3 kA HTS cable of the Dutch project*, Physics Procedia 36, pp. 1285-1289, 2012.
- [24] TenneT: *TenneT Kwaliteits- en Capaciteitsplan 2010 - 2016 / deel II A*, november 2010, Arnhem, page 21.
- [25] R. Zuijderduin, O. Chevtchenko, J.J. Smit, G. Aanhaanen, I. Melnik, A. Geschiere, *Integrating HTS components into the futures grid of the Netherlands*, ISH 2011 17th International Symposium on High Voltage Engineering August 22nd-26th 2011, Hannover, Germany, DVD published, ISBN: 978-3-8007-3364-4.
- [26] Ministerie van economische zaken, *cost comparison between underground cables and O.H. line and Report on network reliability aspects of the choice line versus cable for the randstad 380 project*, BLG15907, 30892, nr 14, published 29-05-2008, April 2008, <https://www.parlementairemonitor.nl/9353000/1/j9vviij5epmj1ey0/vhvbent1ftzr>.
- [27] K. Shimoyama, et al, *Experimental results of tri-axial HTS cable*, Cryogenics 49, pp. 398–401, 2009.
- [28] J. Howe, et al, *Very low impedance (VLI) superconductor cables: concepts, operational implications and financial benefits*, A White Paper, November 2003.
- [29] Private communication with G. Aanhaanen, TenneT, Januari 2010.
- [30] P. Kundur, *Power System Stability and Control*, Publication Date: January 1994, ISBN-13: 978-0070359581.
- [31] E. Zaccone (Prysmian Powerlink), *Synthetic description of performances and benefits of undergrounding transmission*, RealiseGRID, 2009.
- [32] Ministerie van economische zaken, *cost comparison between underground cables and O.H. line and Report on network reliability aspects of the choice line versus cable for the randstad 380 project*, April 2008

- [33] Realisegrid, Final WP1: report on cost/benefit analysis of innovative technologies and grid technologies roadmap report validated by the external partners, project supported by the European Commission under the 7th Framework programme, 2011, <http://realisegrid.rse-web.it/Publications-and-results.asp> consulted 2016.
- [34] IEC TR 60071-4 part 4: *Computation guide to insulation co-ordination and modelling of electrical networks first*, edition 2004-06.
- [35] Phase to Phase BV, Vision Network analysis, version 7.4.1; P.M. Van Oirsouw, Netten voor distributie van elektriciteit, ISBN/EAN: 9789081798302.
- [36] H.G.J. Kamp, *Letter to the (Dutch) Lower Chamber: Wonen in de buurt van hoogspanningsverbindingen*, 16 April 2013.
- [37] E. Zaccone, Presentation E-highway2050: *High voltage underground and subsea cable technology options for future transmission in Europe*, WP3 Workshop, April 15th 2014 Brussels.
- [38] Cigré Technical Brochure 250, *General guidelines for the integration of a new underground cable system in the network*, working group B1.19, August 2004.
- [39] Cigré Technical Brochure 199, *Superconducting cables impact on network structure and control*, task force 38.01.11, 2005.
- [40] *EHV AC Undergrounding electrical power: Performance and Planning (Power Systems)*, Springer, 1st edition, May 2010, ISBN: 139781848828667.
- [41] R. D. Zimmerman, C. E. Murillo-Sánchez, and R. J. Thomas, "MATPOWER: Steady-State Operations, Planning and Analysis Tools for Power Systems Research and Education," *IEEE Transactions on power systems*, vol. 26, no. 1, pp. 12-19, Feb. 2011.
- [42] SER, *Energieakkoord voor duurzame groei*, September 2013.
- [43] Parsons Brinckerhoff in association with cable consulting international Ltd', *Electricity Transmission Costing Study, An independent report endorsed by the institution of engineering & technology*, issued 31 January 2012 with errata April 2012.
- [44] R. Faulkner, *Hybridizing HVDC Transmission with Non-Local Energy Storage and Large Dispatchable Loads for Load Leveling*, Power and Energy Society General Meeting, 2011.
- [45] Y. Yamada, et al. *Whats new in the World of Superconductivity*, ISTE, Superconductivity Web 21, August 2013.

- [46] *Program on Technology Innovation: a Superconducting DC Cable*. EPRI, Palo Alto, CA: 2009. 1020458.
- [47] S.P. Ashworth, P. Metra, R.J. Slaughter, *A techno-economic design study of high-temperature superconducting power transmission cables*, ETEP vol. 4, no. 4, pp 293-300, July/August 1994.
- [48] R. Zuijderduin, O.A. Chevtchenko, J.J. Smit, G. Aanhaanen, I. Melnik, A. Geschiere, *Sustainable future Dutch Grid by integration of high temperature superconducting cables*, Applied Superconductivity and Electromagnetics (Special Issue – Proceedings of Cigré D1-WG38 Workshop), November, 2013.
- [49] ENTSO-E (European network of transmission system operators), *Research and development roadmap*, September 2012.
- [50] Private communication Prof. Mart van der Meijden, TenneT / TUDelft.
- [51] *Annual Report TenneT TSO B.V.*, 2012.
- [52] TenneT, *The Wintrack pylon, an innovative solution for new high-voltage lines*, CE1063OB.EN1210, October 2013.
- [53] ECOFYS, *Study on the comparative merits of overhead electricity transmission lines versus underground cables*, pp. 120, 2013.
- [54] TenneT, *Underground high voltage cable study to enter next phase*, 8 February 2011
http://www.tennet.eu/nl/index.php?id=491&tx_ttnews%5Btt_news%5D=303 consulted 2016.
- [55] J.F.Maguire, et al., *Progress and Status of a 2G HTS Power Cable to Be Installed in the Long Island Power Authority (LIPA) Grid*, IEEE transactions on applied superconductivity, vol. 21, issue 3, 2011
- [56] O.Maruyama, T.Ohkuma, T.Masuda, Y.Ashibe, S.Mukoyama, M.Yagi, T.Saitoh, T.Hasegawa, N.Amemiya, A.Ishiyama, and N.Hayakawa, *Development of 66 kV and 275 kV Class REBCO HTS Power Cables*, IEEE Transactions on applied superconductivity, vol. 23, issue. 3, 2012.
- [57] EPRI, *Superconducting Power Equipment: Technology Watch 2012*, 2013, ISBN: 1024190.
- [58] M.Kosaki and et al., *Development and tests of extruded ethylenepropylene-rubber-insulated superconducting cable*, Cryogenics 35, 805-807.
- [59] ABB, *XLPE Land Cable Systems User's Guide*, Rev 5, 2013.

- [60] RD.Rosevear and et.al, *Insulation coordination for HV AC underground cable system*, joint working group, 21/33, 2013.
- [61] H. Okubo and et.al, *Development and Application Trend of Superconducting Materials and Electrical Insulation Techniques for HTS Power Equipment*, Cirg  D1-306, Working group SC D1. 15, 2004.
- [62] M. Yagi, et al., *The Development of 275 kV-3 kA YBCO High-Tc Superconducting Power Cable*, Special issue Smart grid Furukawa review, no. 34, 2013.
- [63] N. Hayakawa and et al., *A Novel Electrical Insulating Material for 275 kV High-Voltage HTS Cable with Low Dielectric Loss*, 11th European Conference on Applied Superconductivity (EUCAS2013), Journal of Physics: Conference Series 507 (2014) 032021 2013.
- [64] H.Okubo, M.Nagino, H.Kojima, N.Hayakawa, T.Takahashi, and K.Yasuda, *Impulse and AC pd inception characteristics of LN₂/polypropylene laminated paper composite insulation system*, International Conference on dielectric liquids, 429-432, 2005.
- [65] S. Mukoyama, et al., *Model Cable Tests for a 275 kV 3 kA HTS Power Cable*, IEEE Transaction on applied superconductivity, vol. 21, no. 3, June 2011.
- [66] H.Neumann, *Concept for thermal insulation arrangement with a flexible cryostat for HTS power cables*, vol. 44, pp. 93-99, 2004,.
- [67] EPRI, *Superconducting cable construction and testing*, EPRI, Palo, Alto, CA, and U.S. Department of Energy, Washington, D.C.: 2000. 1000160.
- [68] O. Chevtchenko, R. Zuijderduin, J. Smit, D. Will n, H. Lentge, C. Thidemann, and C. Traeholt, *Low friction cryostat for HTS power cable of Dutch project*, Published by Elsevier B.V., 36, 1309-1312, 2012.
- [69] A.Sasaki, Yu.Ivanov, and S.Yamaguchi, *LN₂ circulation in cryopipes of superconducting power transmission line*, Cryogenics 51, 471-476, 2011.
- [70] J.A.Waynert, F.C.Prenger, T.A.Jankowski, and J.A.Stewart, *Long term vacuum maintenance in HTS equipment without external pumping*, American Institute of Physics 0-7354-0186-1/04, 49, 2004.
- [71] J.A.Demko, *Thermal Management of High-Temperature Superconducting Power Cables*, Space Technology and Applications International Fomm-STAIF, CP608, edited by M.S. El-Genk, 2013.

- [72] J.F.Maguire and et.al, *Program update on the development and demonstration of a HTS power cable to operate in the long island power authority transmission grid*, IEEE Power Engineering Society General Meeting, 2007.
- [73] M.Stemmler and et.al, *Superconducting HVDC Power Cables for Voltage Source Converter Systems*, Cigré B1-302, 2013.
- [74] Fesmire, J. E., Augustynowicz, S.D., and Darve, C., *Performance Characterization of Perforated MLI Blanket*, Proceedings of the Nineteenth International Cryogenic Engineering Conference, ICEC 19, Narosa Publishing House, New Delhi, pp. 843-846, 2003.
- [75] S.Kalsi, *Applications of high temperature superconductors to electric power equipment*, April 2011, Wiley-IEEE Press, ISBN: 978-0-470-16768-7.
- [76] J.Gerhold and T.Tanaka, *Cryogenic electrical insulation of superconducting power transmission lines: transfer of experience learned from metal superconductors to high critical temperature superconductors*, Elsevier, 1998, 38, 11, 1173-1188
- [77] C. Traeholt, *Termination Unit*, pub. No. US 2010/0126748A1, 2013, pub. No. US 2010/0126748A1
- [78] C.N.Rasmussen and C.Rasmussen, *Optimization of termination for a high temperature superconducting cable with a room temperature dielectric design*, IEEE transactions on applied superconductivity, 2013, 9, 1
- [79] H. Thomas, *Some socio-economic aspects of long-distance energy transport by superconducting power lines with a focus on MgB₂*, presentation IASS, 2015.
- [80] Gate, 2013, <http://www.gate.nl/en/gate-terminal.html>, consulted January 2015.
- [81] WG B1.19, *General guidelines for the integration of a new underground cable system in the network*, TB 250, 2004.
- [82] Karen Fan, *Liquid nitrogen cost*, 2007 <http://hypertextbook.com/facts/2007/KarenFan.shtml> consulted 2016.
- [83] S. Meijer, et al., *Availability and Risk Assessment of 380 kV Cable Systems in Transmission Grids*, B1-104, Paris, Cigré 2012.
- [84] M. Yagi, *275 kV transmission Cables – Current Status and Future efforts -*, Supernet Symposium, TUDelft, The Netherlands, November 11th 2015.

- [85] H. Yumura, et al., *Update of Yokohama HTS cable project*, *IEEE transactions on applied superconductivity*, vol 23, no 23, June 2013.
- [86] United States Department of Energy Office of Electric Transmission and Distribution, *National Electric Delivery Technologies Roadmap, Transforming the grid to Revolutionize Electric Power in North America*, January 2004.
- [87] A. M. Wolsky, “*A roadmap to future use of HTS by the power sector (HTS from pre-commercial to commercial)*”, executive summary”, September 2013.
- [88] A. M. Wolsky, *From Pre-Commercial to Commercial: a roadmap to future use of HTS by the power sector*, presentation at IEA ExCo Meeting held in Lausanne, Switzerland, 22-24 May 2013.
- [89] I. Melnik, *System study on interaction of HTS cables with power grids* (presentation), EUCAS 2011.
- [90] A. Geschiere, et al., *Long distance triax HTS cable*, 19th International Conference on Electricity Distribution, Cired, Vienna, 21-24 May 2007.
- [91] NKT cables, *High voltage cable system*, brochure, 2009.
- [92] M. Stemmler et. al., *Medium voltage superconducting cable system for inner city power supply*, Second Seminar on Undergrounding of Electric Distribution Networks, Calbos 2011.
- [93] A. Breuer, et. al., *Superconducting medium-voltage cables for urban power supply as an alternative scenario to 110 kV installations*, B1-301 Cigré, Paris 2012.
- [94] H. Yumura, et. al., *Phase II of the Albany HTS Cable Project*, *IEEE transactions on applied superconductivity*, vol. 19, no. 3, June 2009.
- [95] D. Willen, et al. *Type testing of a 13.2 kV, 69 MVA Triax HTS cable*, 7th international conference on insulated power cables, Jicable, Versailles France, 2007.
- [96] M. Ohya, et al., *Japan’s First Live Power Transmission Using 3-in-One Superconducting Cable (High-Temperature Superconducting Cable Demonstration Project)*, SEI technical review, number 76, 2013.
- [97] D. Willen et. al., *A superconductive multi-phase cable system, a method of its manufacture and its use*, patent number WO 2006111170 A2, October 2006.

- [98] A. Geschiere, et. al., *Breakthrough in development of superconducting cables*, 21st International Conference of Electricity Distribution, Frankfurt, 6-9 June 2011.
- [99] J.J. Rabbers et al., *Self-field loss of BSCCO/Ag tape in external AC magnetic field*, *Physica C*, vol. 300, issues 1-2, pp. 1-5, May 1998.
- [100] O. Chevtchenko, *Modeling of high temperature superconducting tapes, arrays and AC cables using COMSOL*, COMSOL Conference, November 17-19, Paris, 2010.
- [101] W.T. Norris, *Calculation of hysteresis losses in hard superconductors carrying AC: isolated conductors and edges of thin sheets*, *J. Physics D: Applied Physics*, vol. 3, 1930.
- [102] S.K. Olsen, et al., *Alternating current losses of a 10 meters long low loss superconducting cable conductor determined from phase sensitive measurements*, *superconducting science and technology*, vol. 12, pp. 360-365, 1999.
- [103] O. Maruyama, et al., *Development of REBCO HTS power cables*, *Physics Procedia*, 2012, 36, 1153-1158; M. Yagi, et. al., *The development of 275 kV-3kA YBCO high-Tc superconducting power cable*, Furukawa review 2013.
- [104] Private communication: D. Willen, Ultera.
- [105] International standard: *Power cables with extruded insulation and their accessories for rated voltages above 30kV up to 170kV*, CEI/IEC 60840:2004.
- [106] S. Mukoyama, et al., *Conceptual design of 275 kV class high-Tc superconducting cable*, *Physica C: Superconductivity*, vol. 470, issue 20, pp. 1563-1566, 2010.
- [107] S. Fink et al., *High voltage testing of short samples of 110 kV high temperature power superconducting transmission cables with HAIhKE facility*, proceedings of 14th International Conference on Dielectric Liquids (ICDL 2002), Graz (Austria), July 7-12, 2002.
- [108] Cirié, *Recommendations for testing superconductive cables*, working group B1.31, June 2013.
- [109] Moody, L. F. *Friction factors for pipe flow*, *Transactions of the ASME* 66 (8): pp. 671-684, 1944.
- [110] B. Zajackowski, A.J.M. Giesbers, M. Holtrust, E. Haenen, R. den Heijer, *Feasibility of inline cooling in long distance HTS power line*, *Cryogenics* vol. 51, nr. 4, pp. 180-186, 2011.

- [111] Lee C. H. W, e.a. *Performance of heat transfer and pressure drop in superconducting cable former*, Cryogenics, vol. 43, nr. 10-11, pp. 583-588, 2003.
- [112] S. Fuchino et. al., *Hydraulic characteristics in superconducting transmission power cables*, Physica C, 354, pp. 125-128, 2001.
- [113] www.iztech.ru, consulted 2016.
- [114] Ultera, *Report on models and results for Alliander 6 km cable*, confidential & proprietary, 2009.
- [115] I. Melnik, et al, *Long length HTS cable with integrated FCL property, 9th European Conference on Applied Superconductivity (EUCAS 09)*, Conference Series 234 032037, 2010.
- [116] Ultera, *Status of FCL computer model results for project Alliander*, confidential and proprietary, 2010.
- [117] J. Howe, et al, *very low impedance (VLI) superconductor cables: concepts, operational implications and financial benefits*, A White Paper, November 2003.
- [118] R. Zuijderduin et al., *Electrical model of balanced AC HTS power cable*, Physics Procedia 36, pp. 1145 – 1148, 2012.
- [119] K. Shimoyama et al., *Experimental results of tri-axial HTS cable*, Cryogenics 49, pp. 398-401, 2009.
- [120] North Sea wind power and the grid: <http://www.ewea.org/index.php?id=196>, consulted at 31-3-2014.
- [121] DESERTEC: <http://www.desertec.org/concept/>, consulted at 31-3-2014.
- [122] European Supergrid: <http://www.friendsofthesupergrid.eu/fosg-report-on-the-preparatory-phase-of-a-supergrid-3/>, consulted at 31-3-2014.
- [123] OffshoreGrid: <http://www.offshoregrid.eu/>; http://www.trecuk.org.uk/resources/airtricity_supergrid_V1.4.pdf, consulted at 31-3-2014.
- [124] W.G.J. Rondeel, *Hydro Electricity and Storage Capabilities in Norway –can they be useful for Europe?*, HIT Telemark University College, 2012.
- [125] Maaïke Noordhuis, *Tennet onderzoekt aanleg hoogspanningskabel tussen Randstad en Duitsland* Energieia, 19 February 2014, <http://energieia.nl/nieuws/610721-1402/tennet-onderzoekt-aanleg-hoogspanningskabel-tussen-randstad-en-duitsland>, consulted at 31-3-2014

- [126] ENTSO-E, *10-Year network development plan*, 2014.
- [127] FOSG <http://www.friendsofthesupergrid.eu/fosg-report-on-the-preparatory-phase-of-a-supergrid-3/>, consulted at 31-3-2014.
- [128] ABB high voltage cables, *The NorNed HVDC Connection*, Norway – Netherlands (leaflet), www.abb.com/cables.
- [129] T.K. Vrana, O.B. Fosso, *Technical aspects of the north sea super grid*, *electra* no. 258, Oktober 2011.
- [130] Nationalgrid, *High Voltage Direct Current electricity – technical information*, June 2010.
- [131] E-Highway2050, *High voltage underground and subsea cable technology options for future transmission in Europe* (Presentation), WP3 workshop April 15th, 2014 Brussels Europe.
- [132] C.M. Frank, *HVDC circuit breakers: A review identifying future research needs*, *IEEE transactions on power delivery*, vol. 26, no. 2, April 2011.
- [133] A. Everaert, *Persbericht: Nexans rondt succesvolle test as van 's werelds eerste supergeleidend 200 kV-gelijkstroomsysteem*, 2010.
- [134] D. van der Laan, et.al, *Development of HTS Conductor on Round Core (CORC) cables for fusion applications at Advanced Conductor Technologies* (Presentation), HTS4Fusion 2014, Villigen, Zwitserland, January 23th, 2014, <http://advancedconductor.com/wp-content/uploads/2011/07/Laan-van-der-D.C.-HTS4Fusion-2014.pdf> consulted 2016.
- [135] Chevtchenko O. A., Smit J. J. and Geschiere A. „*Cryostat for a high-temperature superconducting power cable*“, patent PCT/NL2009/000251, WO2010/095925, published 26.08.2010.
- [136] T.Worzyk, *Submarine power cables – design, installation, repair, environmental aspects*, Springer, 2009, ISBN: 978-3-642-01269-3.
- [137] N.M. Macleod et. al., *Tres Amigas: an innovative HVDC link between three asynchronous AC networks*, Cigré SCB4 Colloquium 2011.
- [138] Nexans, *60-500 kV High Voltage Underground Power Cables XLPE insulated cables*, 2013.
- [139] T. Masuda et al., *Test results of a 30 m HTS Cable for Yokohama project*, *IEEE transaction on applied superconductivity*, vol. 21, no. 3, June 2011.
- [140] IEEE std. 13.13.1-1996.

List of abbreviations

Abbreviation	Description
AC	Alternating Current
AT	Auto Transformer
BIL	Basic Insulation Level
BSCCO	Bismuth Strontium Calcium Copper Oxide
CC	City Cable
CC	Circuit Cost
CB	Circuit Breaker
CD	Cold Dielectric
CO ₂	Carbon Dioxide
CPR	Cost Performance Ratio
CSC	Current Source Convertor
CT	Current Transformer
DC	Direct Current
DER	Distributed Energy Resources
DMC	Dismantling costs
DSMVC	Dutch Superconducting Medium Voltage Cable
DSO	Distribution System Operator
DTU	Danish Technical Univerisity
EBIT	Earnings Before Interest and Taxes
EHV	Extra High Voltage
ENTSO-E	European Network of Transmission System Operators for Electricity
EPR	Ehylene-Propylene Rubber
EPRI	Electric Power Reasearch Institute
EU	European Union
FACTS	Flexible Alternating Current Transmission
FCL	Fault Current Limiter
FPR	Glass Fiber Reinforced Plastic
G	Generator

VM	Voltage Measurement
GFPR	Glass Fibre Reinforced Plastic
GPC	Gas Pressure Cable
GTB	Geertruidenberg
HK	Hoogte Kadijk
HTS(C)	High Temperature Superconductor (Cable)
HV(DC/AC)	High Voltage (Direct Current/Alternating Current)
IEC	International Electricaltechnical Commission
IVC	Investment Costs
KIJ	Krimpen
KIT	Karlsruhe Institute of Technology
LCC	Line-commutated convertors
LELC	Lifetime Energy Loss Costs
LGCC	Lifetime Generation Capital Costs
LIA	Lock-In-Amplifier
LIPA	Long Island Power Authority
LN ₂	Liquid Nitrogen
LTS	Low Temperature Superconductor
M	Motor
MgB ₂	Magnesium diboride
MLI	Multilayer Insulation
MNC	Maintenance Costs
MV	Medium Voltage
N	Number of tapes
NDK	Noord Klapprozenweg
OHL	Overhead Line
PDIE	Partial Discharge Inception Electric field strength
PE	Poly Ethylene
PPLP	Poly Propylene Laminated Paper
R&D	Research and Development
RC	Rogowski Coil
(RE)BCO	Rare earth - Barium - Copper Oxide
RES	Renewable Energy Sources
SM	Submarine

RMS	Root Mean Square
ROI	Return on Investment
ROW	Right Of Way
RWE	Rheinisch Westfalische Elektrizitatswerke
SFCL	Superconducting Fault Current Limiter
SIL	Surge Load Impedance
SS	Stainless steel
$\tan \square$	Dissipation factor
TEPCO	Tokyo Electric Power Company
TIVC	Total Investment Cost
TLTC	Total Life Time Cost
TP	Twist Pitch
TSO	Transmission System Operator
TUD	Delft University of Technology
TWh	Tera Watt Hour
UCTE	Union for the Coordination of the Transmission of Electricity
UGD	Underground Distribution Cable
UGC	Underground Cable
UHV	Ultra High Voltage
UK	United Kingdom
US	United States
VSC	Voltage Source Converter
VM	Voltage measurement
WD	Warm Dielectric
XLPE	Crosslinked polyethylene
YBCO	Yttrium Barium Copper Oxide

List of symbols

Symbol	Unit	Description
ω		Angular frequency
α		Expansion coefficient
ρ	kg/m ³ / Ω m	Fluid density or conductor resistivity
μ	m ² /s	Fluid dynamic viscosity
ε		Cooling penalty
Δp	bar	Pressure drop along the tube
C	F/m	Electrical capacitance
$C_{ab,bc,a}$	F/m	Capacitance
$\cos \varphi$		Power factor
C_v	J/kg/K	Heat capacitance
D_c	m	Cable outer surface diameter
D_h	m	Hydraulic diameter of the tube
D_h	m	Hydraulic diameter
D_i	m	Inner cryostat wall diameter
E_m	V/m	Electrical peak stress
f		Friction factor
F_c	m ²	Cross-sectional area of the flow
F_c	m	Cross-sectional area of the flow
G	kg/s	Mass flow rate
H^*	T	Irreversible field
H_c	T	Critical field
I	A	Current
i		Scaled transport current amplitude
I_2	A	Electrical current at
I_c	A	Tape critical current
I_c	I	Critical current
I_{ch}	A	Charging current
I_k''	kA	Subtransient fault current
$I_{n(om)}$	A	Nominal current

I_p	kA	Peak short circuit power
K	Km/W	Thermal conductivity
L	H/m	Electrical inductance
l	m	Connection length
L	m	Tube length
l_1	m	Critical length 1
l_2	m	Critical length 2
l_3	m	Critical length 3
$L_{a,b,c}$	H/m	Self inductance
l_{exp1}	m	Room temperature length
l_{exp2}	m	Cryogenic temperature length
L_v	J/kg	Latent heat evaporation
$M_{ab, bc, ca}$	H/m	Mutual inductance
N		Number of tapes
$n-1$		Redundancy criteria 1
$n-2$		Redundancy criteria 2
n -value		V-I transition to the normal state
P	W	Input power of cooling
P_1	W	Electrical Power of
P_k	W	Short circuit losses
P_L	W	Transferrable power
P_n	W	Natural power
P_w	m	Wetted perimeter of the flow
P_w	m	Wetted perimeter
Q	W	Cooling power
Q_1	VAR	Electrical reactive power at sending end
Q_2	VAR	Electrical reactive power at receiving end
R	Ω /m	Electrical resistance
R_1	m	Outer core radius
R_1	mm	Outer core radius
Re		Reynolds number
R_{th}	Ω	Thévenin resisitance
S_g	VAR	Apparent power
S_k ''	VA	Short circuit power
T_1	K	Room temperature
T_2	K	Cryogenic temperature
$\tan\delta$		Dissipation factor
T_{in}	K	Temperature inlet
t_{ins}	mm	Insulation thickness

T_o	K	Operating temperature
T_{out}	K	Temperature outlet
T_p	K	Heat rejected temperature
$TP_{a,b,c}$	m	Twist pitch
T_Q	K	Temperature at cold end
U	V	Electrical System Voltage
U_0	V	Phase to earth voltage
U_f	V	Phase voltage
V	V	Conductor voltage
$V_{1,2,3,4}$	V	Bus Voltage
w	m/s	Fluid velocity
X_{th}	Ω	Thévenin reactance
Z_0	Ω	Characteristic impedance
Z_{th}	Ω	Thévenin impedance
ρ	Ωm	Matrix resistivity
ΔT	K	Temperature difference
α		Winding angle
$\delta l_{1,2,3,4}$	deg	Bus voltage angle
η		Anisotropy or relative efficiency of thermal cycle

Acknowledgements

After receiving my master degree at the Department of Electrical Engineering in the High Voltage Technology and Management group at the Technical University of Delft in 2008, I was offered a PhD position. I was very pleased by the opportunity, because of the catchy subject, the pleasurable working environment and great colleagues to work with.

I'm now working on the final pages of this book, and with pleasure (however there were some hurdles along the way)! In this period I have learned very much but also grew many years older. As they say, wisdom comes with the years... I did not reach this point without the support of my colleagues, family and friends. Therefore this book is also partly your merit. There are a few people whom I want to thank personally since without their contribution this thesis would not be a success.

First of all, I want to thank my promotor Prof. dr. Johan Smit, for giving me the opportunity and trust to work on this inspiring project. Thanks for the many (skype) hours spend on finalizing this thesis.

My co-promotor, Dr. Oleg Chevtchenko, your time spent to guide me through the PhD process is very much appreciated. You were always inspiring to me, with your thoughts. You have taught me to go beyond my possibilities. As you told me, the hands on work we did together, will always stay valuable.

I would like to thank Edward Gulski and Jur Erbrink for their trust and for putting me forward for this PhD position after finalizing my master thesis. The coaching year at the start of this project was valuable to me and I want to thank Edward Gulski for that. Peter Morshuis and Dhiradj Djairam thanks for the nice cooperative work on our student teaching courses.

Projects like these need the expertise and guidance of the laboratory assistants. Therefore I want to thank Paul van Nes for his availability during the project. Our diner with pfifferlingen was special. And I want to thank Wim Termorshuizen, Aad de Graaf and Bertus Nagen for the discussions and technical support.

I was involved in the Dutch cable project existing of the consortium NKT cable, Alliander and TUDelft. I'm grateful to have worked in beautiful surroundings of Copenhagen with Dag Willén whom I admire for his enthusiasm and skills. Also many thanks to your team members Heidi Lengte, Carsten Thidemann and Cresten

Traeholt. I would like to thank Alex Geschiere and Irina Melnik, for creating the opportunity to work on this subject and the many valuable discussions we had in our meetings and during after work dinners. From TenneT I want to thank Gert Aanhaanen en Rob Ross for their commitment to this project. In the beginning of the project I was invited at University of Twente to learn more about superconductors and did some hands on work. Marc Dhallé many thanks for transferring valuable knowledge about superconductors, I enjoyed it very much.

Having fun in your daily work goes along with nice colleagues around you. I want to thank my roommates Qikai and Barry, (Piotr also partly) for the very good atmosphere! And off course the other members of our group: Jur, Muhannad, Lukasz, Ravish, Roman, Thomas, Dennis, Huifei, Alex, Tom, and Gautam (ones I forgot please include yourself).

My fellow PhD students of the other group Arjen, thanks for being available for many helpful discussions, and Rick, thanks for joining the coffee (and the stronger drinks on other occasions).

Sander Meijer, thank you for giving me the opportunity to work at DNV GL and for being my fellow villager in Driel! I would also like to express my gratitude to my DNV GL colleagues for the possibility to finish my PhD next to my daily work, especially Frank de Wild.

I'm very grateful for the support of my family, without their perseverance it would have been very hard to finish my thesis. Many thanks to Maarten Witteveen, who helped me with preparing the cover and, Herman Witteveen for the editorial help and support in printing the book, both within a limited timeframe. Ans Schellekens thanks for the support and being available at any time of the day when there was a need!

I would like to thank my parents, Arie and Erna Zuijderduin, for supporting me all those years. I'm thankful that you have encouraged me to get the most out of myself.

Dear Janneke thank you for your patience in seeing my book finished. It was a hard time, in particular the last bits and pieces, but we have managed it together. Within this period we have shared many things together such as renovating a house in Delft, your PhD graduation, birth of our lovely son Thijn, my new job at DNV GL, moving to Driel (near Arnhem), your new job at Radboudumc, birth of our lovely daughter Linde, buying our new house in Oosterbeek. You ended your book with the phrase that it is time for a new project. I would like to state that it is now time to spend more time with my family and friends!

Curriculum Vitae

Roy Zijderduin was born on February 11th, 1980 in Pijnacker, the Netherlands. He received his master degree in 2008 in Electrical Engineering at the Technical University of Delft at the faculty of Electrical Engineering, Mathematics and Computer Science (EEMCS). He graduated on methods to determine the remaining life of on-load tap changers in the High Voltage Technology and Management Group (currently Intelligent Electrical power Grid group). After his graduation he started as a PhD student at the Technical University of Delft with the focus on the application of superconductors in the Dutch power grid, which was funded by SenterNovem (nowadays RVO “Rijksdienst voor Ondernemend Nederland (RVO)”). Since 2013 he is working at DNV GL - Energy as a consultant in the Power Links Group.